

IMPERIAL COLLEGE LONDON

Department of Earth Science and Engineering

Centre for Petroleum Studies

**Production Monitoring of Condensate Gas Ratio Transients Based on Dynamics of
Produced Fluid Composition**

By

Anastasia Alyapina

**A report submitted in partial fulfilment of the requirements for
the MSc and/or the DIC.**

September 2012

DECLARATION OF OWN WORK

I declare that this thesis

Production Monitoring of Condensate Gas Ratio Transients Based on Dynamics of Produced Fluid Composition

is entirely my own work and that where any material could be construed as the work of others, it is fully cited and referenced, and/or with appropriate acknowledgement given.

Signature:.....

Name of student: Anastasia Alyapina

Name of supervisor: Professor Alain Gringarten

Name of the company supervisor: Denis Rudenko, Schlumberger

Acknowledgements

I would like to express my deepest gratitude to Schlumberger Moscow Research for the opportunity and support offered for my Master's Project. The knowledge and experience shared over these three months and also during my previous internships have made an indispensable contribution to my studies and personal development. I am grateful to my supervisor, Denis Rudenko, for his patience, guidance and encouragement, to Bertrand Theuveny for his continuous support throughout and to Valery Shako for his help and advice. This project would not have been possible without their help.

A very special thank to Professor Alain Gringarten and all those at Imperial College who have provided invaluable teaching and guidance over the last year. I truly thank my classmates who have been a great and academically conducive company on this journey.

I am most grateful to my family for their undivided support and encouragement in all my undertakings.

Table of Contents

Abstract	1
Introduction	1
Problem Formulation.....	2
Methodology	2
Reservoir Models	4
Fluid Models	5
Base Case Analysis	5
Rich Gas Condensate.....	5
Lean Gas Condensate	7
Extra Rich Gas Condensate	8
Sensitivity Study: Reservoir and Production Parameters	9
Rich Gas Condensate.....	9
Lean Gas Condensate	11
Extra Rich Gas Condensate	12
Sensitivity: Tuned Reservoir Model and Field Production History	13
Sensitivity to Error in Composition Measurements	14
Conclusions	15
Recommendations for Further Study.....	15
Acknowledgements	16
Nomenclature	16
References	16
Oilfield Units Conversion Factors.....	16
Appendix A: Literature Review	17
Appendix B: Single Well Sector Model.....	33
Appendix C: Rich Fluid Base Case Analysis	34
Appendix D: Sensitivity Study Results	35
Rich Fluid	35
Lean Fluid.....	42
Extra Rich Fluid.....	48
Appendix E: Base Case Final Condensate Saturation	56
Rich Fluid	56
Lean Fluid.....	56
Extra Rich Fluid.....	57
Appendix F: Analytical Solution for Simulation Model Used	58

List of Figures

Figure 1: Production and testing sequence	3
Figure 2: Relative permeability used in base case scenario	4
Figure 3: Fluid phase envelopes with reservoir conditions (RC) marked	5
Figure 4: Rich fluid CGR variation with changing (a) $\Delta C1$; (b) $\Delta C3-C5$; (c) $\Delta C6+$	6
Figure 5: Rich fluid CGR variation with changing $\Delta C2$	6
Figure 6: Rich fluid CGR based on simulation results and calculated from correlations obtained	6
Figure 7: Lean fluid ΔCGR variation with changing (a) $\Delta C1$; (b) $\Delta C2$; (c) $\Delta C3-C5$; (d) $\Delta C6+$	7
Figure 8: Lean fluid CGR based on simulation results and calculated from correlations obtained.....	8
Figure 9: Extra rich fluid ΔCGR variation with changing (a) $\Delta C1$; (b) $\Delta C6+$	8
Figure 10: Extra rich fluid CGR based on simulation results and calculated from correlations obtained	9
Figure 11: Relative permeability used in sensitivity study.....	9
Figure 12: Rich fluid sensitivity study results for $k=10mD$, CGR from simulation results and based on proposed correlations	10
Figure 13: Rich fluid sensitivity study results for (a) $P_{res}^o=350bar$; (b) $P_{res}^o=600bar$; CGR from simulation results and based on proposed correlations	11
Figure 14: Lean fluid sensitivity study results for $k=70mD$, CGR from simulation results and based on proposed correlations	11
Figure 15: Lean fluid sensitivity study results for (a) $P_{res}^o=275bar$; (b) $P_{res}^o=400bar$; CGR from simulation results and based on proposed correlations	12
Figure 16: Extra rich fluid sensitivity results for $k=70mD$, CGR from simulation results and based on proposed correlations..	12

Figure 17: Extra rich fluid sensitivity study results for (a) $P_{res}^o=300\text{bar}$; (b) $P_{res}^o=400\text{bar}$; CGR from simulation results and based on proposed correlations	13
Figure 18: Field production history	13
Figure 19: Rich fluid CGR based on simulation results and calculated from correlations obtained using field production history	14
Figure 20: Rich fluid CGR estimates based on underestimated and overestimated composition (due to measurement errors) compared to actual values (a) C1; (b) C3-C5 (c) C6+	15

List of Figures – Appendices

Figure B- 1: Well placement schematic with sector model considered.....	33
Figure B- 2: Model gridding (left) with zoomed section containing well and hydraulic fracture (right)	33
Figure C- 1: Rich fluid ΔCGR variation with changing ΔC1 , $k=40\text{mD}$	34
Figure D- 1: Rich fluid sensitivity study, $k=0.1\text{mD}$	35
Figure D- 2: Rich fluid sensitivity study, $k=10\text{mD}$	35
Figure D- 3: Rich fluid sensitivity study, $\Phi=0.15$	36
Figure D- 4: Rich fluid sensitivity, $\Phi=0.25$	36
Figure D- 5: Rich fluid sensitivity study, $h=10\text{m}$	37
Figure D- 6: Rich fluid sensitivity study, $h=100\text{m}$	37
Figure D- 7: Rich fluid sensitivity, $L_f=50\text{m}$	38
Figure D- 8: Rich fluid sensitivity, $L_f=200\text{m}$	38
Figure D- 9: Rich fluid sensitivity, $k_{fw}=500\text{mD}\cdot\text{m}$	39
Figure D- 10: Rich fluid sensitivity, $k_{fw}=1500\text{m}$	39
Figure D- 11: Rich fluid sensitivity study, pressure depression factor 0.1	40
Figure D- 12: Rich fluid sensitivity study, pressure depression factor 0.9	40
Figure D- 13: Rich fluid sensitivity study, relative permeability	41
Figure D- 14: Lean fluid sensitivity study, $k=10\text{mD}$	42
Figure D- 15: Lean fluid sensitivity study, $k=70\text{mD}$	42
Figure D- 16: Lean fluid sensitivity study, $\Phi=0.15$	43
Figure D- 17: Lean fluid sensitivity study, $\Phi=0.25$	43
Figure D- 18: Lean fluid sensitivity study, $h=40\text{m}$	44
Figure D- 19: Lean fluid sensitivity study, $h=60\text{m}$	44
Figure D- 20: Lean fluid sensitivity study, $L_f=50\text{m}$	45
Figure D- 21: Lean fluid sensitivity study, $L_f=200\text{m}$	45
Figure D- 22: Lean fluid sensitivity study, $k_{fw}=500\text{mD}\cdot\text{m}$	46
Figure D- 23: Lean fluid sensitivity study, $k_{fw}=1500\text{mD}\cdot\text{m}$	46
Figure D- 24: Lean fluid sensitivity study, pressure depression factor 0.85	47
Figure D- 25: Lean fluid sensitivity study, pressure depression factor 0.95	47
Figure D- 26: Lean fluid sensitivity study, relative permeability.....	48
Figure D- 27: Extra rich fluid sensitivity study, $k=10\text{mD}$	49
Figure D- 28: Extra rich fluid sensitivity study, $k=70\text{mD}$	49
Figure D- 29: Extra rich fluid sensitivity study, $\Phi=0.15$	50
Figure D- 30: Extra rich fluid sensitivity study, $h=40\text{m}$	50
Figure D- 31: Extra rich fluid sensitivity study, $h=60\text{m}$	51
Figure D- 32: Extra rich fluid sensitivity study, $L_f=50\text{m}$	51
Figure D- 33: Extra rich fluid sensitivity study, $L_f=200\text{m}$	52
Figure D- 34: Extra rich fluid sensitivity study, $k_{fw}=500\text{m}$	52
Figure D- 35: Extra rich fluid sensitivity study, $k_{fw}=1500\text{m}$	53
Figure D- 36: Extra rich fluid sensitivity study, pressure depression factor 0.85.....	53
Figure D- 37: Extra rich fluid sensitivity study, pressure depression factor 0.95.....	54
Figure D- 38: Extra rich fluid sensitivity study, relative permeability	54
Figure E- 1: Rich fluid final condensate saturation for whole model (left) and detailed view of condensate banking phenomena around the well and hydraulic fracture (right).....	56

Figure E- 2: Lean fluid final condensate saturation for whole model (left) and detailed view of condensate banking phenomena around the well and hydraulic fracture (right)56

Figure E- 3: Extra rich fluid final condensate saturation for whole model (left) and detailed view of condensate banking phenomena around the well and hydraulic fracture (right)57

Figure F- 1: Log-log plot for model analytical solution above dew point58

Figure F- 2: Semi-log plot for model analytical solution above dew point58

Figure F- 3: History plot for pressure and rate for model analytical solution above dew point59

List of Tables

Table 1: Reservoir and production parameters 4

Table 2: Fluid properties 5

Table 3: Rich fluid RMS Error for obtained correlations 7

Table 4: Lean fluid RMS Error for obtained correlations 8

Table 5: Extra rich fluid RMS Error for obtained correlations..... 9

Table 6: Reservoir and production parameters uncertainty used in sensitivity study..... 9

Table 7: Rich fluid sensitivity study RMS Error (highest among three intervals)10

Table 8: Lean fluid sensitivity study RMS Error (highest among three intervals)11

Table 9: Extra rich fluid sensitivity study RMS Error (highest among three intervals)13

Table 10: Rich fluid RMS Error for obtained correlations, sensitivity to production history14

Table 11: Table: Error in CGR estimates caused by a 5% error in input data15

List of Tables – Appendices

Table A- 1: Key Milestones Related to this Study17

Table D- 1: Rich fluid sensitivity study, RMS Error41

Table D- 2: Lean fluid sensitivity study, RMS Error48

Table D- 3: Extra rich fluid sensitivity study, RMS Error54

MSc in Petroleum Engineering 2011-2012**Production Monitoring of Condensate Gas Ratio Transients Based on Dynamics of Produced Fluid Composition**

Anastasia Alyapina

Professor Alain C. Gringarten, Imperial College

Denis Rudenko, Schlumberger

Abstract

One of the main measurements of interest from gas condensate production flow metering is the condensate content. This knowledge has a significant impact on accurate prediction of condensate reserves, and hence surface facility planning and the field development strategy selected. High condensate production requires provisions for processing and transportation. Therefore it may not always be desirable to produce the maximum amount of condensate at surface. However, a large amount of condensate drop-out in the reservoir also raises issues. Overall recovery of reserves decreases and condensate blockage impairs well productivity. With on-going pressure depletion and also changing production regimes, the condensate content of the produced fluid also changes. It is thus necessary to monitor production of both gas and liquid phases in real-time. Multiphase flow metering is currently widely used for gas condensate field production monitoring. Multiphase flow metering should facilitate characterisation of the produced fluid; in particular, measurements should provide the Condensate Gas Ratio (CGR) for the produced fluid. A potential method for increasing multiphase flow metering results interpretation reliability is investigated. The method proposes to monitor well effluent composition and uses a correlation based on this composition to estimate the produced fluid CGR. Feasibility of the proposed approach is illustrated.

A single well sector model with a hydraulic fracture is used to model production. Hydraulic fracturing is widely used to enhance gas condensate production in Western Siberia. A series of production and testing sequences are applied. Three fluid models corresponding to a rich, lean and extra rich gas condensate mixture are considered. Reservoir model parameters selected corresponded to those typical for Western Siberian gas condensate fields. Relative changes in composition of C1, C2, C3-C5, C6+ and produced CGR were considered. Correlations based on several of the component groups to estimate CGR are proposed for each of the fluid models. Correlation sensitivity to uncertainty in reservoir and production parameters is tested. Findings are such that correlations are robust to variations in reservoir and production parameters, with the exception of initial reservoir pressure. When the pressure under consideration is close to the fluid dew point pressure, variations in phase saturations in the far-zone of the reservoir lead to changing mobile fluid composition. Therefore the composition of the fluid reaching the wellbore is different. This suggests that the correlation needs to be reconsidered. The correlations show significant sensitivity to errors in composition measurements.

Introduction

One of the main measurements of interest from gas condensate production flow metering is the condensate content. This knowledge has a significant impact on accurate prediction of condensate reserves, and hence surface facility planning and the field development strategy selected. High condensate production requires provisions for processing and transportation. Therefore it may not always be desirable to produce the maximum amount of condensate at surface. However, a large amount of condensate drop-out in the reservoir also raises issues. Overall recovery of reserves decreases and condensate blockage impairs well productivity. With on-going pressure depletion and also changing production regimes, the condensate content of the produced fluid also changes. It is thus necessary to monitor production of both gas and liquid phases in real-time.

The first work considering the dynamics of gas condensate fluid properties with on-going reservoir depletion by Niemtschik et al. (1993) considered the dynamics of well stream effluent with changes in reservoir fluid composition.

Variation in produced fluid CGR had been previously studied by Zhang and Wheaton (2000). A general trend had been identified. In the case of a homogenous reservoir, the produced CGR would continuously decline. For a heterogeneous reservoir, the CGR could increase.

A more recent study by Ovalle et al. (2007) has addressed obtaining an estimate of the decrease in condensate yields once the reservoir pressure falls below the dew point pressure. A correlation for estimating the surface condensate yield was proposed. The condensate yield is considered as a function of initial stock-tank oil gravity, the original reservoir-gas specific gravity and reservoir temperature. All three variables are constant for a given reservoir and are determined at the onset of

production, when the reservoir pressure is above the dew point pressure. The condensate yield is estimated for a given reservoir pressure (below the dew point pressure). This method relies on reliable knowledge of the current reservoir pressure. This requires either a complex reservoir model or well tests. Using the former is computationally expensive. The latter, on the other hand, requires long buildups and is costly. Therefore, the proposed correlation cannot be used for real-time produced fluid condensate content monitoring.

The two existing options for production monitoring of gas condensates are separators and multiphase flowmeters. The current trend is an increasing use of multiphase flowmeters, which carries a number of advantages. Multiphase metering has no limitations regarding flow rates. Using separators requires lower flow rates to allow sufficient time for phase segregation. Multiphase flow meters can be used for each individual well. Separators are typically used for well pads due to their large footprint.

When a decision in favour of multiphase flow metering is made, a further issue arises. Overall, two main approaches to multiphase flow metering exist (Falcone et al. 2002). One approach is to measure the parameters of the flow that are functions of the three flow rates: gas, oil and water phases. The second approach is to measure the parameters of phase velocities and phase holdups. Various tools, using technologies such as gamma densitometry, impedance and microwave and differential pressures exist. The reliability of metering results depends on the accurate estimation of phase properties for measurement interpretation (Theuveny et al. 2007). Monitoring gas condensate production poses technical challenges. The gas volume fraction is much greater than the oil volume fraction. The contrast between phase properties is not as distinct as for oil. Both gas and liquid phases are essentially the same fluid. Some liquid can also be dispersed in the gas phase.

Accurate prediction of phase properties requires complex compositional fluid models. This is associated with high computational costs. Therefore what is often used is a relationship to describe fluid properties for a range of pressure and temperature conditions, but for a fixed fluid composition. As produced fluid composition changes with reservoir depletion, the applicability of this simplified model suffers. Flow metering interpretation reliability becomes questionable. The only solution is to update the fluid model. Re-sampling and laboratory analysis is required. This is time-consuming and costly. It is desirable to be able to identify when the fluid composition has changed to such an extent that a new fluid model is necessary.

The possibility for permanent monitoring of changing fluid properties would improve the efficiency of currently available multiphase flow metering technologies. Downhole Fluid Analysis (DFA) is a technique that has emerged recently and suggests potential for such permanent monitoring. DFA allows fast and approximate real-time fluid composition analysis in terms of C1, C2, C3-C5 and C6+ groups (Zuo et al. 2008). Suppose there is an explicit relationship between the change in fluid composition and the change in fluid properties. This suggests that monitoring produced fluid composition could allow an estimation of the corresponding change in fluid properties. If the change in fluid composition is associated with a significant change in fluid properties, a new fluid model is required. In this way, reliability of flow metering results interpretation can be improved.

The major difference between this approach and the ones that had been proposed before is that it is proposed to monitor fluid property changes at surface conditions, rather than considering the changing conditions in the reservoir.

Increasing reliability of flow metering data would also contribute to understanding and thus optimising well performance.

Problem Formulation

The aim of this study is to validate the feasibility of real-time monitoring of produced fluid properties based on changes in produced fluid composition. It investigates the possibility of establishing a correlation between changes in produced fluid composition and changes in one of the fluid properties used for production characterisation, the produced fluid Condensate/Gas Ratio (CGR). A single well sector reservoir model, with a hydraulic fracture, will be used with production and testing sequences. Our study targeted Western Siberia Gas Condensate production where the most of the vertical wells are stimulated with hydraulic fractures. Presence of the fracture changes the flow and therefore the condensate distribution patterns in the zone around the well with spatial extent of about several fracture lengths. It is impossible to accurately imitate the process of condensate bank formation around the fractured well using a model of non-fractured well with negative skin. Carlson and Myer (1995) demonstrated that modelling hydraulically fractured systems requires that the fracture is modelled explicitly.

Production and testing sequences are selected based on final reservoir depletion and pressure drop across the reservoir. Three fluid models, corresponding to a lean, rich and extra rich gas condensate are used. Reservoir model parameters are based on actual gas condensate formation properties of Western Siberia.

Studies by Roebuck Jr. et al (1968) concerning gas condensate reservoirs have shown that compositional simulation is required to represent the system behaviour. Since the system under consideration is that of a gas condensate, non-Darcy flow must be taken into account, as suggested by Belhaj et al (2003).

Methodology

Single Well Sector Model

A rectangular reservoir sector model with impermeable boundaries was used in this study. A vertical multi-segment (with 10 segments) well produced from the whole reservoir thickness. A vertical, homogenous and rectangular fracture penetrated the

reservoir from top to bottom. Two-phase flow was modelled. Homogenous flow within the well (i.e. no backflow and no slippage between phases) was assumed.

A compositional reservoir simulator, ECLIPSE 300 (2011.2 version), was used. As the model was simplified, only long-term production trends were considered. Simulation results on short time-scales (1-10 hours) were not taken into account due to questionable reliability.

A system above the oil-water contact with only gas and oil phases present was assumed.

The base case fluid model considered was that of a rich gas condensate. Lean and extra rich gas condensate models were also used to demonstrate that it is possible to establish correlations for various fluid models.

Model reliability has been verified by comparing with an analytical solution above dew point pressure. A well with a finite conductivity fracture in a closed rectangle homogenous reservoir was considered for the case of a dry gas. The model matched the analytical solution. The corresponding graphs can be observed in Appendix E.

Production and Testing Sequences

A fixed production and testing sequence was used for all simulations, with ten cycles of a constant rate production period followed by a multirate test and a buildup (Figure 1).

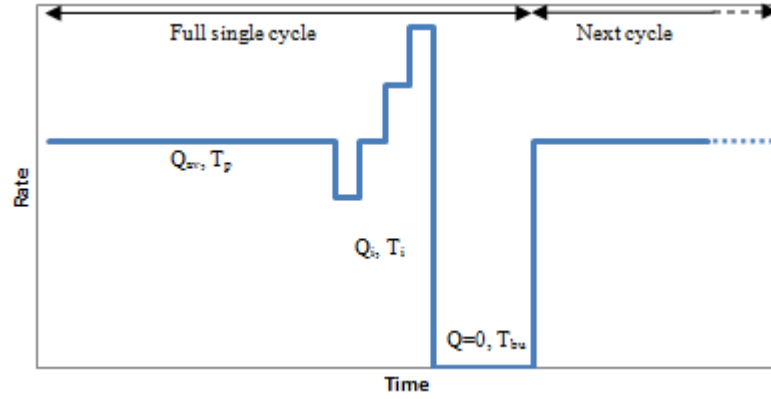


Figure 1: Production and testing sequence

The average gas production rate (Eq. 1) was estimated based on Darcy's law for single-phase gas:

$$Q_p = \frac{kh\pi}{\mu} \frac{P_i^2}{P_{st}} \left(1 - \left(\frac{P_{bh}}{P_f} \right)^2 \right) \left[\ln \left(\frac{r_e}{r_w} \right) + S \right]^{-1}$$

where Q_p is the production gas rate, k the formation permeability, h the pay thickness, μ the fluid viscosity, P_f the final reservoir pressure, P_{bh} the bottomhole pressure, r_e the extent of the model, r_w the wellbore radius and S the skin.

Skin was estimated from

$$S = \ln \left[2 \ln \left(e - \frac{0.17}{\frac{2}{\sqrt{\pi}} \frac{r_e}{L_f} - 0.87} \right) + \pi \frac{kL_f}{k_f w} \right] \quad (\text{Meyer and Jacot, 2005})$$

where L_f is the fracture half-length and $k_f w$ the fracture conductivity.

Adjusting the rate each time according to varying reservoir parameters ensured rates were sustainable for the reservoir model. Fixed final reservoir depletion and pressure drop across the reservoir for each fluid model sensitivity study were introduced for valid comparison. Reservoir depletion was taken into account through the use of a depletion factor:

$$\text{depletion factor} = \frac{P_i}{P_{res}^o}$$

where P_{res}^o is the initial reservoir pressure.

A similar depression factor was introduced to account for the pressure drop across the reservoir:

$$\text{depression factor} = \frac{P_{bh} - P_{bh}^{min}}{P_i - P_{bh}^{min}}$$

where P_{bh} and P_{bh}^{min} are the bottomhole pressure and the constraining minimum bottomhole pressure respectively. The minimum bottomhole pressure was fixed at 100bar for all cases under consideration.

Total production time was estimated by considering the same recovery factor for each fluid model cases:

$$T_{tot} = \frac{RF \cdot GIP}{Q_{av}}$$

where RF is the Recovery Factor and GIP the initial Gas In Place.

Production flow period duration was assumed to be the same for each of ten cycles:

$$T_p = \frac{T_{tot}}{10}$$

where T_p and T_{tot} are the production flow period duration and total production time respectively.

Multirate test rates and durations were defined as follows:

$$Q_i = 0.75Q_p, Q_p, 1.25Q_p, 1.5Q_p, T_i = 10 \text{ days}, T_{bu} = 40 \text{ days}$$

where Q_i are the multirate test gas rates, T_i the duration of each test and T_{bu} the duration of the buildup test.

Reservoir Models

Reservoir parameters for two specific gas condensate fields in Western Siberia were used in this study. Low permeability and typical permeability cases were selected (Table 1).

Table 1: Reservoir and production parameters

Parameter	Low Permeability	Typical Permeability
k, mD	1	40
Φ	0.2	0.2
h, m	50	20
L_f , m	100	
k_{fW} , mD·m	1000	
P_{res}^o , bar	500	350
Depression factor	0.5	0.95
Non-Darcy flow β -factor, m^{-1}	5.E+09	

Relative permeability curves used in the base case scenario for both reservoir models are presented in Figure 2.

Relative permeabilities were calculated from

$$k_r^g = \left(\frac{S_g - S_g^c}{1 - S_g^c} \right)^{m_g} \text{ and } k_r^o = \left(\frac{S_o - S_o^c}{1 - S_o^c} \right)^{m_o}$$

where k_r^g is the relative permeability of the gas phase, S_g the gas saturation, S_g^c the critical gas saturation, m_g the Corey exponent for gas, k_r^o the relative permeability of the condensate phase, S_o the condensate saturation, S_o^c the critical condensate saturation and m_o the Corey exponent for condensate.

For the matrix, $S_{gc}=0$, $m_g=1.5$, $S_{oc}=0.05$, $m_o=3$. For the fracture, $S_{gc}=0$, $m_g=2$, $S_{oc}=0$, $m_o=2$. Usually, straight lines are used as a simplification of the relative phase permeability in the fracture, however there are indications in literature (Jamiohlahmady et al. 2007) that this is not necessarily good assumption. This correlates with internal experience of Schlumberger Moscow Research Centre (Butula et al. 2005). Unlike the case of a non-fractured vertical well, taking into account dependence of the relative phase permeability on capillary number does have not a significant effect for the case of a hydraulically fractured well. This could be explained by the fact that a hydraulic fracture reduces the pressure drop for the same production rates and therefore reduces the severity of condensate banking. Additionally, the fracture reduces the zone of the high flow velocities to the small areas around the fracture tips. Therefore the effect of condensate stripping is reduced. High flow velocities in the fracture do not significantly increase the total velocity stripping effect, as most of the condensate is deposited in the formation around the fracture. Relative phase permeabilities in the fracture are already close to ‘‘miscible’’ relative permeabilities that are assumed to have effect at high capillary numbers.

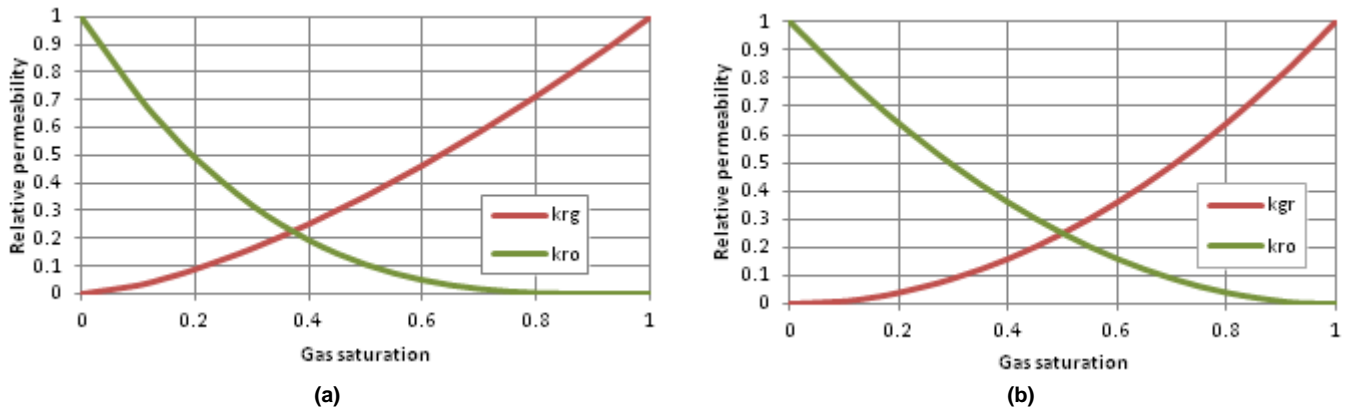


Figure 2: Relative permeability used in base case scenario (a) matrix (b) fracture

Fluid Models

Three fluid models were used in this study. They correspond to a lean, rich and extra rich gas condensate mixture (Table 2, Figure 3). The fluid models are suitable for correlation establishment based on component groups that can be identified using DFA techniques: C1, C2, C3-C5 and C6+.

For the purposes of this study, the term fluid was used to describe a gas condensate mixture. The term composition refers to the total fluid composition.

The rich gas condensate corresponds to the low permeability reservoir. The lean gas condensate model corresponds to the typical permeability reservoir. The extra rich fluid model is synthetic, used to represent the rare case of gas condensate that is close to volatile oil due to a very high heavy ends composition. The typical permeability reservoir was used with this fluid model.

Table 2: Fluid properties

	Lean	Rich	Extra rich
GOR, sm^3/sm^3	10860	3375	774
CGR, l/sm^3	0.0921	0.296	1.292
T_{res} , °C	87	108	267
P_{dew} , bar	291	386	374

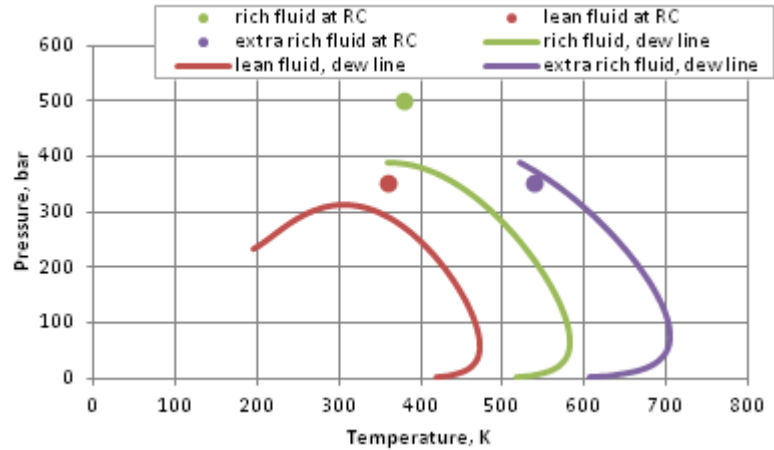


Figure 3: Fluid phase envelopes with reservoir conditions (RC) marked

Base Case Analysis

A correlation of the following form has been proposed:

$$\Delta CGR = f(\Delta C_i)$$

where $\Delta CGR = \frac{CGR - CGR_{ref}}{CGR_{ref}}$ and $\Delta C_i = \frac{C_i - C_{i,ref}}{C_{i,ref}}$.

Relative differences for both CGR and component group composition were used. Initial values at the start of production were taken as reference points.

For such a correlation to be established, base case results have been analysed to produce curves of changes in CGR versus changes in component or component group compositions.

Components considered for correlations were selected for each fluid model individually. A component was used if it showed monotonous behaviour suitable for correlation establishment.

An exponential function was considered for the correlation:

$$\Delta CGR = A[e^{b(\Delta C_i)} - 1]$$

The purpose of this study was to determine the possibility to establish a correlation.

Rich Gas Condensate

Correlations based on C1, C3-C5 and C6+ have been established (Figure 4 (a), (b) and (c) respectively). C2 composition demonstrated non-monotonous behaviour (Figure 5) making it an unsuitable candidate for correlation establishment.

The pressure considered was above the dew point pressure.

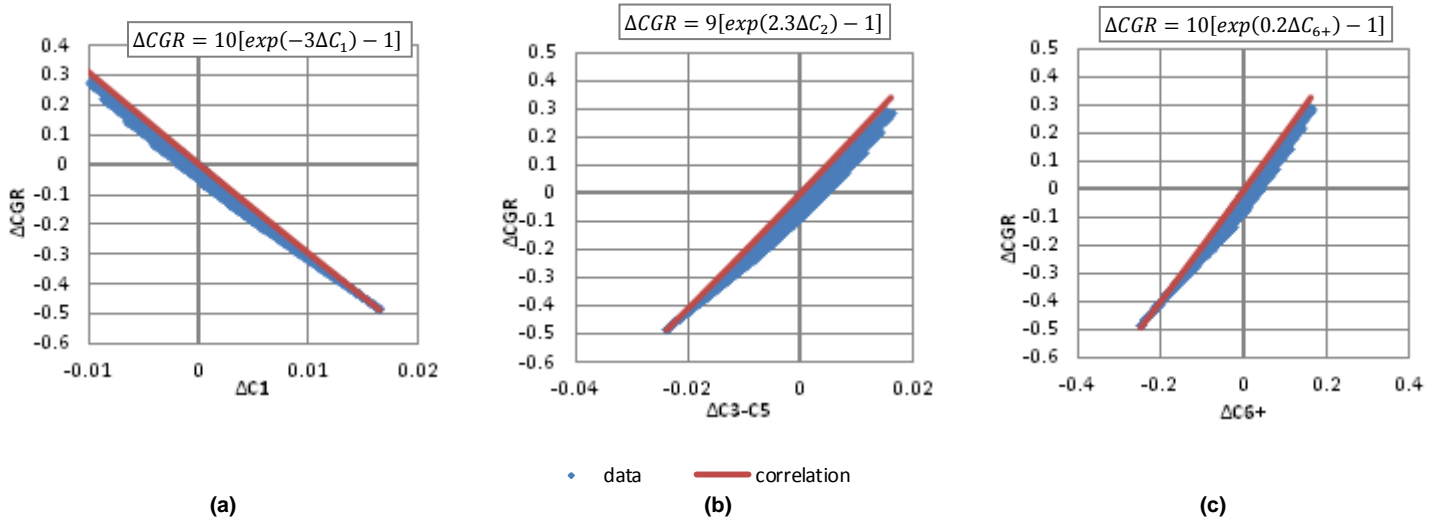


Figure 4: Rich fluid CGR variation with changing (a) ΔC_1 ; (b) ΔC_{3-5} ; (c) ΔC_{6+}

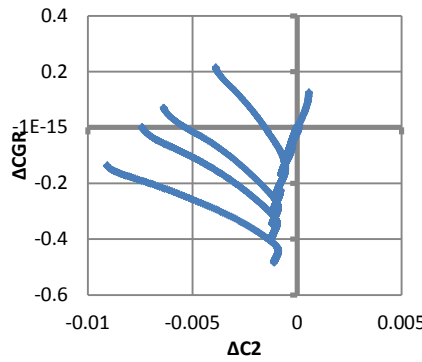


Figure 5: Rich fluid CGR variation with changing ΔC_2

The correlations obtained are based on obtaining an envelope for the data, neglecting the scatter. An assumption made is that no change in composition leads to no change in CGR. The scatter is due to changing trends in ΔCGR with ΔC_i over time due to reservoir depletion. Pressure variation across the reservoir can be significant and therefore mobile fluid composition varies over time. Phase saturations and hence phase mobilities change across the reservoir due to pressure variation. This is expected to introduce errors in CGR estimation. CGR calculated based on the proposed correlations is compared to the actual values in Figure 6 below. Results of using a higher permeability reservoir model in the C1 case, as an example, can be found in Appendix C.

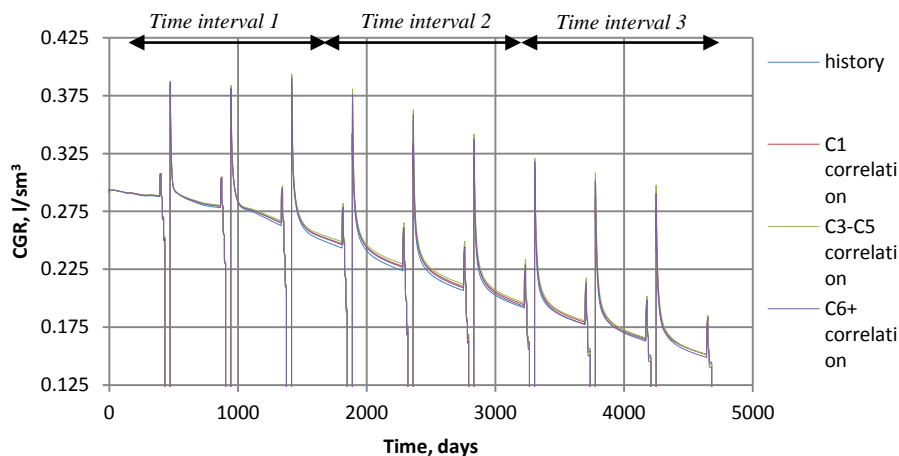


Figure 6: Rich fluid CGR based on simulation results and calculated from correlations obtained

The quality of the match between CGR from simulation results and values based on correlation has been assessed by considering the Root Mean Square (RMS) Error (Table 3). The error has been calculated on three intervals of equal duration

over the total production time (as marked on Figure 6). At early times the match is better (Interval 1). At middle and late times (Intervals 2 and 3 respectively) the error increases. It was expected that the error would be greatest in Interval 3. This is not always the case. As mentioned already, the correlation obtained does not cover all data points and this is a potential cause for this variation in error. All errors are below 3%, however the correlation giving the highest errors is the one based on C3-C5 component group.

Although at initial time reservoir pressure is above dew point, during production reservoir pressure goes below dew point and condensate drop out occurs throughout the reservoir. Nevertheless, the correlations remain valid until significant changes in composition of the mobile fluid in the far zone of the reservoir are observed. Variation of the mobile fluid composition is most sensitive to the rate of condensate deposition with the pressure drop and condensate mobility threshold, rather than the pressure change itself.

Table 3: Rich fluid RMS Error for obtained correlations

Correlation	C1			C3-C5			C6+		
Time interval	1	2	3	1	2	3	1	2	3
RMS Error %	0.56	1.7	1.4	0.84	2.6	2.2	0.52	1.4	1.5

Lean Gas Condensate

Correlations based on all four component groups under consideration: C1, C2, C3-C5 and C6+ (Figure 7 (a), (b), (c) and (d) respectively) have been established. The heavy component composition is smaller for this fluid, compared to the rich fluid, and therefore less interaction is expected between components. All component groups show monotonous behaviour.

The pressure considered was above the dew point pressure.

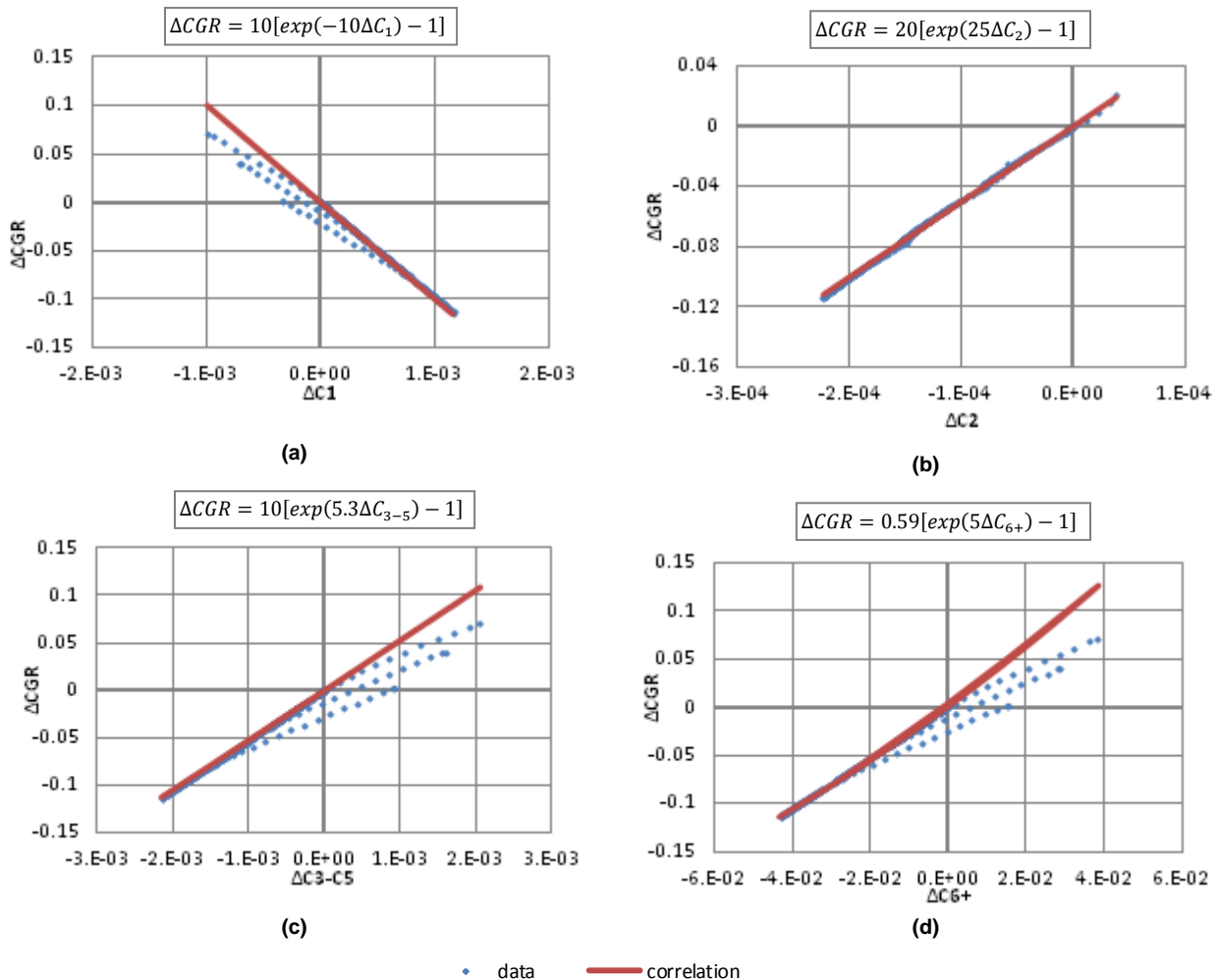


Figure 7: Lean fluid ΔCGR variation with changing (a) ΔC1; (b) ΔC2; (c) ΔC3-C5; (d) ΔC6+

As can be seen from the Figures above, the correlations match the data closely, and there is no scatter as in the case of the rich fluid. The outlying points were not considered. They were deemed to be due to the lack of model reliability for short-time results. A higher permeability reservoir model was used for this fluid, and therefore the pressure variation across the reservoir

was not as significant. The mobile fluid composition did not change substantially. Smaller errors are expected for the lean fluid correlations than for those for the rich fluid. CGR values based on proposed correlations show a good match with simulation results (Figure 8).

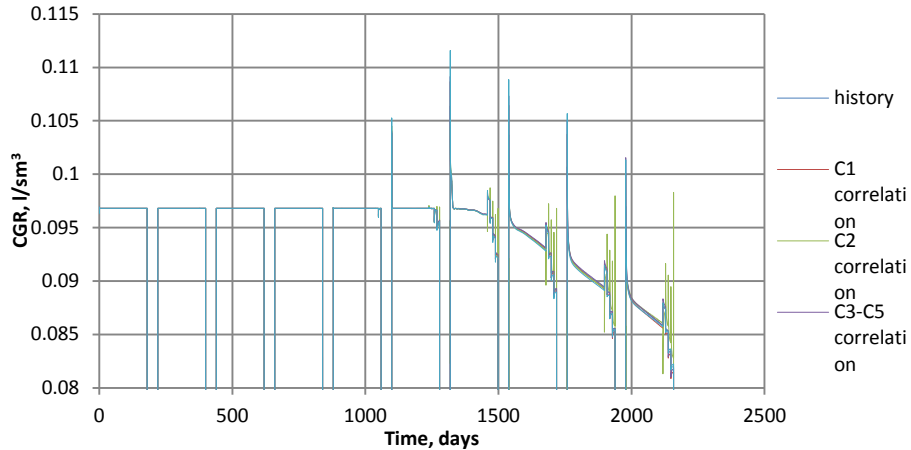


Figure 8: Lean fluid CGR based on simulation results and calculated from correlations obtained

Observing the RMS Error (Table 4), it is negligible at early and middle times, and a very low error appears towards the end of the simulation time considered. With ongoing reservoir depletion, fluid phase saturations change and therefore correlation validity is reduced. The highest error is observed for the correlation based on C2 component. Overall, all errors remain very low.

Table 4: Lean fluid RMS Error for obtained correlations

Correlation	C1			C2			C3-C5			C6+		
Time interval	1	2	3	1	2	3	1	2	3	1	2	3
RMS Error %	0	0	0.092	0	0	0.13	0	0	0.054	0	0	0.13

Extra Rich Gas Condensate

Correlations based on C1 and C6+ have been established (Figure 9 (a) and (b) respectively). C2 and C3-C5 compositions demonstrated non-monotonous behaviour.

The pressure considered was below the dew point pressure.

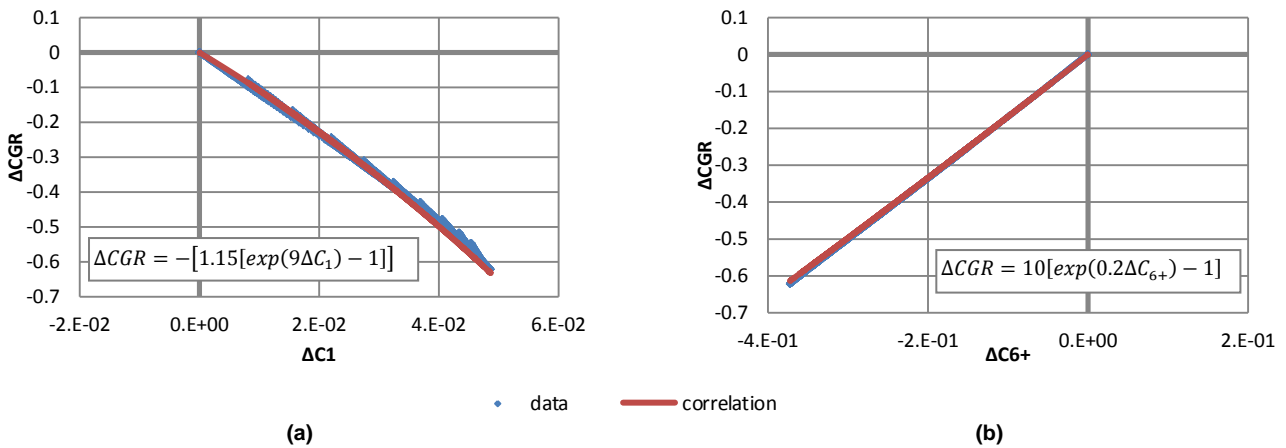


Figure 9: Extra rich fluid ΔCGR variation with changing (a) ΔC1; (b) ΔC6+

As can be seen from the Figures above, the correlations match the data closely, and there is no scatter as in the case of the rich fluid. A greater error is expected for values based on the C1 correlation. Figure 9 (a) demonstrates that there is a changing trend in the relationship between ΔCGR and ΔC1, which is not accounted for by the correlation.

CGR calculated based on correlations match the simulation values closely at early times (Figure 10). However, approaching mid-time, they begin to show a more significant error. Such an observation has not been made for the lean and rich fluids. As the fluid is heavy, phase saturation changes are sudden and lead to significant changes in phase mobilities in the far-zone. This alters the composition of the mobile fluid reaching the wellbore. The validity of the correlation is affected. If

compared to the rich and lean fluid models, significant condensate drop-out can lead to the critical oil saturation, when the condensate becomes mobile, to be reached quite early in production in the case of the extra rich fluid. This will also affect correlation applicability.

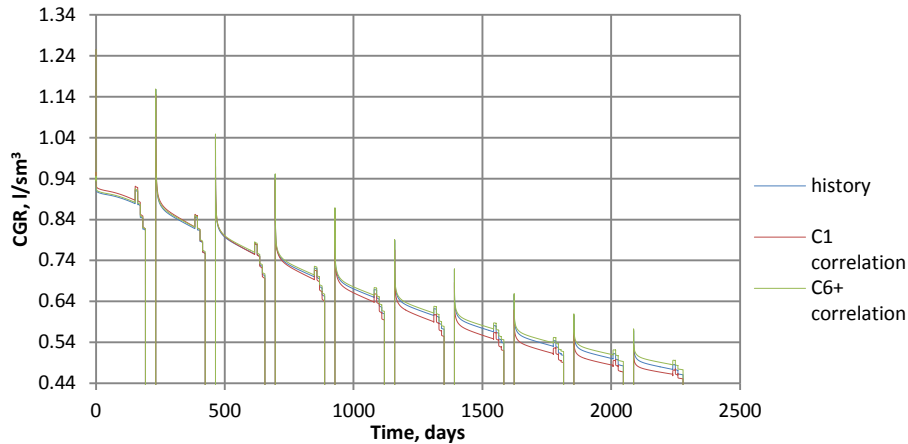


Figure 10: Extra rich fluid CGR based on simulation results and calculated from correlations obtained

Considering the RMS Error (Table 5), considerably higher than that for the lean fluid. Compared to the rich fluid model, the error for the C1 correlation is higher for the extra rich fluid. However, the C6+ correlation shows a lower error than that for the rich fluid.

Table 5: Extra rich fluid RMS Error for obtained correlations

Correlation	C1			C6+		
Time interval	1	2	3	1	2	3
RMS Error %	0.62	1.9	2.8	0.39	0.83	1.7

Sensitivity Study: Reservoir and Production Parameters

Uncertainty ranges corresponding to the two Western Siberian gas condensate fields were used in this study for reservoir parameters sensitivity study (Table 6). Relative permeability sensitivity was tested by using relative permeability curves for the matrix as shown in Figure 11. For the matrix, $S_g^c=0, m_g=3, S_o^c=0.2, m_o=5$.

For production parameters sensitivity study, pressure drop across the reservoir was considered to vary the production rates. The CGR values based on simulation results and that calculated using the proposed correlations were compared. Thus the range of validity of the correlations was tested.

Table 6: Reservoir and production parameters uncertainty used in sensitivity study

Parameter	Rich fluid	Lean fluid	Extra rich fluid
k, mD	0.1, 1, 10	10, 40, 70	
ϕ	0.15, 0.2, 0.25		
h, m	10, 50, 100	20, 40, 60	
L_f , m	50, 100, 200		
kfw, mD·m	500, 1000, 1500		
P_{res}^o , bar	350, 500, 600	275, 350, 400	300, 350, 400
Depression factor	0.1, 0.5, 0.9	0.85, 0.9, 0.95	

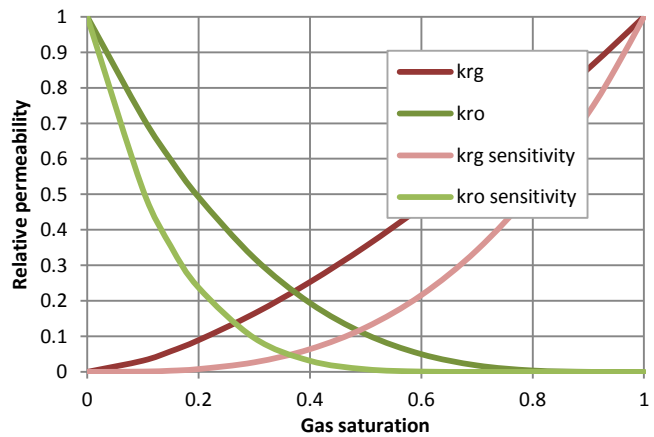


Figure 11: Matrix relative permeability used in sensitivity study

Rich Gas Condensate

Figure 12 demonstrates the match between simulation results CGR and the values obtained using the proposed correlation for the case of higher reservoir permeability. The results for varying all parameters apart from the reservoir pressure behave in a similar manner. A full set of results can be found in Appendix D. The correlations are valid for a wide range of reservoir parameters, excluding varying initial reservoir pressure.

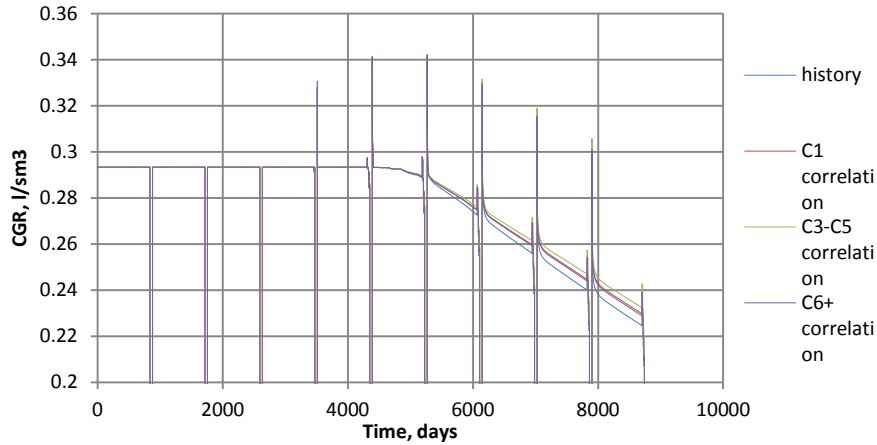


Figure 12: Rich fluid sensitivity study results for $k=10\text{mD}$, CGR from simulation results and based on proposed correlations

The RMS Error was considered in a similar manner to the Base Case Analysis (Table 7). The results are consistent with what had been seen before: the greatest error is observed when using the correlation based on C3-C5. All errors remain below 3%.

Table 7: Rich fluid sensitivity study RMS Error (highest among three intervals)

Parameter	RMS Error, %		
	C1	C3-C5	C6+
k , mD	1.8	2.7	1.5
Φ	1.7	2.6	1.7
h , m	1.7	2.7	2.1
L_f , m	1.7	2.7	2.0
k_{rw} , mD·m	1.7	2.7	1.7
P'_{res} bar	20	15	4.6
Depression factor	1.8	2.7	1.6
Relative permeability	1.4	2.2	1.1

It is expected that varying the initial reservoir pressure will require the correlations to be reconsidered. Changes in pressure are associated with changes in phase saturations and phase mobilities in the far-zone of the reservoir. Therefore, the flowing fluid composition varies, resulting in changes in composition of the fluid that reaches the wellbore. The correlation is based on the case where the initial reservoir pressure, 500bar, is above the fluid dew point pressure (386bar). Considering an initial pressure of 350bar, below the dew point pressure, affects the correlation applicability (Figure 13 (a)). All correlations begin to show a considerably higher error. The correlation based on C6+, however, is noticeably better than the other two. As the initial reservoir pressure is below the dew point, the fluid phase saturations and hence mobilities change considerably. Component group phase distribution in the produced fluid is affected.

Initial reservoir pressure of 600bar, on the other hand, is well above the dew point pressure. Mobile fluid composition is not expected to change significantly and therefore the correlations provide reasonable estimates of CGR (Figure 13 (b)). These estimates are better than those for the Base Case Analysis. In the latter the initial reservoir pressure used was 500bar. The dew point pressure was reached earlier in the 500bar initial reservoir pressure and therefore phase saturations changed, affecting correlation applicability.

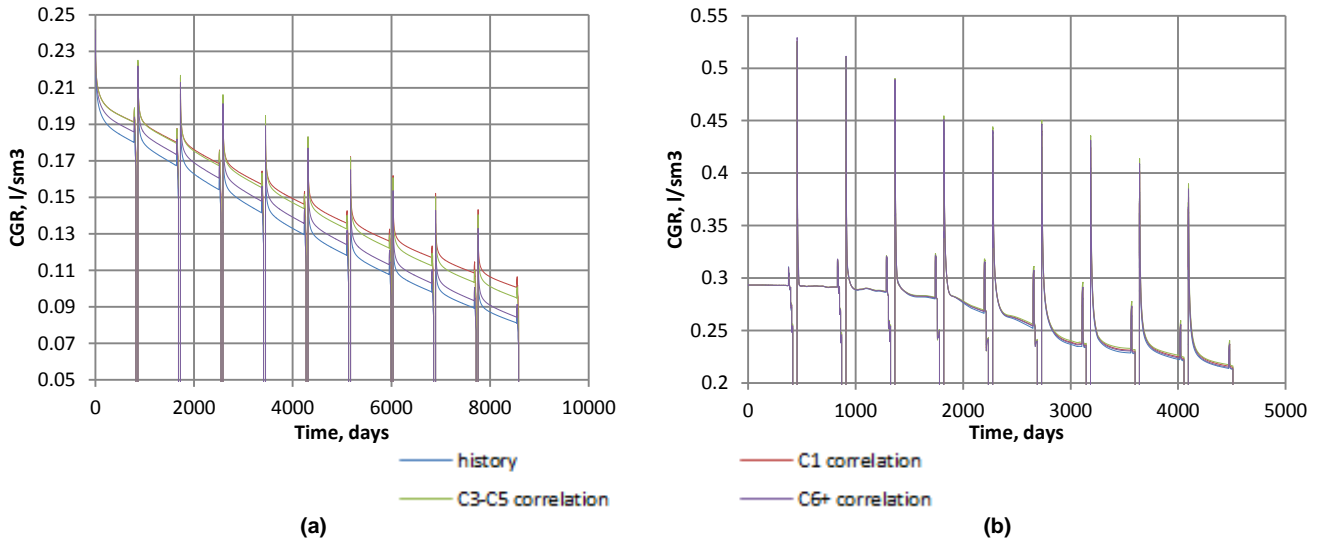


Figure 13: Rich fluid sensitivity study results for (a) $P_{res}^o=350\text{bar}$; (b) $P_{res}^o=600\text{bar}$; CGR from simulation results and based on proposed correlations

Lean Gas Condensate

Figure 14 demonstrates the match between simulation results CGR and the values obtained using the proposed correlation for the case of higher reservoir permeability. The results for varying all parameters apart from the reservoir pressure behave in a similar manner. A full set of results can be found in Appendix D. It can be said the correlations are valid for a wide range of reservoir parameters, excluding varying initial reservoir pressure.

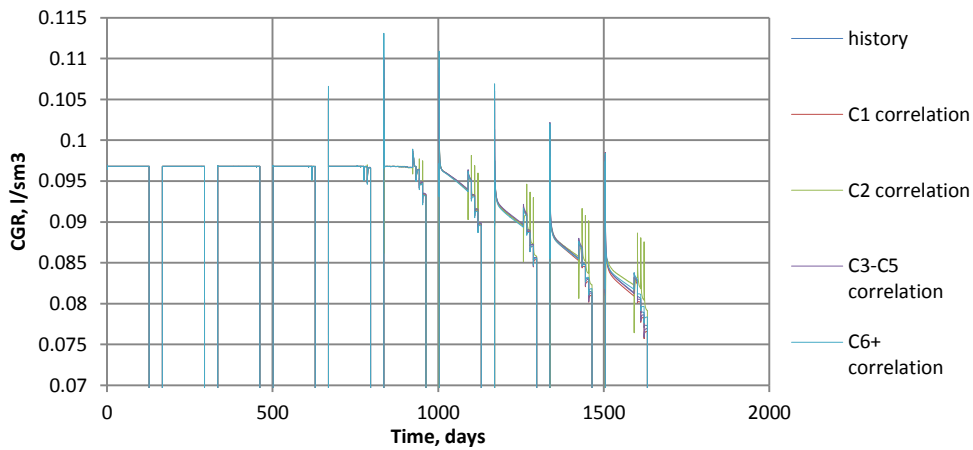


Figure 14: Lean fluid sensitivity study results for $k=70\text{mD}$, CGR from simulation results and based on proposed correlations

The RMS Error was considered in a similar manner to the Base Case Analysis (Table 8). The results are consistent with what had been seen before: the greatest error is observed when using the correlation based on C3-C5. All errors remain below 3%.

Table 8: Lean fluid sensitivity study RMS Error (highest among three intervals)

Parameter	RMS Error, %			
	C1	C2	C3-C5	C6+
k, mD	0.17	0.36	0.068	0.18
Φ	0.14	0.25	0.061	0.14
h, m	0.72	2.4	0.43	1.4
L_{fs} , m	0.095	0.14	0.055	0.13
k_{fW} , mD·m	0.11	0.17	0.060	0.13
P_{res}^o , bar	0.82	29	0.95	9.1
Depression factor	0.25	0.60	0.13	0.24
Relative permeability	0.11	0.17	0.068	0.13

The correlation is based on the case where the initial reservoir pressure is 350bar, which is above the fluid dew point pressure (291bar). An initial reservoir pressure of 275bar is below the fluid dew point pressure. Fluid phase saturations will be different and hence mobilities will change. Correlations based on C1 and C3-C5 provide a good estimate of the CGR (

Figure 15 (a)). In the case of a 400bar initial reservoir pressure (which is above dew point) the correlation shows a good match for CGR values (Figure 15 (b)). The pressure is well above dew point and therefore no significant change in phase saturations and mobilities is expected.

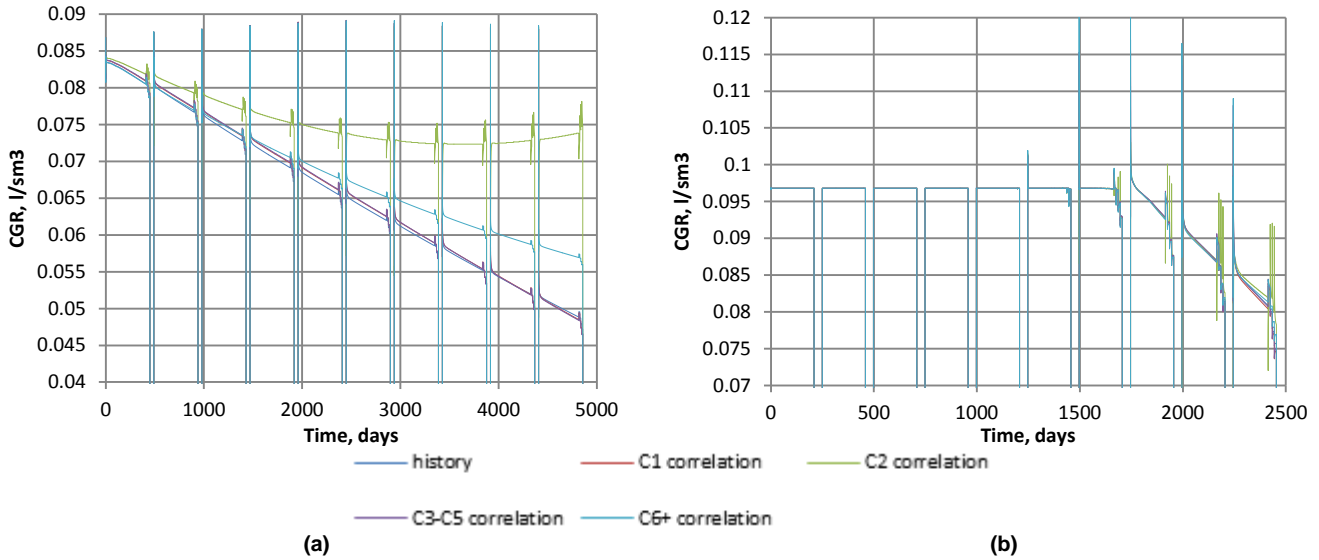


Figure 15: Lean fluid sensitivity study results for (a) $P_{res}^o=275\text{bar}$; (b) $P_{res}^o=400\text{bar}$; CGR from simulation results and based on proposed correlations

Extra Rich Gas Condensate

The correlations proposed for the extra rich fluid showed a shorter validity time than those for lean and rich fluids. The sensitivity study results are consistent with this statement. The correlations are valid for a wide range of reservoir parameters. However, correlations remain valid for a shorter time after production had started.

Figure 16 demonstrates the match between simulation results CGR and the values obtained using the proposed correlation for the case of higher reservoir permeability. The results for varying all parameters apart from the reservoir pressure behave in a similar manner. Also, unlike the lean and rich fluid models, one of the correlations showed higher sensitivity to uncertainty in relative permeability. The error observed when applying the C1 correlation increased significantly, while that for C6+ remained consistent with the rest. A full set of results can be found in Appendix D. The correlations are valid for a wide range of reservoir parameters, excluding varying initial reservoir pressure and relative permeability.

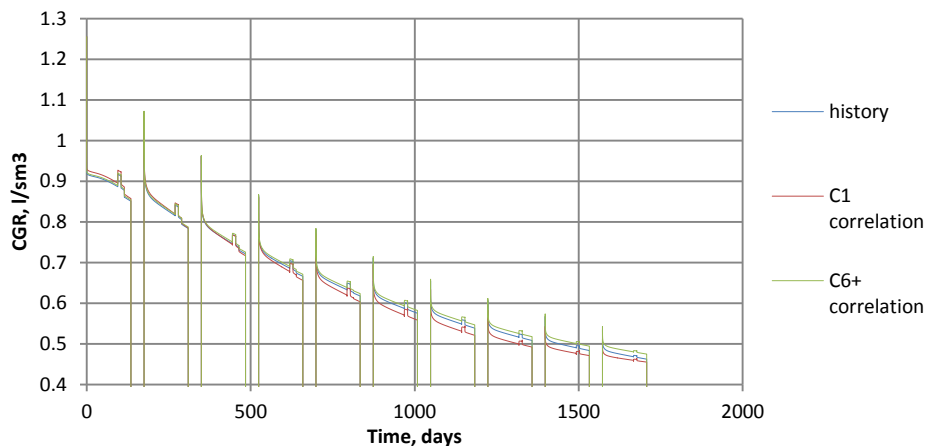


Figure 16: Extra rich fluid sensitivity results for $k=70\text{mD}$, CGR from simulation results and based on proposed correlations

The RMS Error was considered in a similar manner to the Base Case Analysis (Table 9). The results are consistent with what had been seen before: the greatest error is observed when using the correlation based on C1. All errors remain below 3%.

Table 9: Extra rich fluid sensitivity study RMS Error (highest among three intervals)

Parameter	Root Mean Square Error, %	
	C1	C6+
k, mD	2.9	1.8
Φ	2.9	1.9
h, m	4.0	1.7
L_f , m	2.8	1.7
k_{fW} , mD·m	2.8	1.7
P_{res}^o , bar	97	15
Depression factor	2.8	1.7
Relative permeability	5.8	1.6

Varying initial reservoir pressure showed that the correlation is only valid for the specific value it has been based upon. As already mentioned in the Base Case Analysis section, in the case of the extra rich fluid model, small changes in pressure lead to significant changes in phase saturation and hence mobilities. Thus the composition of the fluid reaching the wellbore can change significantly. An initial pressure below the dew point pressure (374bar) (Figure 17 (a)) results in both correlations significantly overestimating the produced fluid CGR. Considering an initial pressure above the dew point pressure (Figure 17 (b)) demonstrates a close match between the C6+ correlation CGR estimates and the simulation results. The correlation based on C1, however, gives a very large error. In both cases, C1 correlation gives a substantially higher error than C6+.

In the case of the extra rich fluid, varying relative permeability also affects correlation applicability. The amount of condensate drop-out is significant and therefore the condensate flow becomes a factor affecting the produced fluid composition.

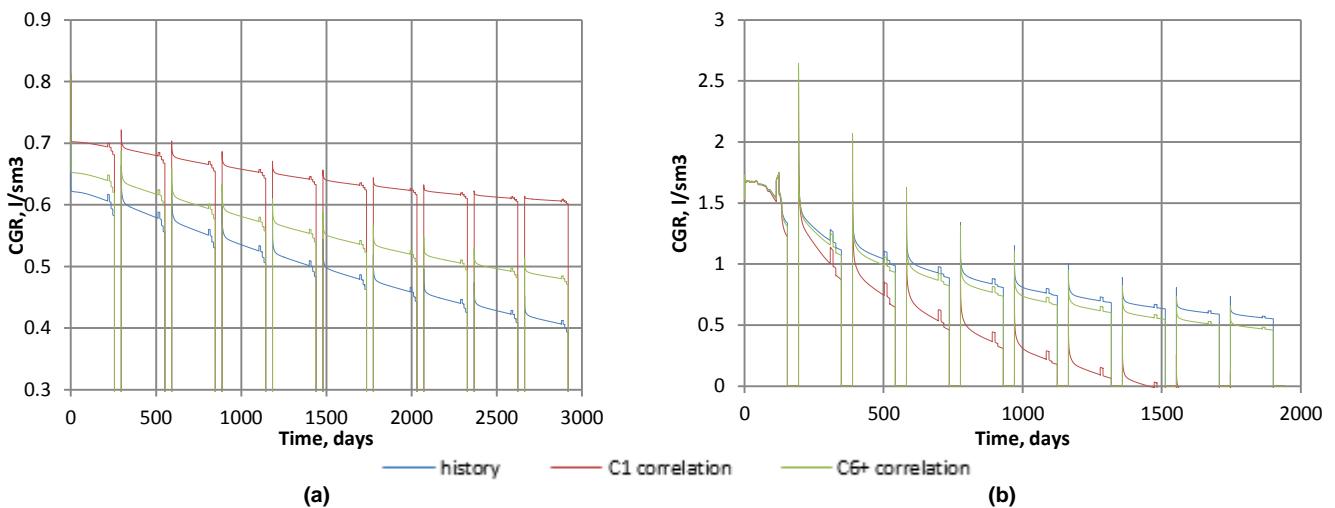


Figure 17: Extra rich fluid sensitivity study results for (a) $P_{res}^o=300\text{bar}$; (b) $P_{res}^o=400\text{bar}$; CGR from simulation results and based on proposed correlations

Sensitivity: Tuned Reservoir Model and Field Production History

A field production history was applied to the rich gas condensate fluid with reservoir parameters based on a tuned model (Figure 18). The initial reservoir pressure considered was 500bar, with fluid dew point pressure being 386bar.

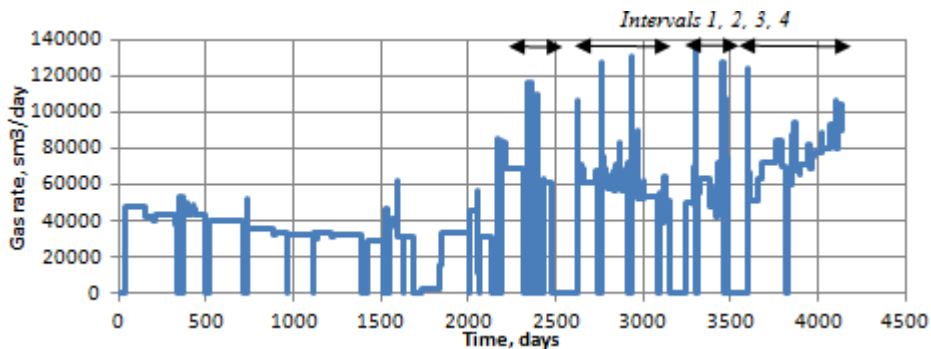


Figure 18: Field production history

This allowed for the correlations to be tested for a wider range of rates and more frequent regime changes, as well confirming correlation robustness to uncertainty in reservoir parameters. Results obtained (Figure 19) show that the correlations provide reasonable estimates of CGR. However, they are not as accurate as for the production and testing sequence considered for the base case and sensitivity study. A number of potential explanations exist. The field production history involves more short-term flow rate changes. The correlations may not represent this short-time behaviour very accurately. Also, as mentioned in the Methodology: Single Well Sector Model section, the well model used is a simplified one. Therefore, the results shown on short-times are deemed not as reliable.

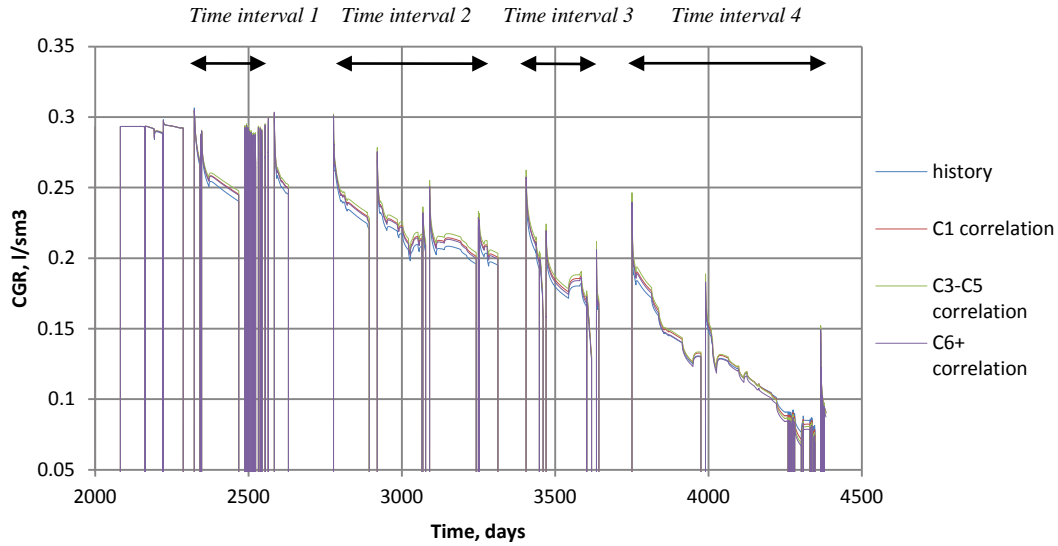


Figure 19: Rich fluid CGR based on simulation results and calculated from correlations obtained using field production history

The RMS Error was considered on four production time intervals (Table 10). The intervals were selected after the point in time when CGR begins to change. The reservoir pressure drops below fluid dewpoint pressure. All errors are below 4%. This is consistent with what had been seen in the Base Case Analysis and Sensitivity Study for the rich fluid model. Therefore, it can be said that correlation reliability does not suffer from applying a different production history. The time for which the correlation will be valid is dependent on the production history, as that will determine the rate of reservoir depletion.

Table 10: Rich fluid RMS Error for obtained correlations, sensitivity to production history

Correlation	C1				C3-C5				C6+			
Time interval	1	2	3	4	1	2	3	4	1	2	3	4
RMS Error %	1.2	1.9	2.3	2.1	1.7	2.8	3.5	3.2	1.0	1.5	1.8	3.2

Sensitivity to Error in Composition Measurements

The proposed correlations rely on accurately measured input data: produced fluid composition. Therefore, it is necessary to assess the potential effect of error in the input data.

For the purposes of this study, the rich gas condensate mixture Base Case Analysis was considered. An arbitrary relative error was taken to be

$$\frac{\Delta(z_i)_{abs}}{z_i} = 0.05$$

where z_i is the component composition and $\Delta(z_i)_{abs}$ is the absolute error, for each of C1, C3-C5 and C6+. This error was then used to calculate two possible compositions:

$$z_i = z_i + \Delta(z_i)_{abs} \text{ and } z_i = z_i - \Delta(z_i)_{abs}.$$

These new composition estimates were then used to calculate the surface CGR from proposed correlations (Figure 20).

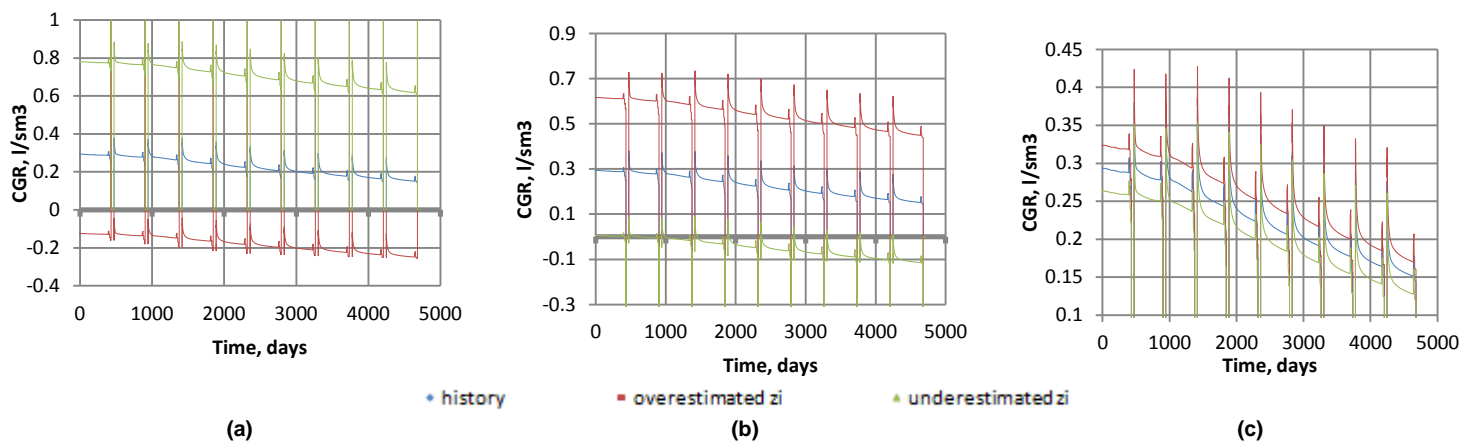


Figure 20: Rich fluid CGR estimates based on underestimated and overestimated composition (due to measurement errors) compared to actual values (a) C1; (b) C3-C5 (c) C6+

The sensitivity to errors in the input data is high as can be observed from the Figure above. C1 correlation shows the highest error, followed by C3-C5 and, finally, by C6+, which is the most robust to errors in the measured composition. The relative errors are summaries below (Table 11). This suggests that a quantitative measure of correlation applicability range is required to assess the required accuracy of the input data. Also, technological capabilities to obtain composition measurements of such accuracy need to be considered.

Table 11: Table: Error in CGR estimates caused by a 5% error in input data

Correlation	C1		C3-C5		C6+	
Error in composition	overestimate	underestimate	overestimate	underestimate	overestimate	underestimate
$\epsilon_{CGR} \%$	-160	140	100	-110	10	-10

Conclusions

In the course of this study, the feasibility of establishing correlations between produced fluid CGR and C1, C2, C3-C5 and C6+ composition had been confirmed. Which components groups are suitable for correlation establishment depends on the particular fluid model. The higher the heavy ends content, the more interaction between components takes place.

1. The sensitivity study carried out demonstrated the correlations robustness to a typical range of uncertainties in reservoir and production parameters, with the exception of reservoir pressure.
2. Correlations can be established with the initial reservoir pressure being both above and below the dew point pressure. In the case of the rich and lean gas condensate mixture, initial reservoir pressure was above dew point. In the case of extra rich gas condensate mixture, initial reservoir pressure was below the dew point. In all cases, correlations were established and their robustness to variation in reservoir and production parameters was confirmed.
3. If the initial reservoir pressure is close to the fluid dew point, a difference between the pressure used for correlation establishment and the actual initial reservoir pressure will affect correlation applicability. The extent of condensate drop-out in the reservoir will change the mobile fluid composition that flows to the wellbore and therefore the well effluent. This also means that for significant field depletion, correlations need to be re-established. Therefore it is necessary to establish a range of reservoir pressure variation for which the correlations remain valid.

Recommendations for Further Study

This study has proposed correlations for surface CGR estimation based on changes in produced fluid C1, C2, C3-C5 and C6+ composition. However, it requires further analysis to validate practical applicability:

1. The sensitivity study carried out demonstrated correlation applicability over a certain range of reservoir and production parameters. It is necessary to extend the sensitivity study to formulate quantitative criteria for the correlation applicability. This applies to both reservoir and production parameter uncertainty and fluid composition uncertainty.
2. This study suggested that advances in DFA technologies could offer the possibility of permanent produced fluid composition monitoring. It is therefore necessary to evaluate DFA capabilities to provide fluid composition measurements with resolution and accuracy within correlations applicability criteria.
3. Following the conclusion drawn from this study on the feasibility of correlation establishment with respect to produced CGR, other produced fluid properties could also be considered. Produced fluid phase densities are also a property of interest for production monitoring. Establishing correlations with respect to these properties could also be considered.

Acknowledgements

The support of the Schlumberger Moscow Research team before and throughout this project is gratefully acknowledged, in particular to Bertrand Theuveny and Valery Shako.

Nomenclature

CGR	Condensate Gas Ratio (l/sm ³)	Q_p	Production flow period gas rate (sm ³ /day)
C_i	Total component mole fraction	Q_i	Multirate test gas rate (sm ³ /day)
GIP	Gas In Place	RF	Recovery factor
GOR	Gas Oil Ratio (sm ³ /sm ³)	r_w	Wellbore radius (m)
h	Net pay thickness (m)	S	Skin
k	Formation permeability (mD)	S_g	Gas saturation
k_g^r	Gas phase relative permeability	S_g^c	Critical gas saturation
k_o^r	Oil phase relative permeability	S_o	Condensate saturation
k_{fw}	Fracture conductivity (mD·m)	S_o^c	Critical condensate saturation
L	Sector model extent (m)	T_{bu}	Build-up duration (days)
L_f	Fracture half-length (m)	T_i	Multirate test duration (days)
m_g	Corey exponent for gas	T_p	Production flow period duration
m_o	Corey exponent for condensate	T_{tot}	Total production time
P_{bh}	Bottomhole pressure (bar)	Δ	Change in given parameter
P_{bh}^{min}	Minimum bottomhole pressure (bar)	μ	Viscosity (Pa·s)
P_i	Reservoir pressure at given time (bar)	Φ	Formation porosity
P_{res}^o	Initial reservoir pressure (bar)		

References

- Belhaj, H.A., Agha, K.R., Nouri, A.M., Butt, S.D., Vaziri, H.F. and Islam, M.R. 2003. Numerical Simulation of Non-Darcy Flow Utilizing the New Forchheimer's Diffusivity Equation. Paper SPE 81499 presented at the Middle East Oil Show, Bahrain, 9-12 June. DOI: 10.2118/81499-MS.
- Butula, K.K., Maniere, J., Shandrygin, A., Rudenko, D. and Zynchenko, I.A. 2005. Analysis of Production Enhancement Related to Optimisation of Propped Hydraulic Fracturing in Gazprom's Yamburgskoe Arctic Gas Condensate Field, Russia. Paper SPE 94727 presented at SPE European Formation Damage Conference, Sheveningen, The Netherlands, 25-27 May. DOI: 10.2118/94727-MS.
- Carlson, M.R. and Myer, J.W.G. 1995. The Effects of Retrograde Liquid Condensation On Single Well Productivity Determined Via Direct (Compositional) Modeling Of A Hydraulic Fracture In A Low Permeability Reservoir. Paper SPE 29561 presented at Low Permeability Reservoirs Symposium, Denver, Colorado, 19-22 March. DOI: 10.2118/29561-MS.
- Falcone, G., Hewitt, G.F., Alimonti, C. and Harrison, B. 2002. Multiphase Flow Metering: Current Trends and Future Developments. *J. Pet Tech* **54** (4), DOI: 10.2118/74689-PA.
- Jamiolahmady, M., Ganesh, D., Sohrabi, M. and Danesh, A., 2007, Impact of Fracture Clean-Up on Productivity of Gas Condensate Wells. Paper SPE 107432 presented at SPE European Formation Damage Conference, Sheveningen, The Netherlands, 30 May – 1 June. DOI: 10.2118/107432-MS.
- Meyer, B.R. and Jacot, R.H. 2005. Pseudosteady-State Analysis of Finite-Conductivity Vertical Fractures. Paper SPE 95941 presented at SPE Annual Technical Conference and Exhibition, Dallas, Texas, 9-12 October. DOI: 10.2118/95941-MS.
- Niemstschik, G.E., Poettmann, F.H. and Thompson, R.S. 1993. Correlation for Determining Gas Condensate Composition. Paper SPE 26183 presented at SPE Gas Technology Symposium, Calgary, Alberta, Canada, 28-30 June. DOI: 10.2118/26183-MS.
- Ovalle, A.P., Lenn, C.P. and McCain, W.D. 2007. Tool To Manage Gas/Condensate Reservoirs; Novel Fluid-Property Correlations on the Basis of Commonly Available Field Data. *SPE Res Eval & Eng* **10** (6). SPE-112977-PA. DOI: 10.2118/112977-PA.
- Roebuck Jr., I.F., Henderson, G.E., Douglas Jr., J. and Ford, W.T. 1969. The Compositional Reservoir Simulator: Case I – The Linear Model. *SPE J.* **9** (1). DOI: 10.2118/2033-PA.
- Theuveny, B., Zinchenko, I.A. and Shumakov, Y. 2007. Testing Gas Condensate Wells in Northern Siberia With Multiphase Flowmeters. SPE Paper 110873 presented at SPE Annual Technical Conference and Exhibition, Anaheim, California, 11-14 November. DOI: 10.2118/110873-MS.
- Zhang, H.R. and Wheaton, R.J. 2000. Condensate Banking Dynamics in Gas Condensate Fields: Changes in Produced Condensate to Gas Ratios. SPE Paper 64662 presented at International Oil and Gas Conference and Exhibition in China, Beijing, China, 7-10 November. DOI: 10.2118/64662-MS.
- Zuo, J.Y., Zhang, D., Dubost, F., Dong, C., Mullins, O.C., O'Keefe, M. and Betancourt, S.S. 2008. EOS Based Downhole Fluid Characterization. Paper SPE 114702 presented at SPE Asia Pacific Oil and Gas Conference and Exhibition, Perth, Australia, 20-22 October. DOI: 10.2118/114702-MS.

Oilfield Units Conversion Factors

bars · 14.5	= psi
metres · 3.281	= ft
litres · 0.035315	= cf
m ³ · 35.315	= cf

Appendix A: Literature Review

Table A- 1: Key Milestones Related to this Study

SPE Paper n°	Year	Title	Authors	Contribution
716	1965	Integration of Partial Differential Equation for Transient Radial Flow of Gas Condensate Fluid in Porous Structures	C. K. Eilerts, E. F. Summer, N. L. Potts	First to numerically solve the second-order, non-linear, partial equation representing the transient radial flow of gas condensate fluid in reservoirs
962	1965	Two-Phase Flow of Volatile Hydrocarbons	V. J. Kniazeff, S. A. Naville	First to numerically model radial gas-condensate well deliverability Confirm that condensate blockage reduced well deliverability
1495	1966	Successfully Cycling in a Low-Permeability, High-Yield Gas-Condensate Reservoir	H. G. O'Dell, R. N. Miller	First gas rate equation using pseudopressure function to describe the effect of condensate blockage
2033	1968	The Compositional Reservoir Simulator: Case 1 – The Linear Model	I. F. Roebuck, G. E. Henderson, J. Douglas, W. T. Ford	First to develop compositional models to study gas condensate Linear model forms the basis for radial and 3D Cartesian models developed later
26183	1993	Correlation for Determining Gas Condensate Composition	G. E. Niemtschik, F. H. Poettmann, R. S. Thompson	First to suggest a procedure for estimating the changes in reservoir gas composition as reservoir pressure declines below the dew point pressure of the reservoir gas
DOE/B C/1465 9-7	1994	Characterization of Non-Darcy Multiphase Flow in Petroleum Bearing Formation	R. D. Evans, F. Civan	First to develop a non-Darcy flow model that could be used in reservoir simulation and give reasonably accurate results
29561	1995	The effects of retrograde liquid condensation on single well productivity determined via direct (compositional) modelling of a hydraulic fracture in a low-permeability reservoir	M. R. Carlson, J. W. G. Myer	First to investigate gas condensate flow around hydraulically fractured wells in gas condensate reservoirs
30714	1996	Modelling Gas Condensate Well Deliverability	O. Fevang, C. H. Whitson	First to model gas condensate wells with having three flow regions First to show that condensate blockage is dictated primarily by the relationship $k_{rg}=f(k_{rg}/k_{ro})$
64662	2000	Condensate Banking Dynamics in Gas Condensate Fields: Changes in Produced Condensate to Gas Ratios	H. R. Zhang, R. J. Wheaton	First to investigate changes of condensate gas ratio with condensate banking dynamics
81499	2003	Numerical Simulation of Non-Darcy Flow Utilising the New Forchheimer's Diffusivity Equation	H. A. Belhaj, K. R. Agha, A. M. Nouri, S. D. Butt, H. F. Vaziri, M. R. Islam	Introduce an alternative diffusivity equation derived from Forchheimer's equation; equation numerically modelled and validated Suggest a new dimensionless group term to verify the onset of non-Darcy behaviour
112977	2007	Tools to Manage Gas/Condensate Reservoirs, Novel Fluid Property Correlations on the Basis on Commonly Available Field Data	A. P. Ovaile, C. P. Lenn, W. D. McCain Jr	First to develop a surface-yield correlation as function of readily available field data (selected reservoir pressure, initial stock-tank oil gravity, specific gravity of the original reservoir gas and reservoir temperature)

114702	2008	EOS-Based Downhole Fluid Characterisation	J. Y. Zuo, D. Zhang, F. Dubost, C. Dong, O. C. Mullins, M. O'Keefe, S. S. Betancourt	First to suggest establishing an EOS model to predict fluid phase behaviour and physical properties on the basis of DFA data as an input
117930	2008	Gas Condensate Pseudopressure in Layered Reservoirs	K. Singh, C. H. Whitson	Confirm that the gas condensate pseudopressure method as proposed by Fevang and Whitson is valid and accurate for layered systems with significant heterogeneity
122611	2012	Non-Darcy Porous-Media Flow According to the Barree and Conway Model: Laboratory and Numerical-Modelling Studies	B. Lai, J. L. Miskimins, Y. Wu	Show that the Barree and Conway (2004) flow model matches the entire range of low to high flow rates, whereas the conventional Forchheimer model may not be sufficient to describe the observed high-flow-rate behaviour

SPE 114702 (2008)

EOS-Based Downhole Fluid Characterisation

Authors: Julian Y. Zuo, Dan Zhang, Francois Dubost, Chengli Dong, Oliver C. Mullins, Michael O'Keefe, Soraya S. Betancourt

Contribution to the understanding of gas condensate reservoirs:

A new method that can help understand dynamics of gas condensate reservoirs.

Objective of the paper:

Describe processing of DFA data and establish an EOS model to predict fluid phase behaviour and physical properties using DFA data as an input.

Methodology used:

Measurements of DFA data are delumped and characterised into full-length compositional data. Based on delumped and characterised compositions, an EOS model is established.

Conclusion reached:

Full-length compositional data predicted by the proposed method was compared with laboratory-measured data and a good agreement has been found.

The EOS model established can be applied to predict fluid phase behaviour and physical properties using DFA data as an input.

Therefore the EOS approach can be used to interpret DFA data and perform QA/QC on DFA data.

Comments:

Depends on reliable and accurate DFA measurements.

Key for this study: describes potential technology to be used for real-time fluid analysis.

SPE 115726 (2008)

Gas Condensate Relative Permeabilities in Propped Fracture Porous Media: Coupling vs. Inertia

Authors: M. Jamiolahmady, M. Sohrabi, Shaun Ireland

Contribution to the understanding of gas condensate reservoirs:

None as it applied and improved existing method for prediction of productivity of hydraulically fractured wells and gas condensate reservoir performance.

Objective of the paper:

Analyse a series of steady-state gas condensate relative permeability values for a proppant filled and a sand packed fracture.

Methodology used:

Gas condensate relative permeability values for proppant filled and a sand packed fracture have been measured experimentally. Results used to demonstrate interaction of capillary, viscous and inertial forces within these highly conductive media. A previously proposed correlation was used to predict relative permeability curves at different interfacial tensions and velocities and compared to corresponding measured values.

Conclusion reached:

Results indicate that inertia is quite dominant at all the tested conditions albeit at lower IFT and higher gas fractional flow rates.

The unique contribution of inertial forces, as observed in the experiments and predicted by the generalised k_r correlation, is mainly attributed to the impact of the fracture properties and the fluid flowing in the fractures.

Results obtained can be used for an improved production of productivity of hydraulically fractured wells and gas condensate reservoir performance.

Comments:

The correlation used to predict relative permeability curves is considered to be widely applicable as it was based on data very different from that for the fracture properties considered, and yet the values obtained matched closely.

SPE 56476 (1999)

Gas Condensate Relative Permeability for Well Calculations

Authors: Curtis H. Whitson, Oivind Fevang, Aud Saevareid

Contribution to the understanding of gas condensate reservoirs:

None, as the focus is on suggesting a better way of describing the near-well flow in gas condensate wells for simulation purposes.

Objective of the paper:

Present engineering approach to treating gas-oil relative permeabilities describing near-well flow in gas condensate wells.

Methodology used:

Special steady-state experimental procedures have been developed to measure k_{rg} as a function k_{rg}/k_{ro} and N_c .

Saturations are not necessary.

Particular attention has been paid to the effect of hysteresis on the $k_{rg}=f(k_{rg}/k_{ro})$ relation.

Fitting steady-state gas condensate relative permeability data and modelling relative permeability curves.

Generalised relative permeability model applied by using a transition function dependent on the capillary number to link the “immiscible” and “miscible” curves.

Conclusion reached:

The approach provided allows incorporating the improvements in k_{rg} at high capillary numbers and the detrimental effect of inertial high velocity flow as part of the two-phase condensate pseudopressure model.

Comments:

Assumes that far-removed areas of condensate accumulation with a reduced gas relative permeability have a negligible effect.

SPE 81037 (2003)

Numerical and Experimental Modelling of Non-Darcy Flow in Porous Media

Authors: H. A. Belhaj, K. R. Agha, A. M. Nouri, S. D. Butt, M. R. Islam

Contribution to the understanding of gas condensate reservoirs:

A more accurate model to describe non-Darcy flow.

Objective of the paper:

Develop a numerical simulation of the Forchheimer's diffusivity equation to describe non-Darcy behaviour, select the non-Darcy coefficient (β).

Establish an experimental analogy model to verify the numerical model.

Methodology used:

A new diffusivity equation based on the Forchheimer equation has been derived to simulate non-Darcy flow.

Conclusion reached:

Satisfactory agreement between the experimental results and numerical model predictions.

The numerical model is capable of addressing single-phase flow behaviour.

A new dimensionless number can be used to determine the commencement of non-Darcy flow.

The non-Darcy behaviour is more affected by the fracture contribution to permeability regardless of fracture geometry, orientation and frequency.

Comments:

The proposed model has been designed for single-phase flow in porous media, and in order to be applied to multiphase flow, which is the case for gas condensate reservoir simulation, it requires modification.

SPE 26183 (1993)

Correlation for Determining Gas Condensate Composition

Authors: G. E. Niemtschik, F. H. Poettmann, R. S. Thompson

Contribution to the understanding of gas condensate reservoirs:

Not much, as the focus is on developing a correlation using methods previously suggested by others.

Objective of the paper:

Develop a correlation relating composition of the well stream effluent at any depleted state to the composition of the reservoir fluid at its initial dew point pressure. Thus it will be possible to reproduce the compositional history of the well stream effluent during pressure depletion.

Methodology used:

1. Theoretical approach using the Peng-Robinson EOS
2. Strictly empirical approach

Conclusion reached:

The compositional history of the well stream effluent being produced from a constant volume reservoir as a function of depletion pressure can be calculated from a knowledge of the composition of a retrograde gas condensate at its initial dew point pressure, the initial reservoir pressure, the reservoir temperature and the gas-condensate specific gravity of the reservoir fluid at the initial dew point pressure.

The correlation was found to be consistent with measured data.

Comments:

Requires accurate determination of initial dew point pressure and initial reservoir pressure.

Key milestone.

SPE 29561 (1995)

The Effects of Retrograde Liquid Condensation on Single Well Productivity Determined via Direct (Compositional) Modelling of a Hydraulic Fracture in a Low Permeability Reservoir

Authors: M. R. Carlson, J. W. G. Myer

Contribution to the understanding of gas condensate reservoirs:

A better understanding of how condensate banking impairs flow in the case of a hydraulically fractured well.

Objective of the paper:

Perform sensitivity analysis for well test interpretation and to predict long term performance.

Methodology used:

Single well model, which included a hydraulic fracture as part of the grid system.

Conclusion reached:

Radial modelling confirmed the results obtained by Fussell [liquid condensing in the reservoir will result in a substantial productivity impairment].

However productivity of fractured wells was not impaired to the degree expected.

Simulation technique allows for direct modelling of a hydraulic fracture instead of using an equivalent well bore radius.

A hydraulic fracture treatment reduces the amount of drawdown in the well and results in a less concentrated condensate precipitation; significant impairment does not occur during the first ten years of production.

Modelling the effects of a hydraulic fracture require that the fracture be included in the grid.

Comments:

Radial flow into the wellbore was assumed.

The work did not cover cases with a full range of liquid dropout levels, i.e. high liquid drop out was not considered.

Key milestone.

SPE 30714 (1996)

Modelling Gas-Condensate Well Deliverability

Authors: O. Fevang, C. H. Whitson

Contribution to the understanding of gas condensate reservoirs:

Considering gas condensate wells producing with BHFP lower than the dew point pressure as having up to three flow regions:

1. An inner near-wellbore region where both gas and oil flow simultaneously (at different velocities)
2. A region of condensate buildup where only gas is flowing
3. A region containing single-phase (original) reservoir gas

Objective of the paper:

Provide method to model the deliverability of gas-condensate wells.

Provide a simple method for calculating BHFP in coarse-grid models.

Methodology used:

Modified form of the Evinger-Muskat pseudopressure to make it applicable for gas-condensate systems.

Consider the gas-condensate well undergoing depletion as consisting of three regions.

Conclusion reached:

Gas-condensate wells producing with BHFP lower than the dew point have up to three flow regions. Most of the deliverability loss is caused by reduced gas permeability in Region 1 (both gas and oil flow simultaneously, constant flowing composition (GOR)).

Multiphase pseudopressure is calculated from producing GOR (composition) and PVT properties.

The primary relative permeability relationship affecting condensate blockage is $k_{rg}=f(k_{rg}/k_{ro})$.

Critical oil saturation has no direct effect on gas-condensate well deliverability.

Comments:

Method relies heavily on knowing the producing GOR accurately.

Key milestone.

SPE 64662 (2000)

Condensate Banking Dynamics in Gas Condensate Fields: Changes in Produced Condensate to Gas Ratios

Authors: H. R. Zhang, R. J. Wheaton

Contribution to the understanding of gas condensate reservoirs:

A better understanding of condensate banking behaviour and well deliverability impairment. Determines dynamics of produced CGR with reservoir depletion.

Objective of the paper:

Conduct a general theoretical study on the CGR behaviour in the processes of condensate banking.

Methodology used:

Theoretical treatment confirmed and supplemented by numerical simulations. Numerical well test results interpreted with the developed analytical model.

Conclusion reached:

For homogenous reservoirs, the produced CGR continuously decreases with time during depletion. For a well producing at constant BHFP, a pseudosteady state may be reached at some stage of condensate banking. No real "steady state" situation exists with regard to either composition or CGR. In heterogeneous reservoirs, the produced CGR may increase with time and is even greater than the initial reservoir CGR at some point.

Comments:

Once a well has been produced with flowing bottomhole pressure below dew point pressure it is no longer possible to accurately determine the initial CGR by the means of well testing.

Key milestone for this study.

SPE 81499 (2003)

Numerical Simulation of Non-Darcy Flow Utilizing the New Forchheimer's Diffusivity Equation

Authors: H. A. Belhaj, K. R. Agha, A. M. Nouri, S. D. Butt, H. F. Vaziri, M. R. Islam

Contribution to the understanding of gas condensate reservoirs:

An alternative diffusivity equation to replace the one derived from Darcy's law. The new equation was derived from the Forchheimer's equation. Non-Darcy flow is an important factor to take into account when considering gas condensate reservoirs.

Objective of the paper:

Obtain numerical model based on a diffusivity equation derived from Forchheimer's equation.

Methodology used:

Partial derivatives representing non-Darcy flow have been transferred into finite differences and modelled numerically using Crank-Nicolson and Barakat-Clark methods. The former was adopted for further parametric analysis.

Conclusion reached:

New two dimensional numerical simulation model based on the diffusivity equation derived from Forchheimer's equation may describe both Darcian and non-Darcian behaviours.
New dimensionless group term to verify the non-Darcy behaviour.

Comments:

Radial flow to the wellbore has been assumed.
Key milestone for this study.

SPE 112977 (2007)

Tools to Manage Gas/Condensate Reservoirs; Novel Fluid-Property Correlations on the Basis of Commonly Available Field Data

Authors: A. P. Ovalle, C. P. Lenn, W. D. McCain

Contribution to the understanding of gas condensate reservoirs:

Not much, focus on aiding management of gas/condensate reservoirs or prediction of condensate reservoirs by using correlations to estimate values of relevant properties before laboratory data becomes available.

Objective of the paper:

Develop correlation equations for gas condensate based on readily available field data.

Methodology used:

A nonparametric approach for estimating optimal transformations of petrophysical data was used to obtain the maximum correlation between observed variables.

Conclusion reached:

Correlations to be used to predict dew point pressures, decreases in surface condensate yields after reservoir pressure has decreased below dew point pressure, and decrease in reservoir-gas specific gravity at reservoir pressures below dew point pressure.

Comments:

Depends on sufficient accuracy of measured values.

Requires knowledge of current reservoir pressure.

Key milestone for this study.

SPE 117930 (2008)

Gas Condensate Pseudopressure in Layered Reservoirs

Authors: K. Singh, C. H. Whitson

Contribution to the understanding of gas condensate reservoirs:

Verifies for the first time that the gas condensate pseudopressure method as proposed by Fevang and Whitson is valid and accurate for layered systems with significant heterogeneity, with and without crossflow, with and without capillary number modification of relative permeabilities, and for widely-ranging fluid compositions in each layer.

Objective of the paper:

Verify previously suggested pseudopressure method for layered gas condensate reservoirs by Fevang and Whitson.

Methodology used:

A compositional reservoir simulator. 3D multi-layer, fine-grid models and equivalent coarse grid models. Depletion and gas injection simulated for a wide range of reservoir fluids.

Conclusion reached:

The gas condensate pseudopressure method as proposed by Fevang and Whitson is valid and accurate for layered systems with significant heterogeneity.

Effect of condensate blockage is most prominent for low-kh reservoirs.

Effect of condensate blockage is greater at higher production rates.

Effect of condensate blockage is smaller with velocity dependent relative permeability.

Comments:

Accuracy is dependent of well grid size.

Coarse grid models without pseudopressure well treatment give optimistic reservoir performance whereas fine grid models capture correctly well treatment and blockage.

Key milestone.

SPE 122611 (2012)

Non-Darcy Porous-Media Flow According to the Barree and Conway Model: Laboratory and Numerical-Modelling Studies

Authors: B. Lai, J. L. Miskimins, Y. Wu

Contribution to the understanding of gas condensate reservoirs:

Shows that the Barree and Conway flow model is a better representation of non-Darcy flow. Non-Darcy flow is an important factor to consider when modelling gas condensate reservoirs.

Objective of the paper:

Present experimental data of high flow rates through proppant packs.

Develop mathematical modelling tools to quantify such high-flow-velocity, non-Darcy-flow behaviour.

Methodology used:

Analytical and numerical approaches for simulating single-phase non-Darcy flow with the Barree and Conway model.

Numerical model is used to perform parameter-sensitivity analysis and to obtain insight into transient non-Darcy flow with the Barree and Conway flow model.

Conclusion reached:

Barree and Conway model is able to describe the entire range of flow velocities from low to high flow rates under tests, while the Forchheimer model fails to cover the high end of flowrates.

Comments:

Key milestone.

SPE 962 (1965)

Two-Phase Flow of Volatile Hydrocarbons

Authors: V. J. Kniazeff, S. A. Nvaille

Contribution to the understanding of gas condensate reservoirs:

Solving problem of unsteady-state gas condensate flow through porous media.

Objective of the paper:

Solve the above mentioned problem on a computer and compare with field data to validate approach.

Methodology used:

Second order non-linear partial differential equations numerically solved for the case of radial two-phase flow around a well.

Conclusion reached:

Transient two-phase flow problem can be solved numerically. Applicable to both volatile oil and gas condensate. Non-Darcy flow needs to be considered and has been taken into account by using a quadratic relationship between the gas phase velocity and the pressure gradient.

Computational costs considered moderate.

Comments:

Assumes radial flow to the wellbore.

Key milestone.

SPE 95941 (2005)

Pseudosteady-State Analysis of Finite-Conductivity Vertical Fractures

Authors: B.R. Meyer, R.H Jacot

Contribution to the understanding of gas condensate reservoirs:

A new solution for pseudosteady-state behaviour of a well with a finite conductivity vertical fracture is proposed. Can be applied for hydraulic fractures often used to enhance gas condensate production.

Objective of the paper:

Present a mathematical model and analytical solution for predicting the pseudosteady-state performance of finite-conductivity vertical fractures and damaged fractures in close-rectangular drainage areas.

Methodology used:

Governing pseudosteady-state equation in terms of dimensionless productivity and pseudo-skin relationships is used.

Two-region, fracture and formation, domain resistivity concept is introduced.

Inverse productivity index for finite and variable-conductivity vertical fractures in rectangular closed formations are developed.

Conclusion reached:

Analytical results have demonstrated the application of the model for a wide range of formation aspect ratios and variable fracture conductivities in closed rectangular systems.

Model can accurately determine the productivity index, pseudo-skin function and an effective wellbore radius for non-uniform finite-conductivity vertical fractures in closed rectangular systems.

Good agreement with previous works achieved.

Comments:

Solution is analytical and is easily implemented.

Equations formulated for rectangular reservoirs.

Wellbore flow is included.

Additional testing and validation are required for highly variable fracture conductivities to determine analysis limits.

Paper findings used directly in this study for skin estimation.

Appendix B: Single Well Sector Model

Objective: Provide schematics of single well sector model used in this study.

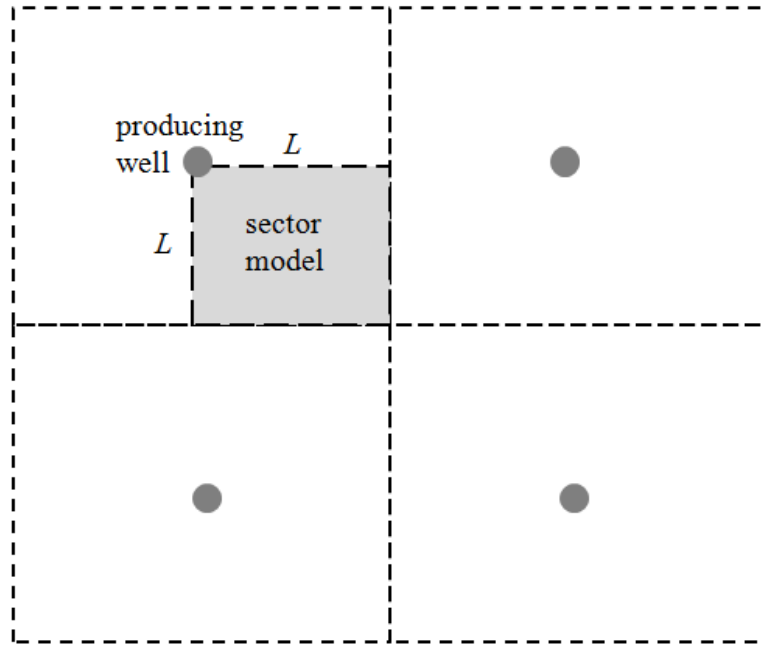


Figure B- 1: Well placement schematic with sector model considered

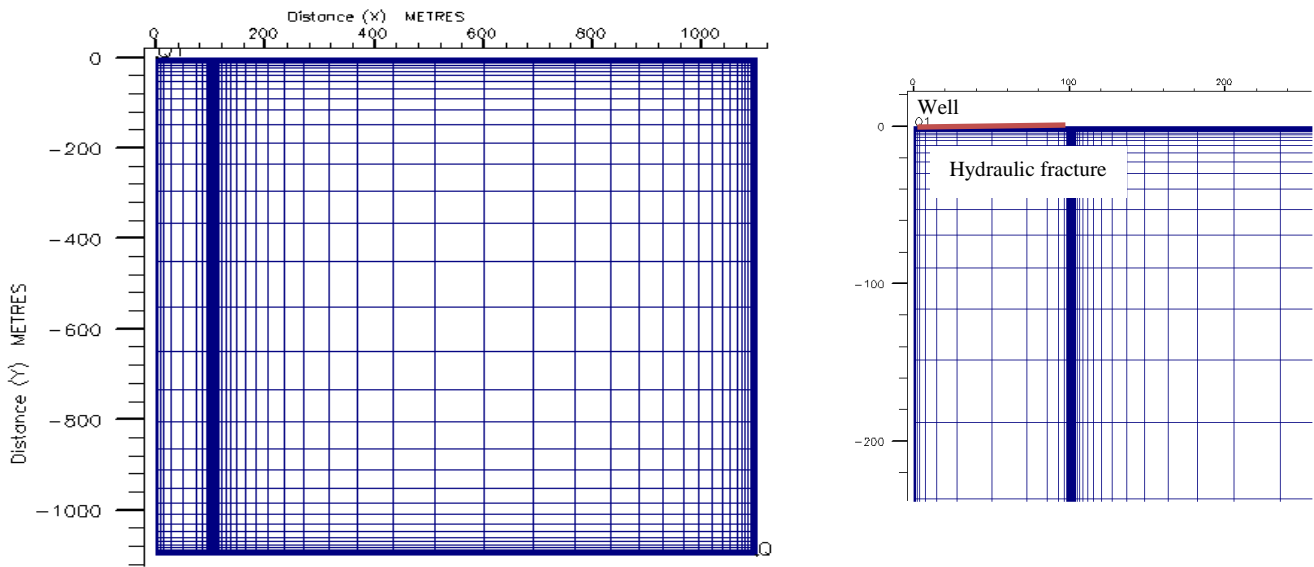


Figure B- 2: Model gridding (left) with zoomed section containing well and hydraulic fracture (right)

Appendix C: Rich Fluid Base Case Analysis

Objective: Demonstrate that low reservoir permeability (1mD) is the cause for significant data scatter for rich fluid base case analysis. If the reservoir permeability is increased (to 40mD) the scatter is significantly reduced due to less pressure variation across the reservoir.

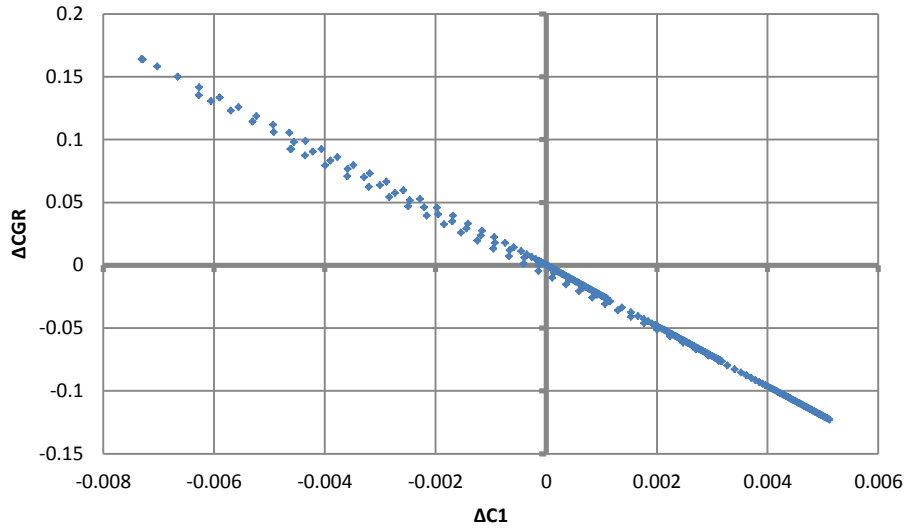


Figure C- 1: Rich fluid ΔCGR variation with changing $\Delta C1$, $k=40mD$

Appendix D: Sensitivity Study Results

Objective: Demonstrate full set of sensitivity study results for all three fluids models. Includes plots of simulation results CGR and that estimated from proposed correlations. RMS Errors are provided on three time intervals as in the Base Case Analysis section.

Rich Fluid

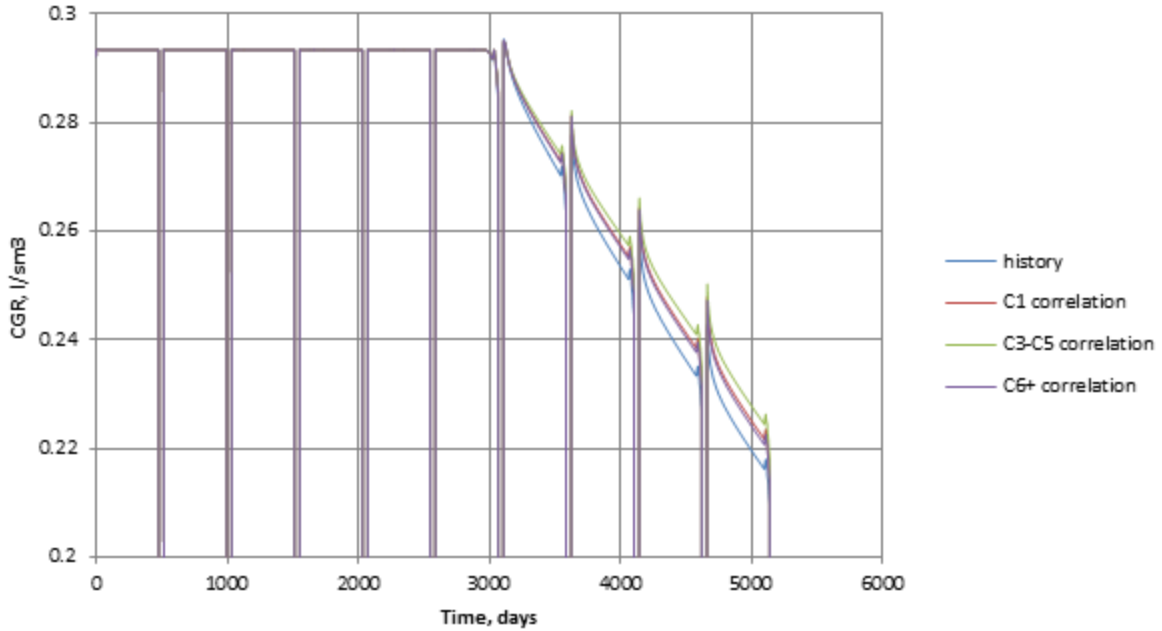


Figure D- 1: Rich fluid sensitivity study, k=0.1mD

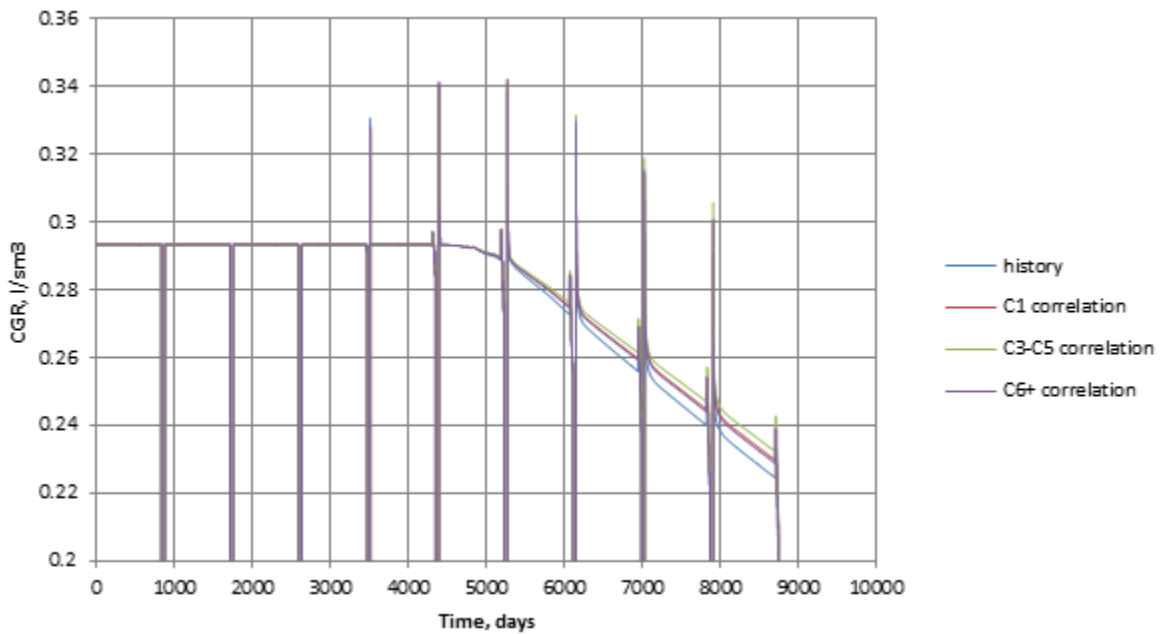


Figure D- 2: Rich fluid sensitivity study, k=10mD

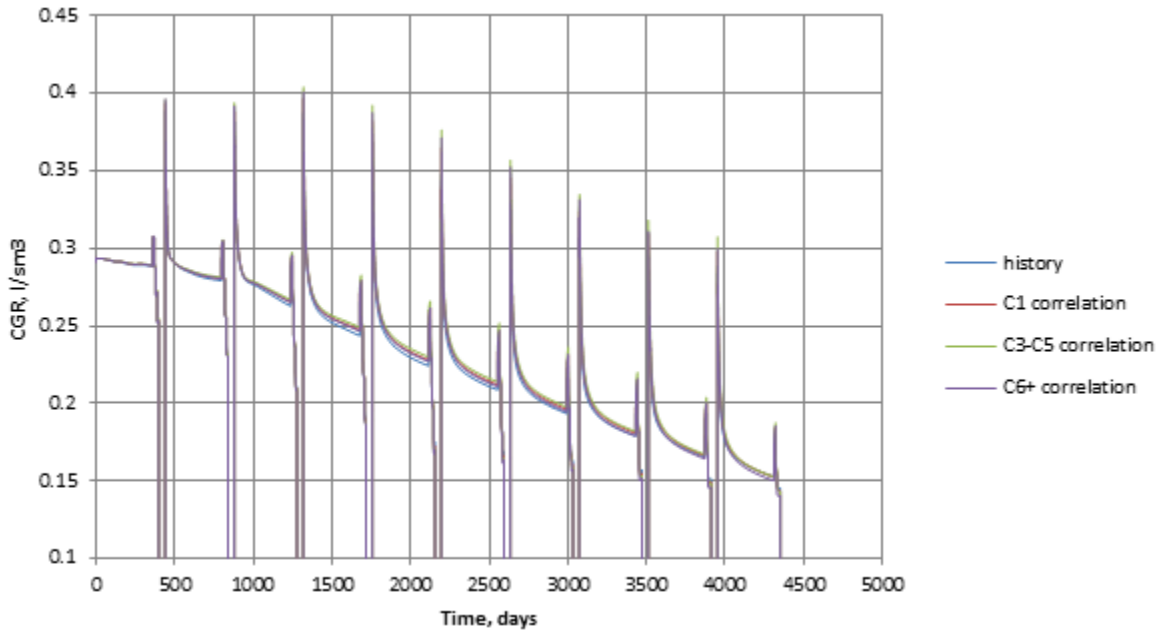


Figure D- 3: Rich fluid sensitivity study, $\Phi=0.15$

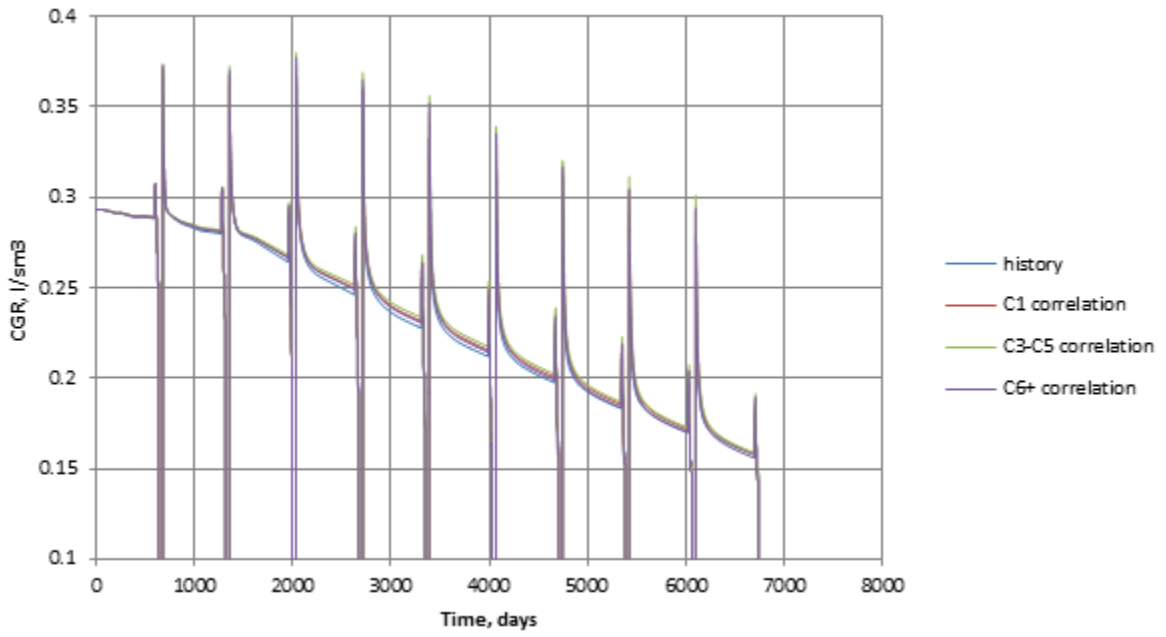


Figure D- 4: Rich fluid sensitivity, $\Phi=0.25$

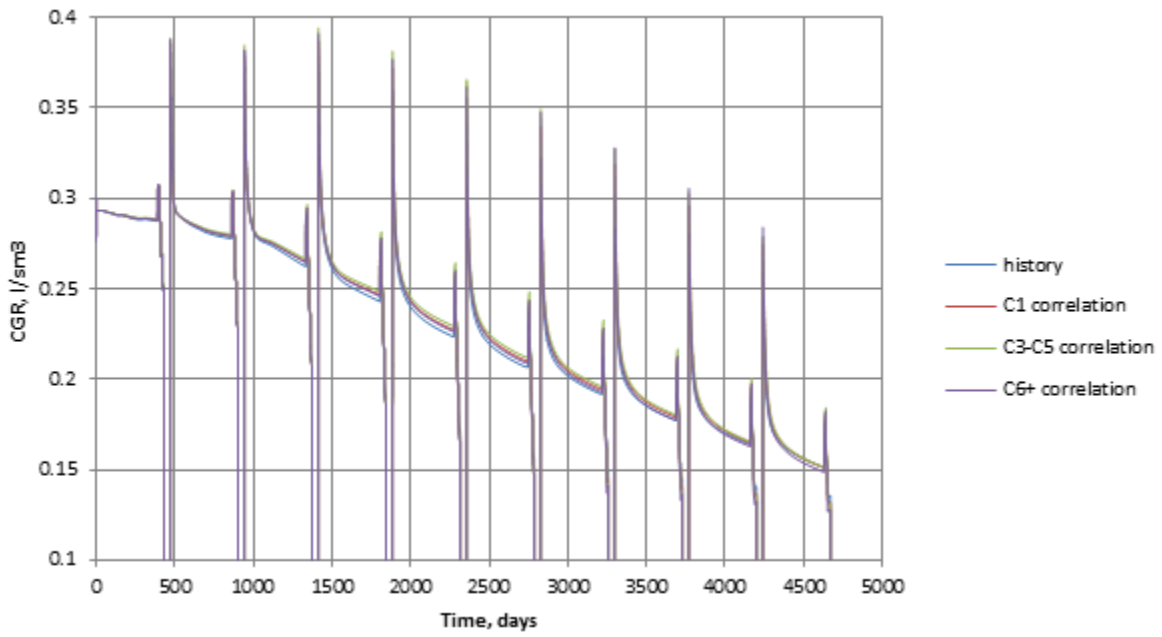


Figure D- 5: Rich fluid sensitivity study, h=10m

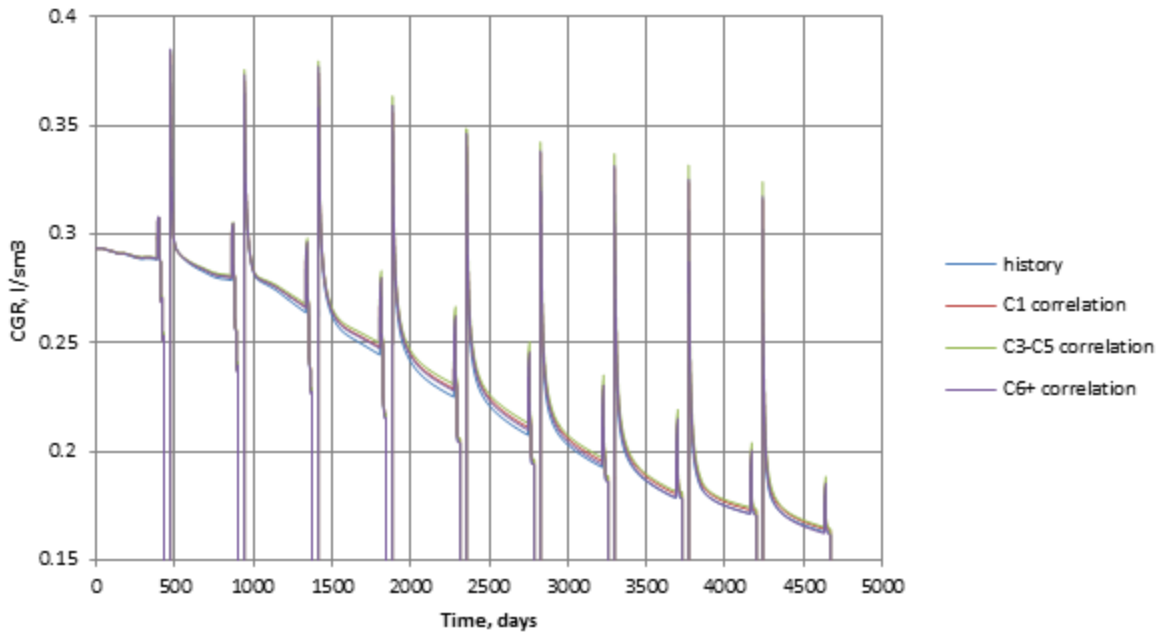


Figure D- 6: Rich fluid sensitivity study, h=100m

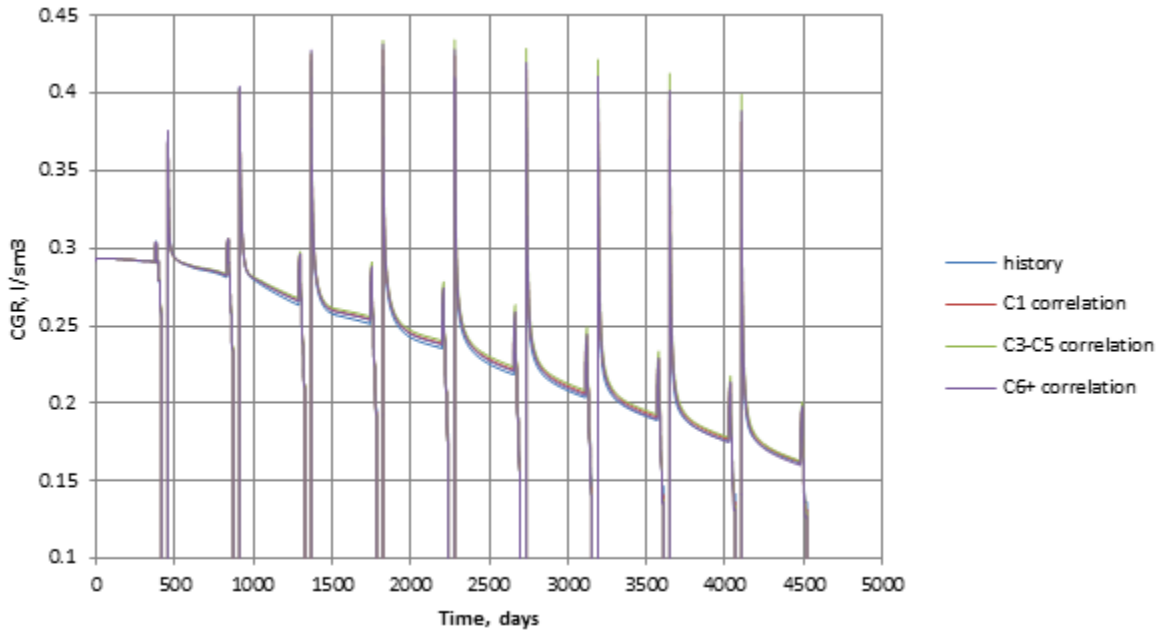


Figure D- 7: Rich fluid sensitivity, $L_r=50m$

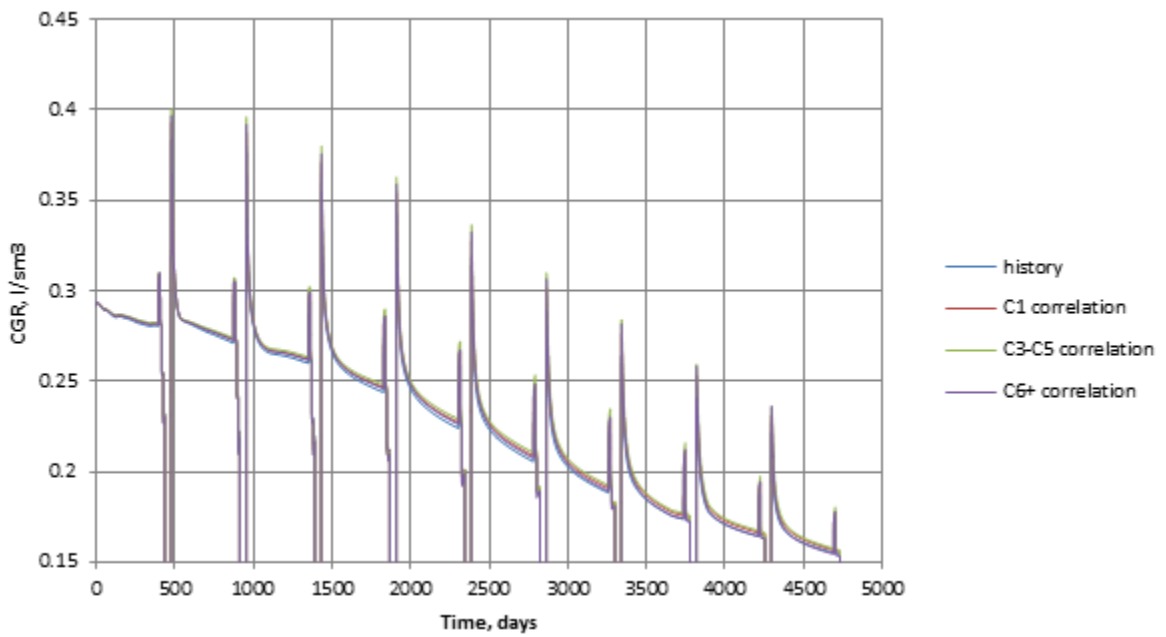


Figure D- 8: Rich fluid sensitivity, $L_r=200m$

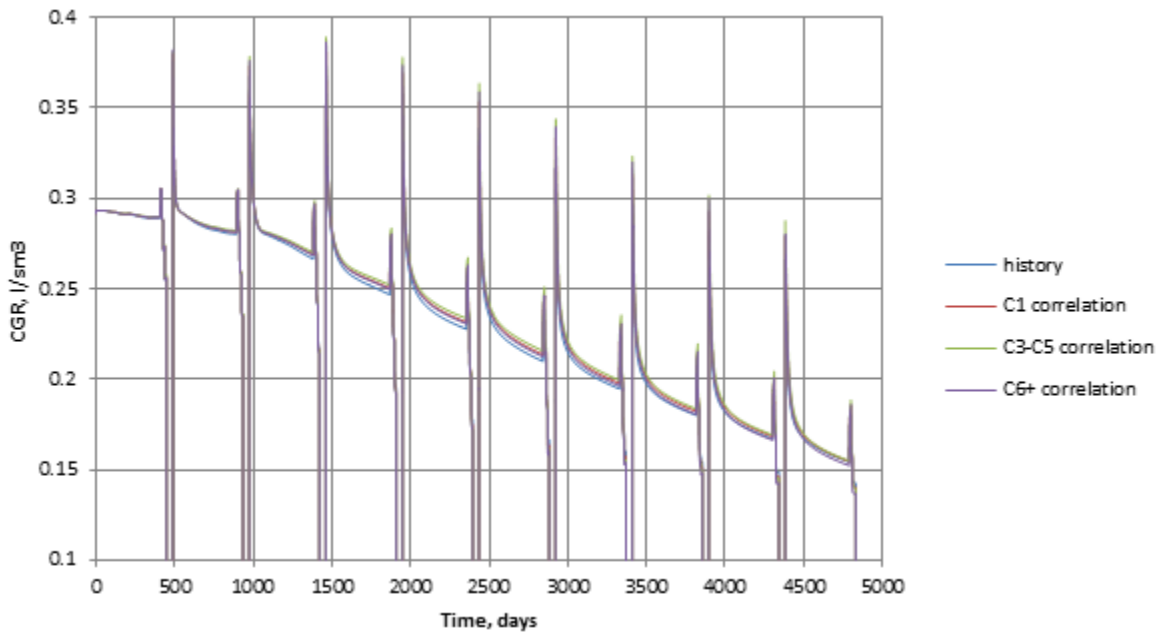


Figure D- 9: Rich fluid sensitivity, $k_r w=500mD\cdot m$

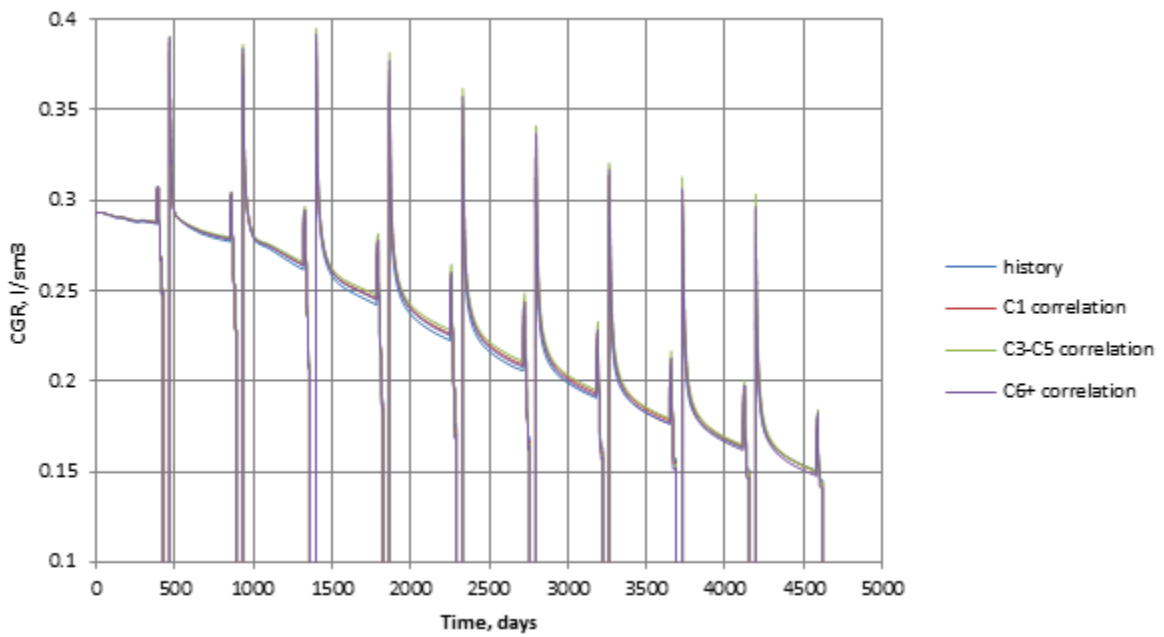


Figure D- 10: Rich fluid sensitivity, $k_r w=1500m$

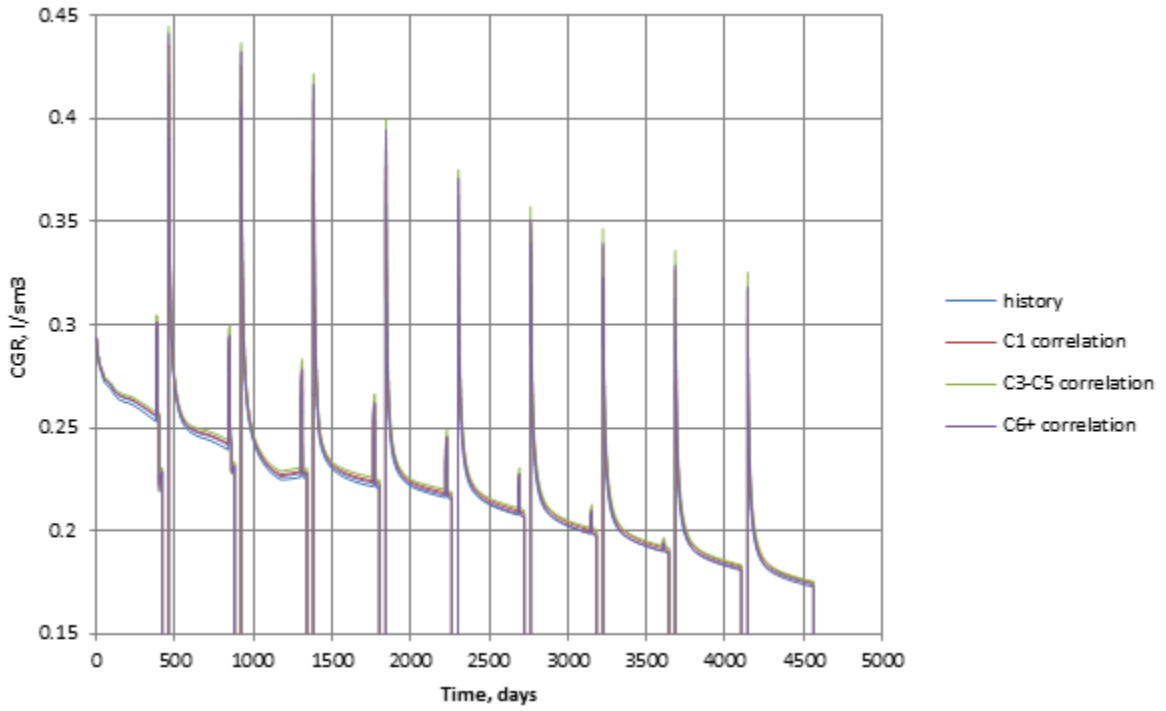


Figure D- 11: Rich fluid sensitivity study, pressure depression factor 0.1

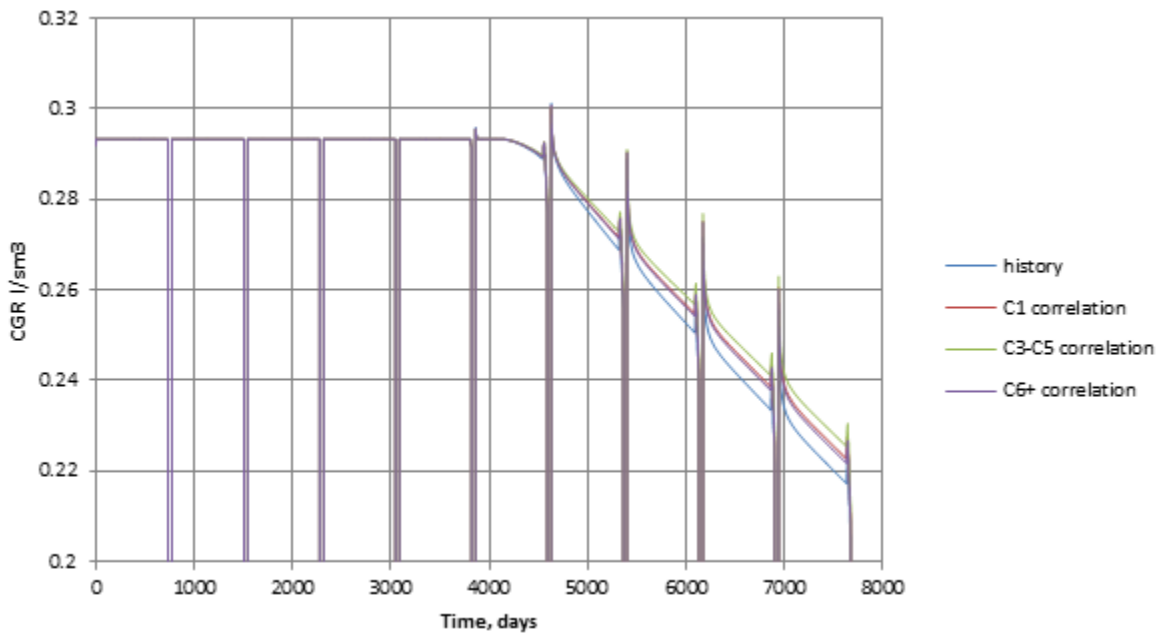


Figure D- 12: Rich fluid sensitivity study, pressure depression factor 0.9

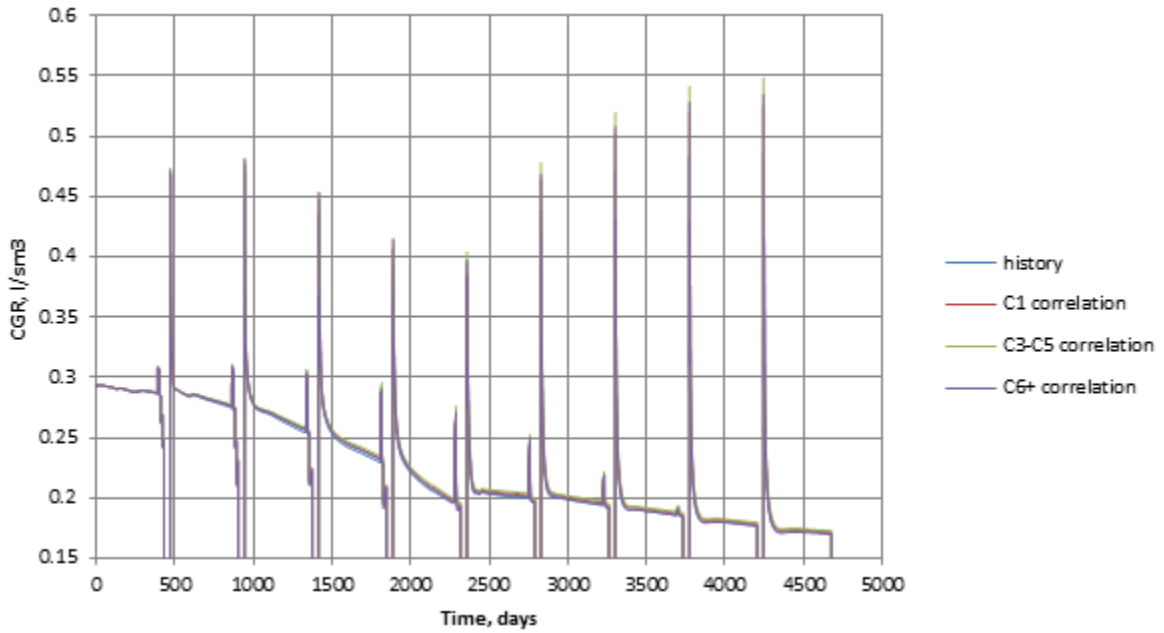


Figure D- 13: Rich fluid sensitivity study, relative permeability

Table D- 1: Rich fluid sensitivity study, RMS Error

Correlation		RMS Error, %								
		C1			C3-C5			C6+		
Time interval		1	2	3	1	2	3	1	2	3
Parameter										
k, mD	0.1	0.00063	0.23	1.8	0.00089	0.34	2.7	0.00050	0.21	1.5
	10	0	0.22	1.6	0	0.32	2.4	0	0.19	1.4
Φ	0.15	0.58	1.7	1.5	0.88	2.6	2.4	0.58	1.5	1.7
	0.25	0.54	1.6	1.4	0.82	2.5	2.3	0.52	1.4	1.5
h, m	10	0.59	1.7	1.6	0.90	2.7	2.5	0.58	1.6	2.1
	100	0.53	1.6	1.5	0.80	2.5	2.4	0.51	1.3	1.2
L _f , m	50	0.56	1.5	1.7	0.84	2.4	2.7	0.52	1.4	2.0
	200	0.69	1.5	1.5	1.1	2.3	2.5	0.74	1.3	1.2
k _{rw} , mD·m	500	0.51	1.7	1.6	0.77	2.6	2.5	0.50	1.5	1.7
	1500	0.58	1.7	1.3	0.92	2.6	2.3	0.60	1.5	1.7
P ^o _{res} , bar	350	1.1	1.3	1.1	1.7	2.0	1.8	0.94	0.95	0.91
	600	0	0.26	1.8	0	0.38	2.7	0	0.23	1.6
Depression factor	0.1	7.2	13	20	6.8	11	15	3.4	4.6	4.6
	0.9	0.20	0.67	1.2	0.30	1.0	1.8	0.19	0.59	0.93
Relative permeability		0.64	1.4	1.2	0.97	2.2	2.0	0.60	1.1	1.0

Lean Fluid

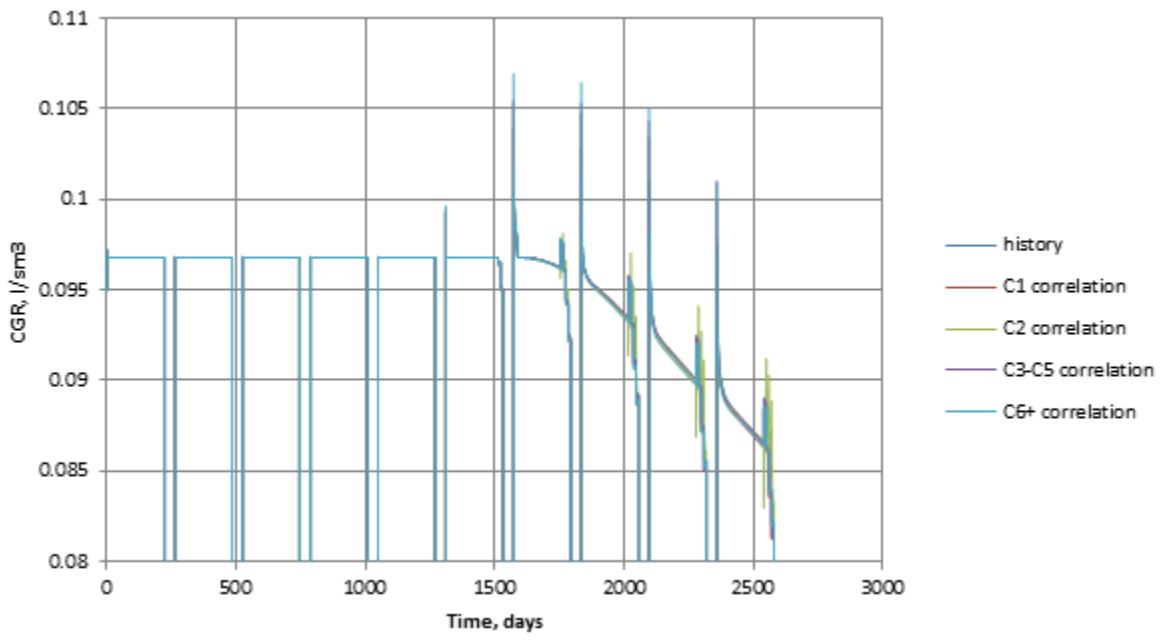


Figure D- 14: Lean fluid sensitivity study, k=10mD

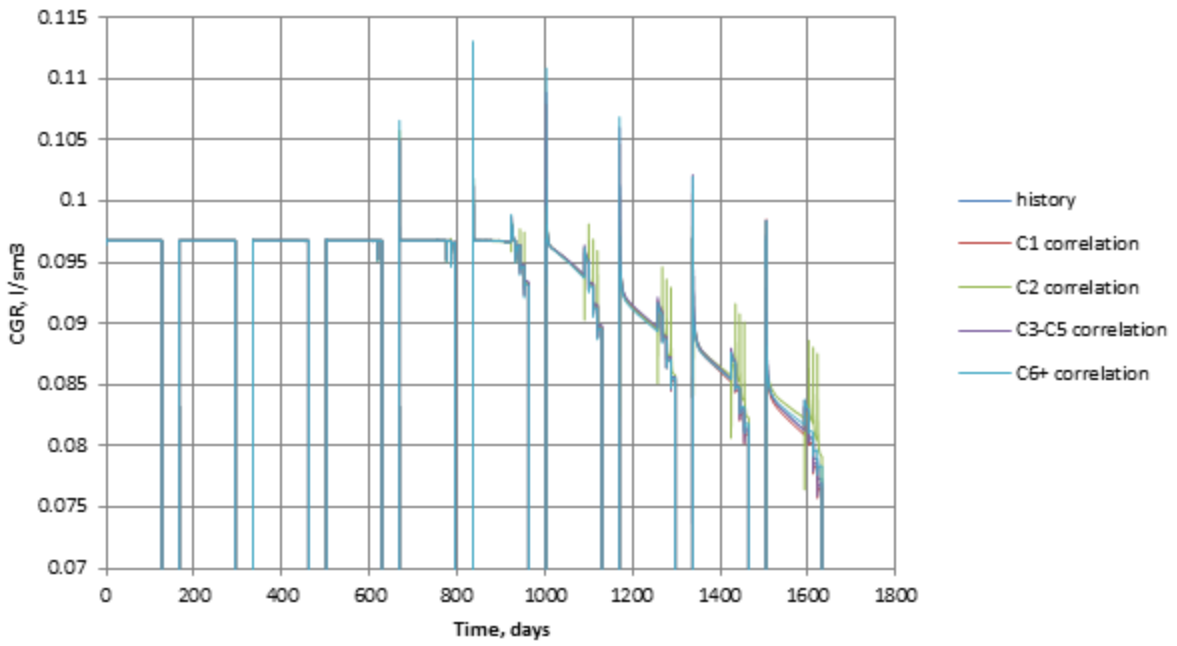


Figure D- 15: Lean fluid sensitivity study, k=70mD

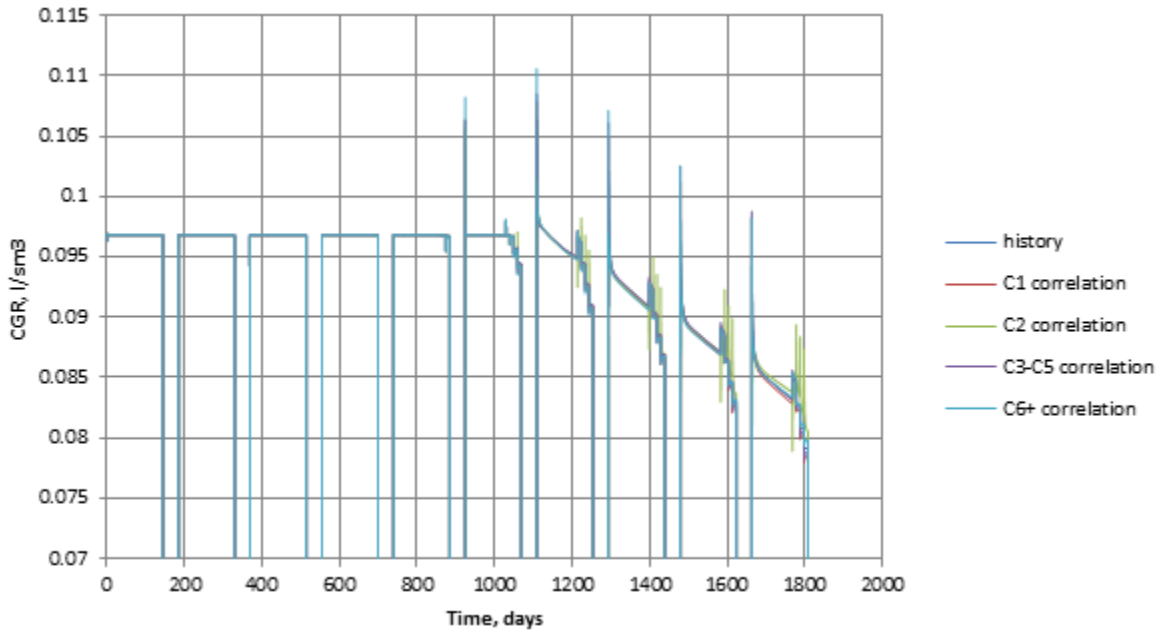


Figure D- 16: Lean fluid sensitivity study, $\Phi=0.15$

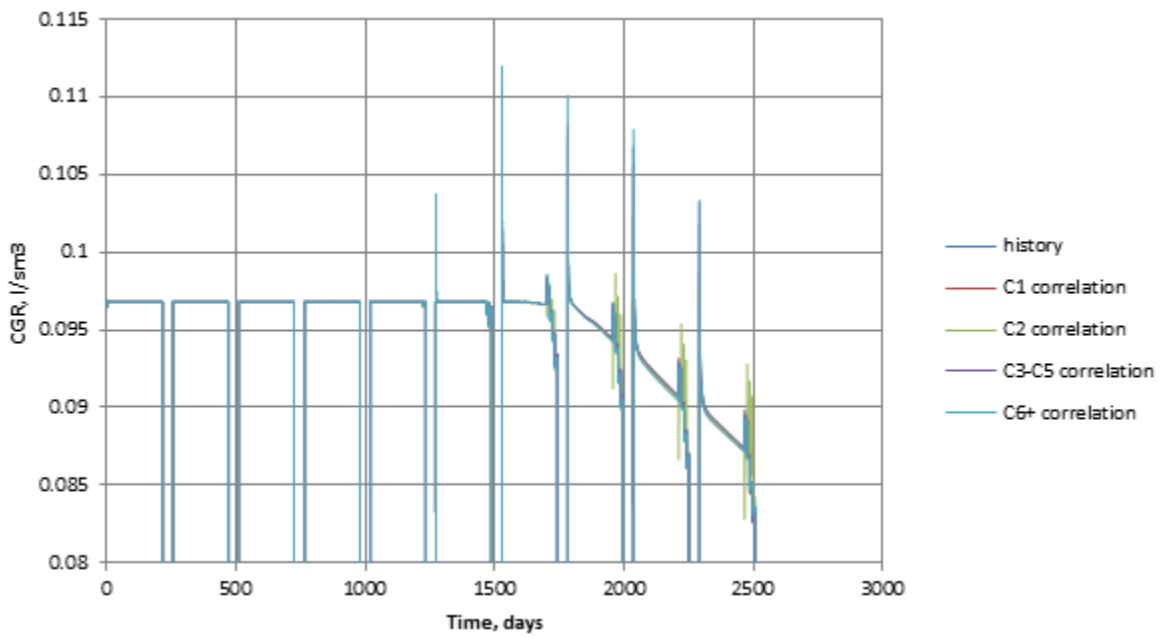


Figure D- 17: Lean fluid sensitivity study, $\Phi=0.25$

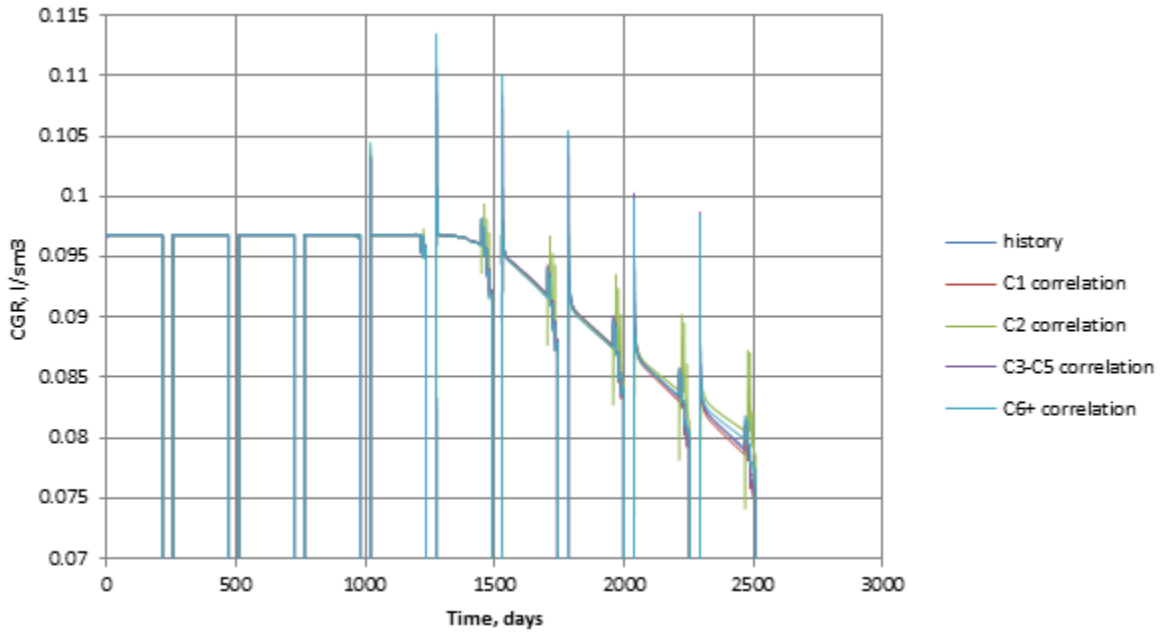


Figure D- 18: Lean fluid sensitivity study, h=40m

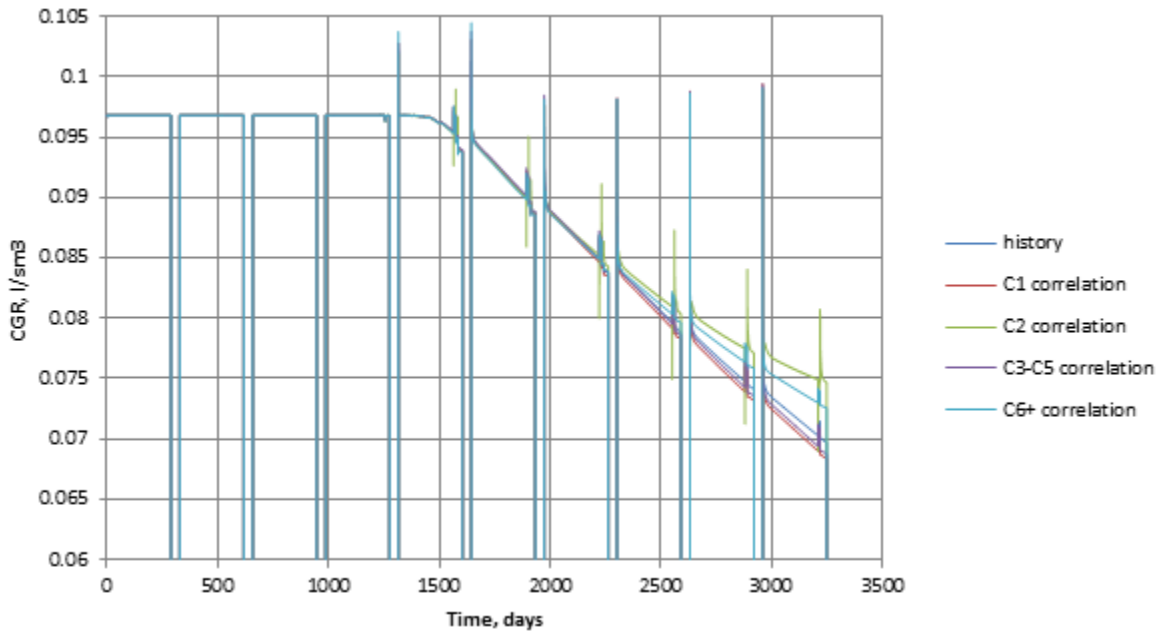


Figure D- 19: Lean fluid sensitivity study, h=60m

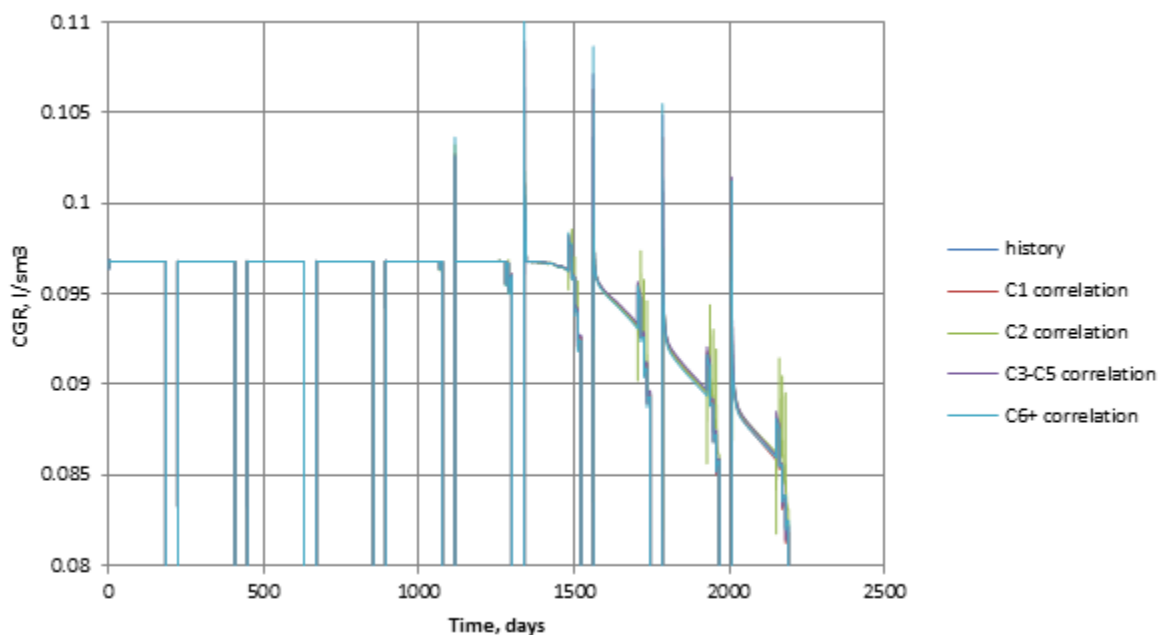


Figure D- 20: Lean fluid sensitivity study, $L_f=50m$

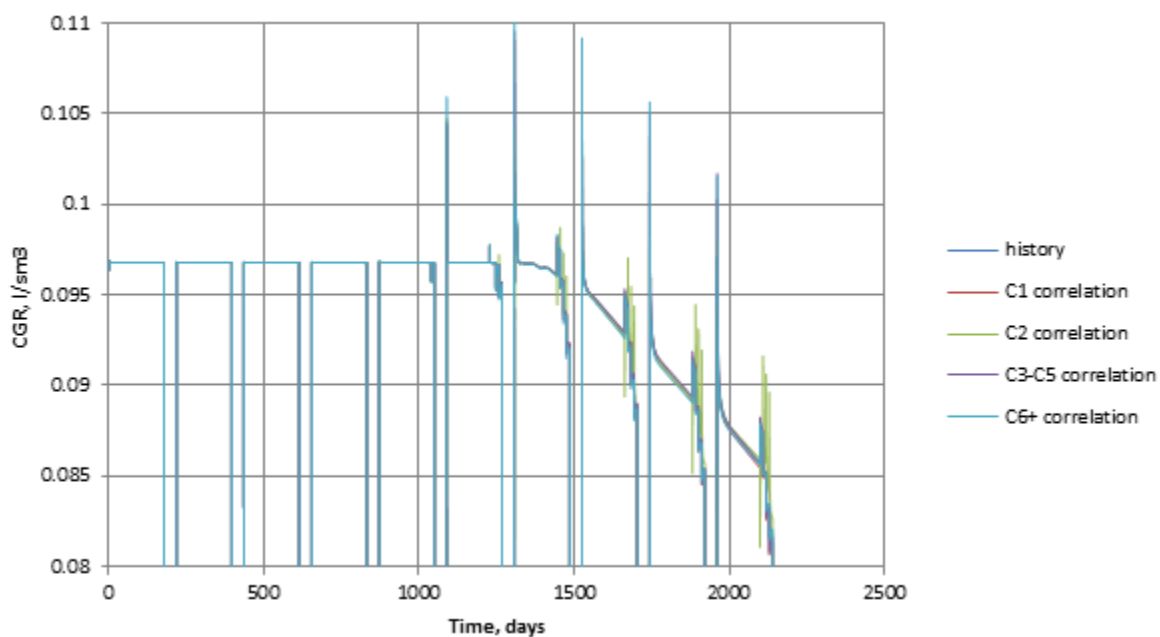


Figure D- 21: Lean fluid sensitivity study, $L_f=200m$

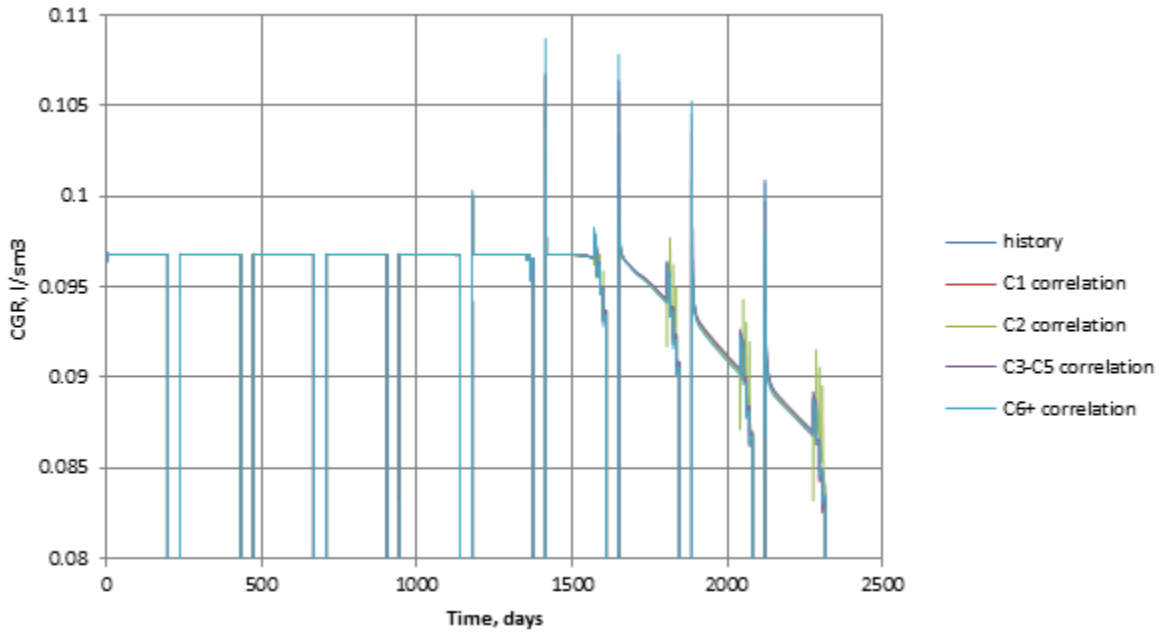


Figure D- 22: Lean fluid sensitivity study, $k_w=500\text{mD-m}$

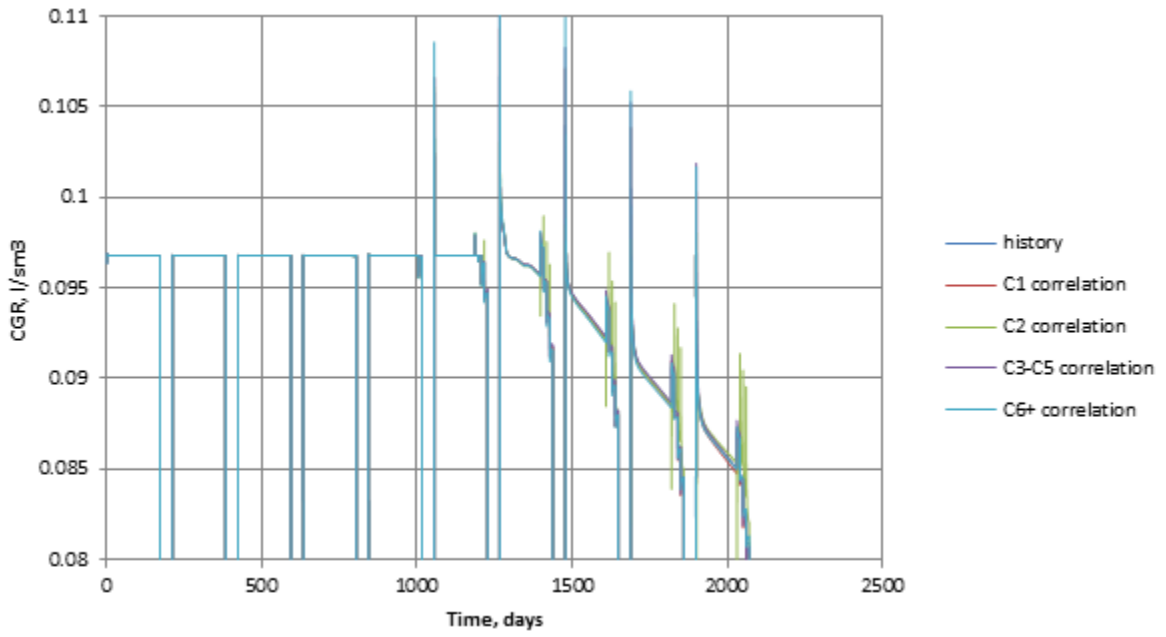


Figure D- 23: Lean fluid sensitivity study, $k_w=1500\text{mD-m}$

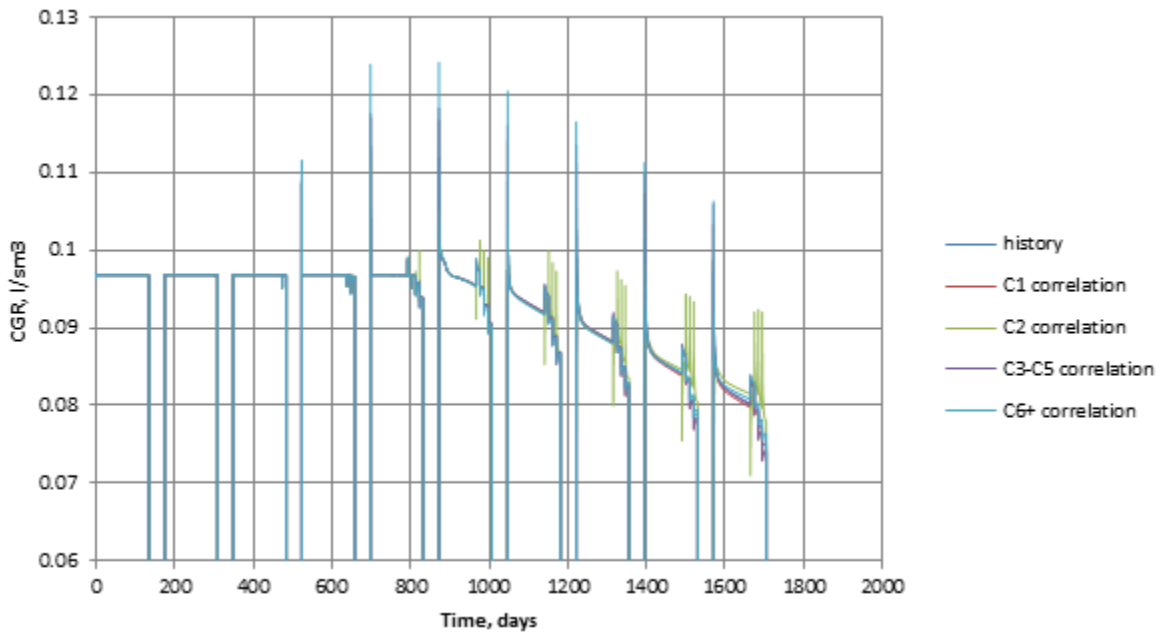


Figure D- 24: Lean fluid sensitivity study, pressure depression factor 0.85

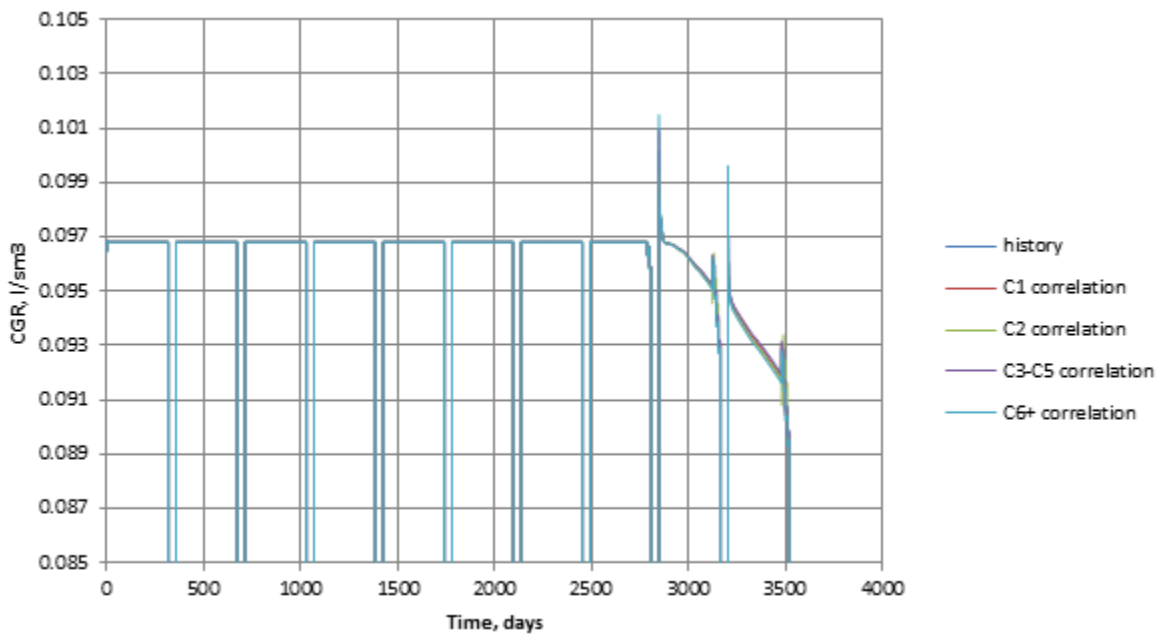


Figure D- 25: Lean fluid sensitivity study, pressure depression factor 0.95

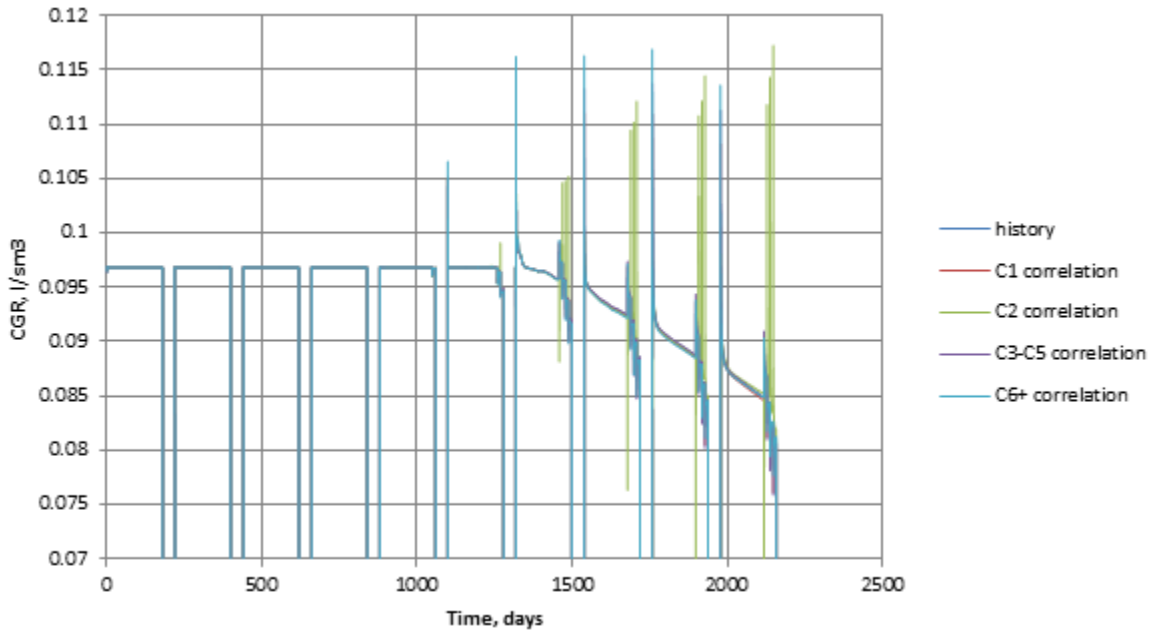


Figure D- 26: Lean fluid sensitivity study, relative permeability

Table D- 2: Lean fluid sensitivity study, RMS Error

Correlation	RMS Error, %												
	C1			C2			C3-C5			C6+			
Time interval	1	2	3	1	2	3	1	2	3	1	2	3	
Parameter													
k, mD	10	0	0	0.092	0	0	0.16	0	0	0.064	0	0	0.14
	70	0	0	0.17	0	0	0.36	0	0	0.068	0	0	0.18
ϕ	0.15	0	0	0.14	0	0	0.25	0	0	0.061	0	0	0.14
	0.25	0	0	0.070	0	0	0.10	0	0	0.052	0	0	0.13
h, m	40	0	0	0.25	0	0	0.58	0	0	0.10	0	0	0.28
	60	0	0	0.72	0	0	2.4	0	0	0.43	0	0	1.4
L _f , m	50	0	0	0.086	0	0	0.12	0	0	0.052	0	0	0.13
	200	0	0	0.095	0	0	0.14	0	0	0.055	0	0	0.13
k _{fw} , mD·m	500	0	0	0.070	0	0	0.094	0	0	0.049	0	0	0.12
	1500	0	0	0.11	0	0	0.17	0	0	0.060	0	0	0.13
P ^o _{res} , bar	275	0.5	0.82	0.63	2.0	6.6	29	0.60	0.95	0.69	0.14	1.4	9.1
	400	0	0	0.18	0	0	0.41	0	0	0.089	0	0	0.18
Depression factor	0.85	0	0	0.24	0	0	0.60	0	0	0.13	0	0	0.24
	0.95	0	0	0.016	0	0	0.065	0	0	0.032	0	0	0.094
Relative permeability	0	0	0	0.11	0	0	0.17	0	0	0.068	0	0	0.13

Extra Rich Fluid

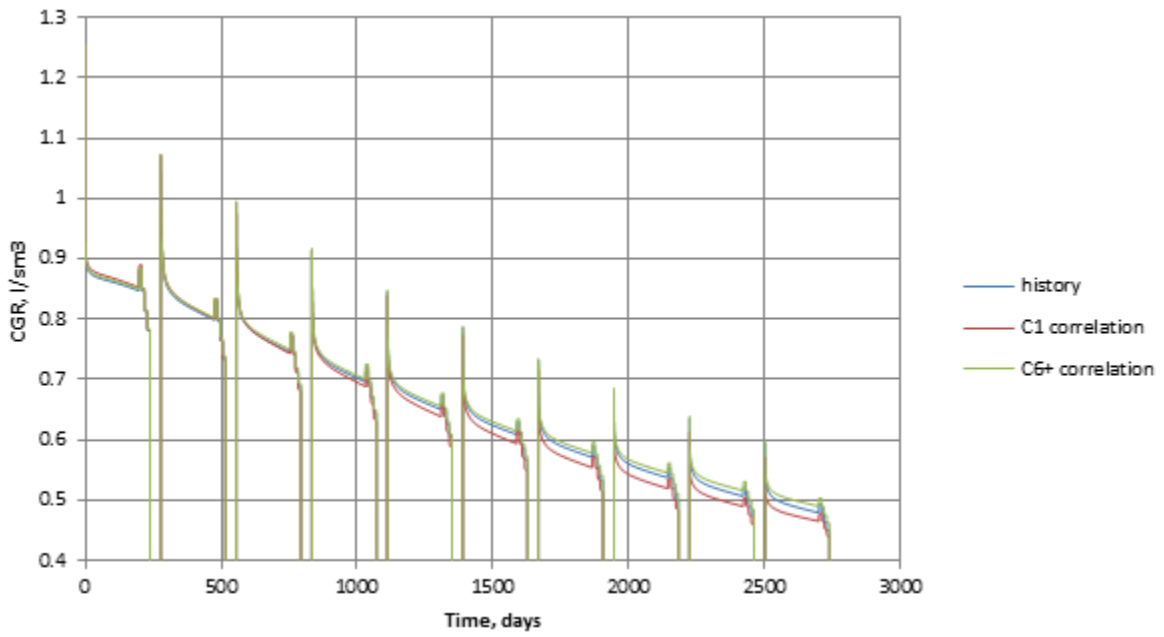


Figure D- 27: Extra rich fluid sensitivity study, k=10mD

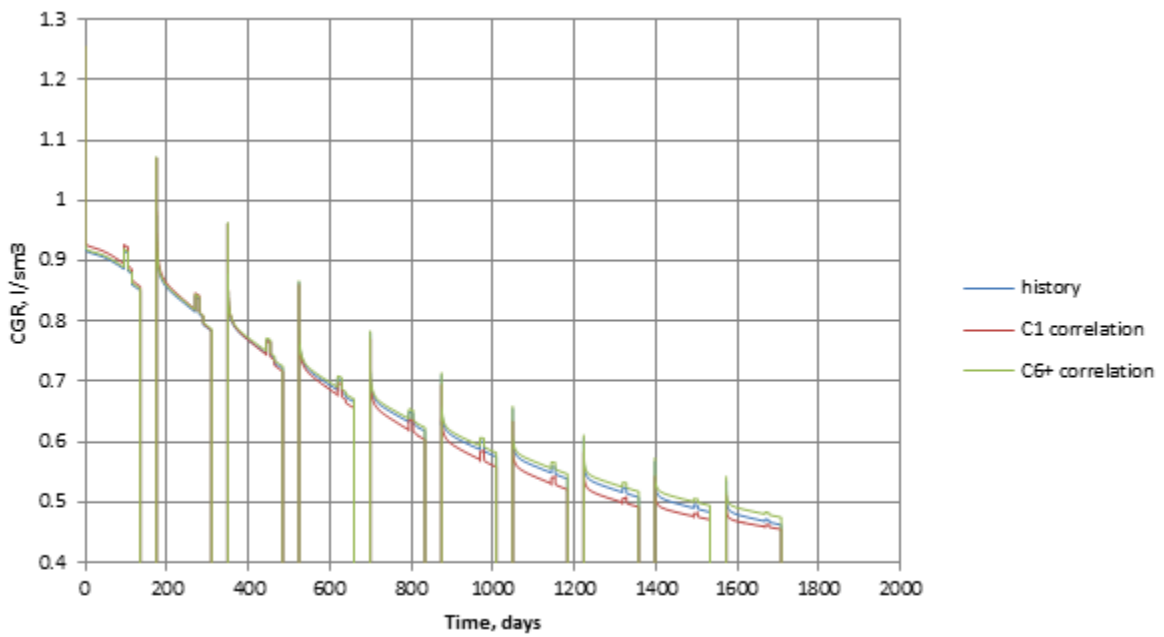


Figure D- 28: Extra rich fluid sensitivity study, k=70mD

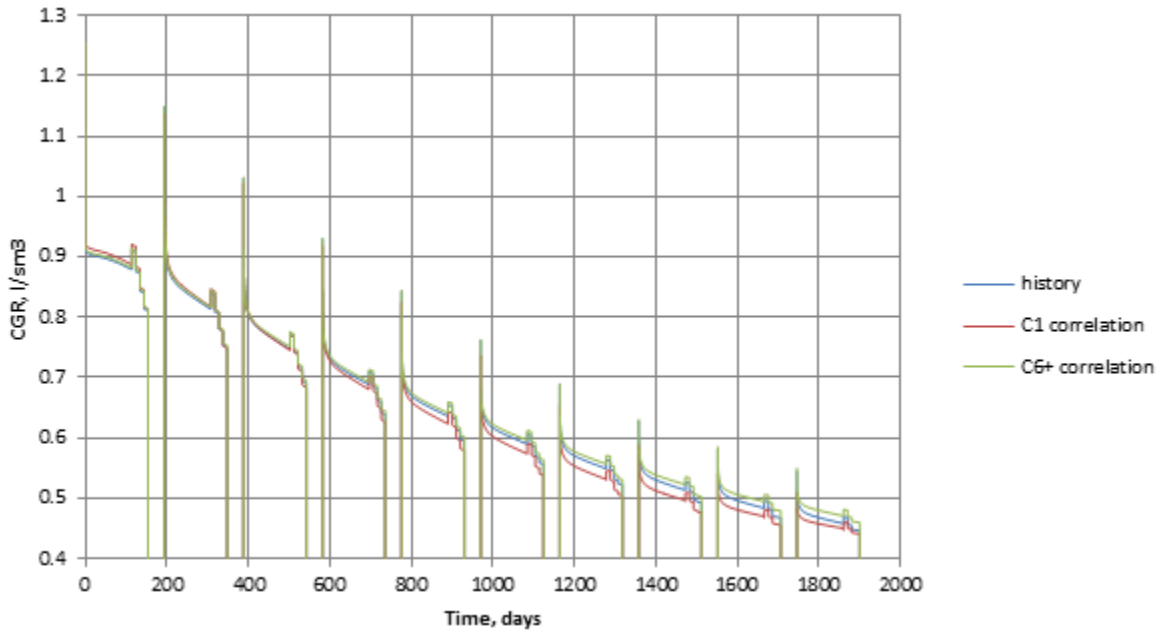


Figure D- 29: Extra rich fluid sensitivity study, $\Phi=0.15$

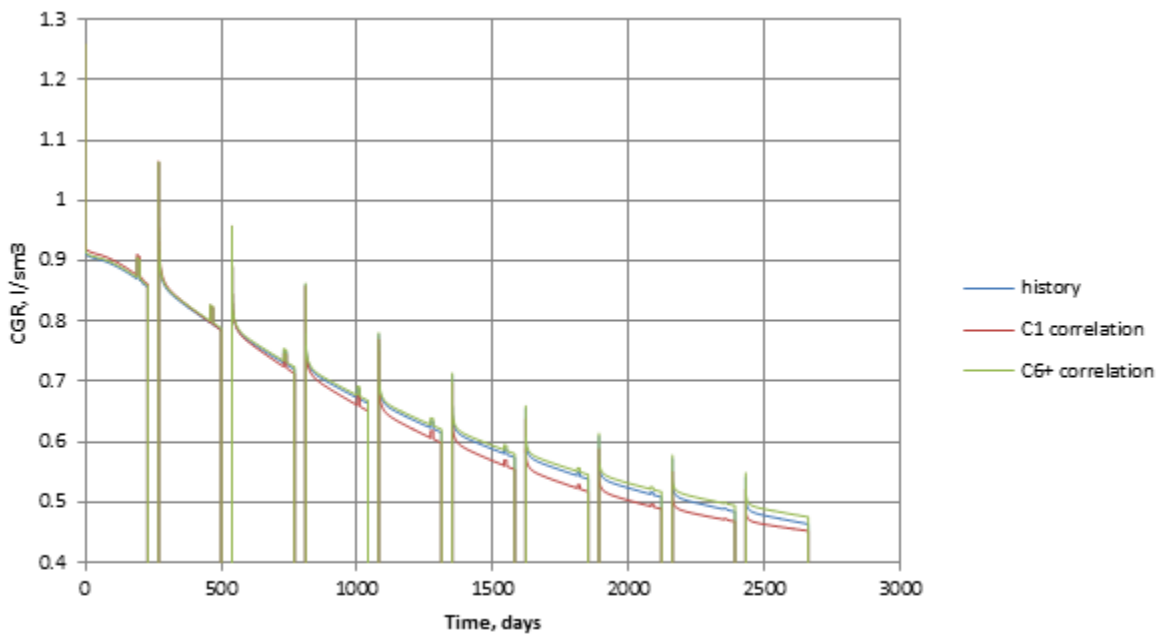


Figure D- 30: Extra rich fluid sensitivity study, $h=40m$

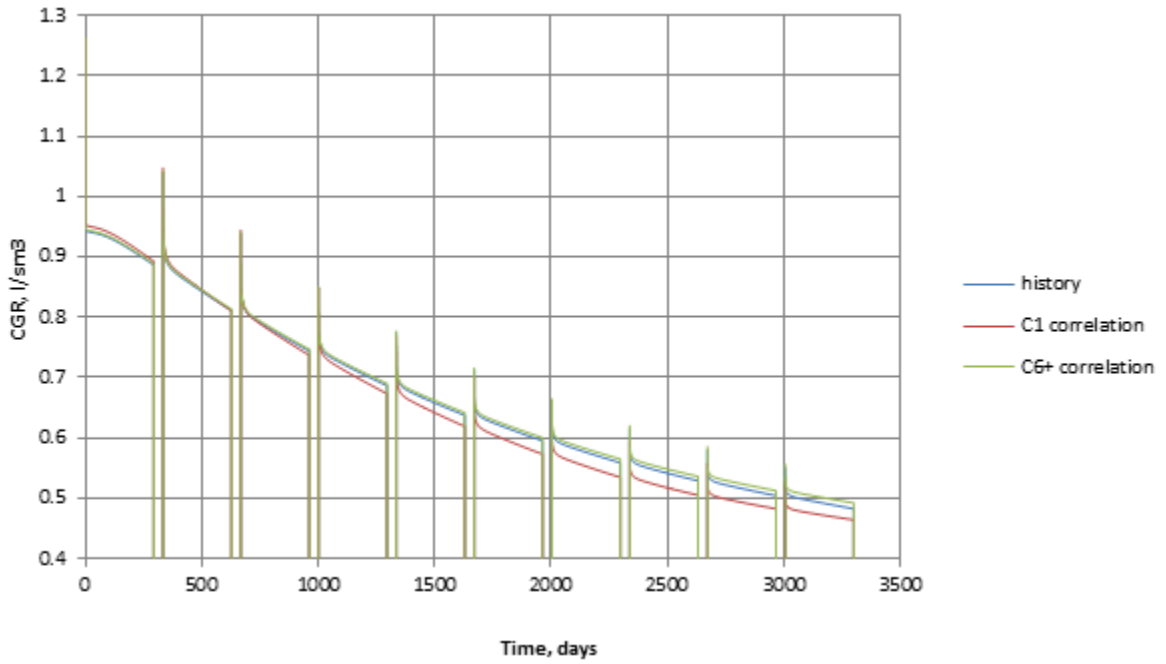


Figure D- 31: Extra rich fluid sensitivity study, h=60m

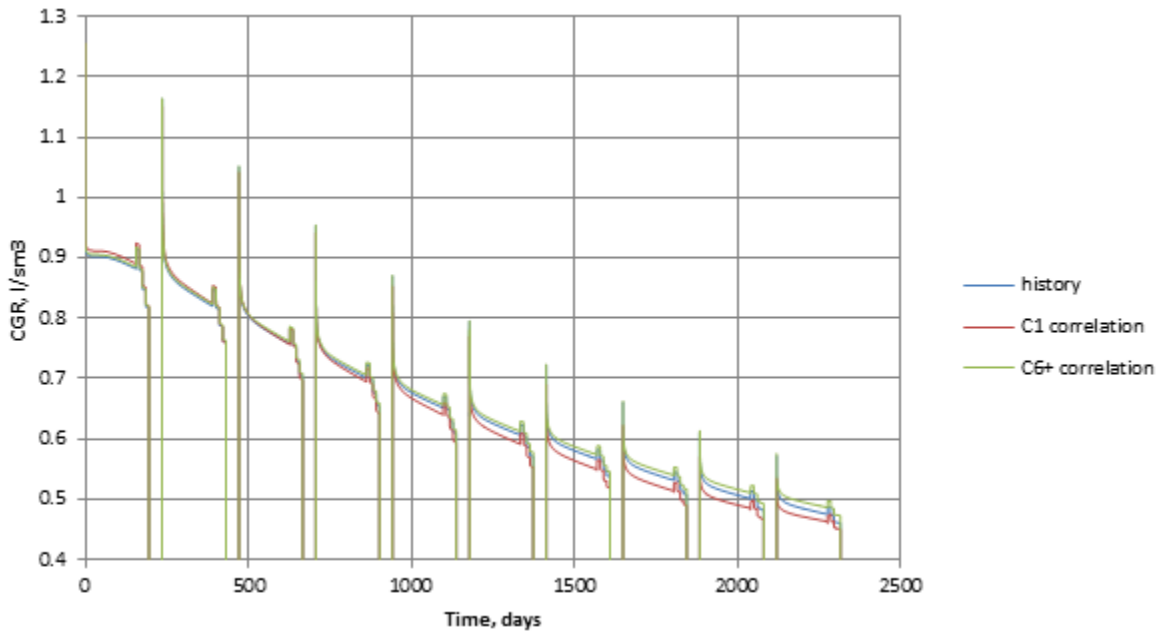


Figure D- 32: Extra rich fluid sensitivity study, L_r=50m

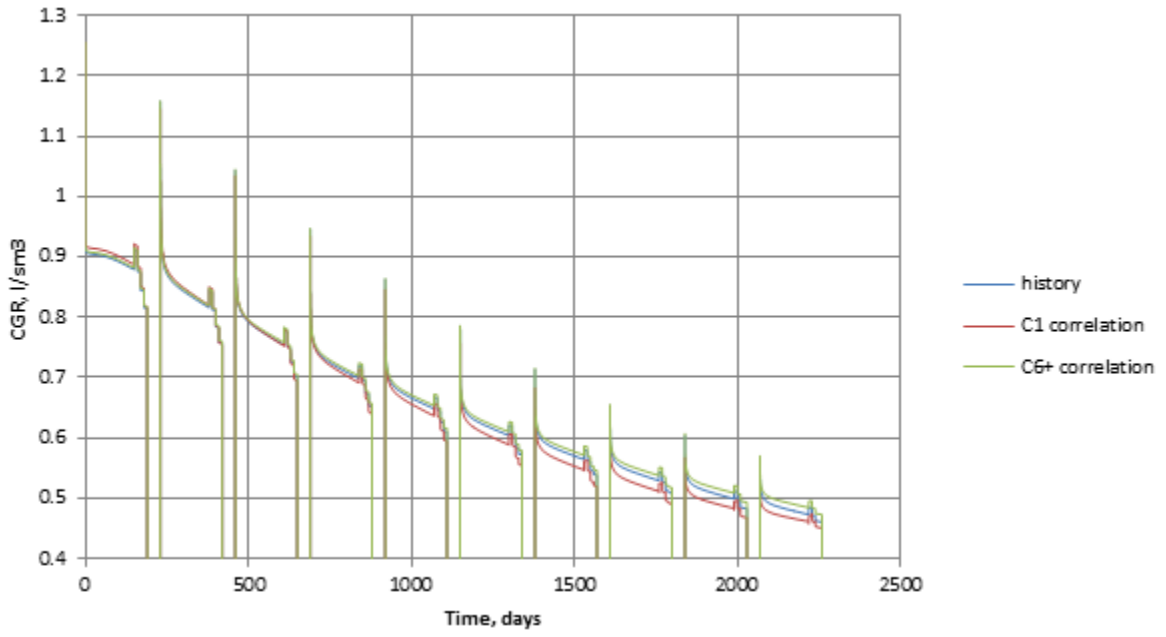


Figure D- 33: Extra rich fluid sensitivity study, $L_r=200m$

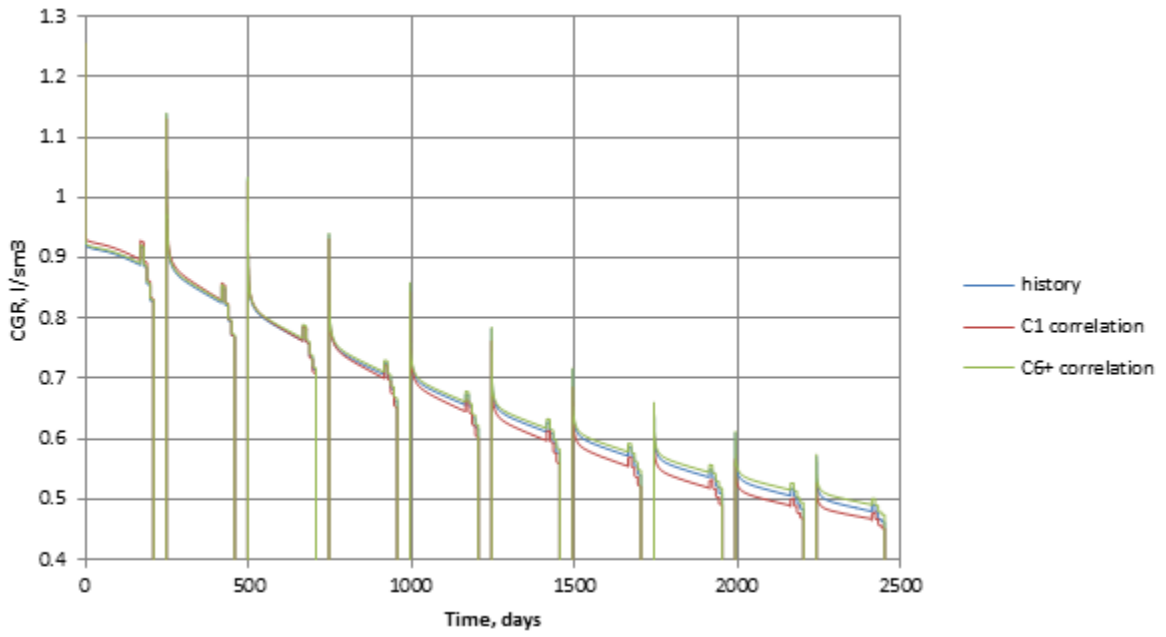


Figure D- 34: Extra rich fluid sensitivity study, $k_{rw}=500m$

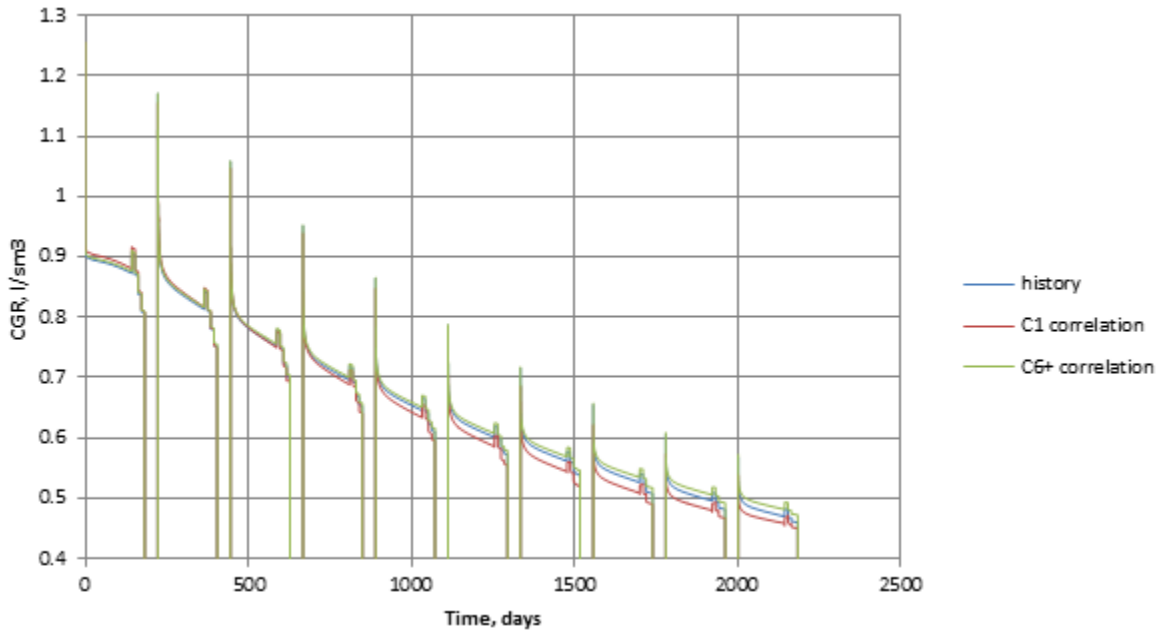


Figure D- 35: Extra rich fluid sensitivity study, $k_w=1500m$

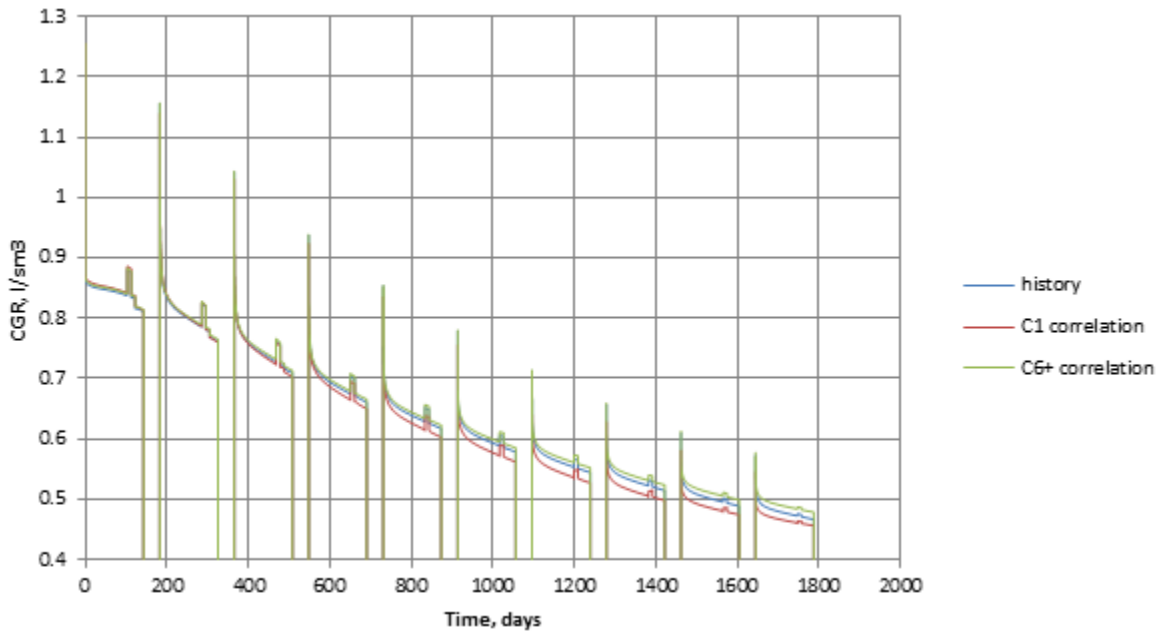


Figure D- 36: Extra rich fluid sensitivity study, pressure depression factor 0.85

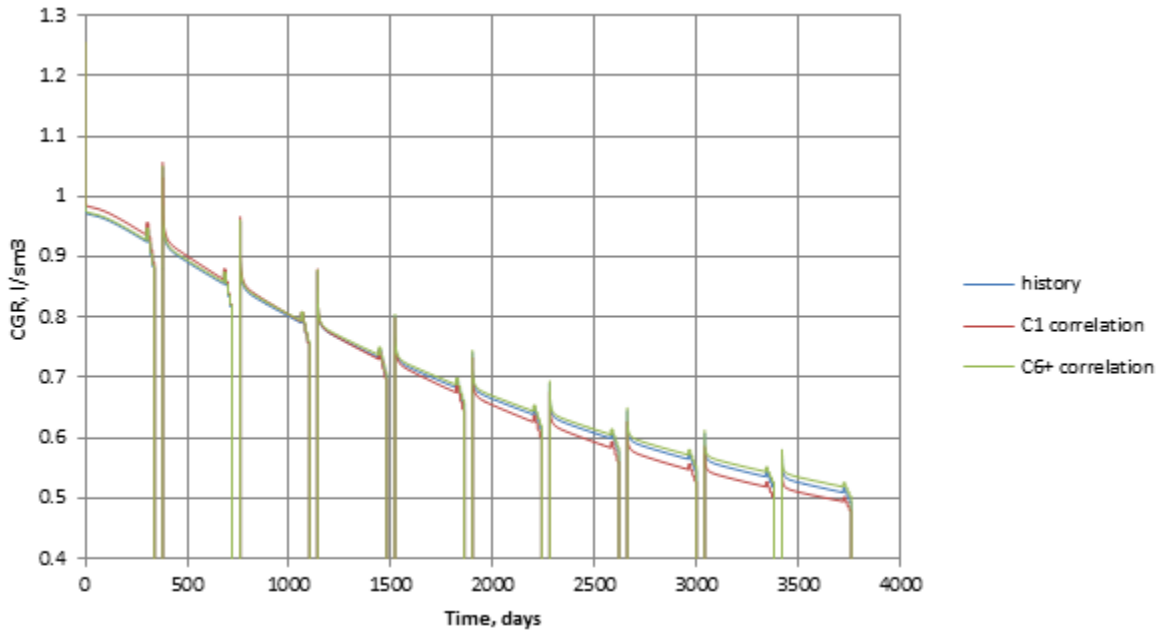


Figure D- 37: Extra rich fluid sensitivity study, pressure depression factor 0.95

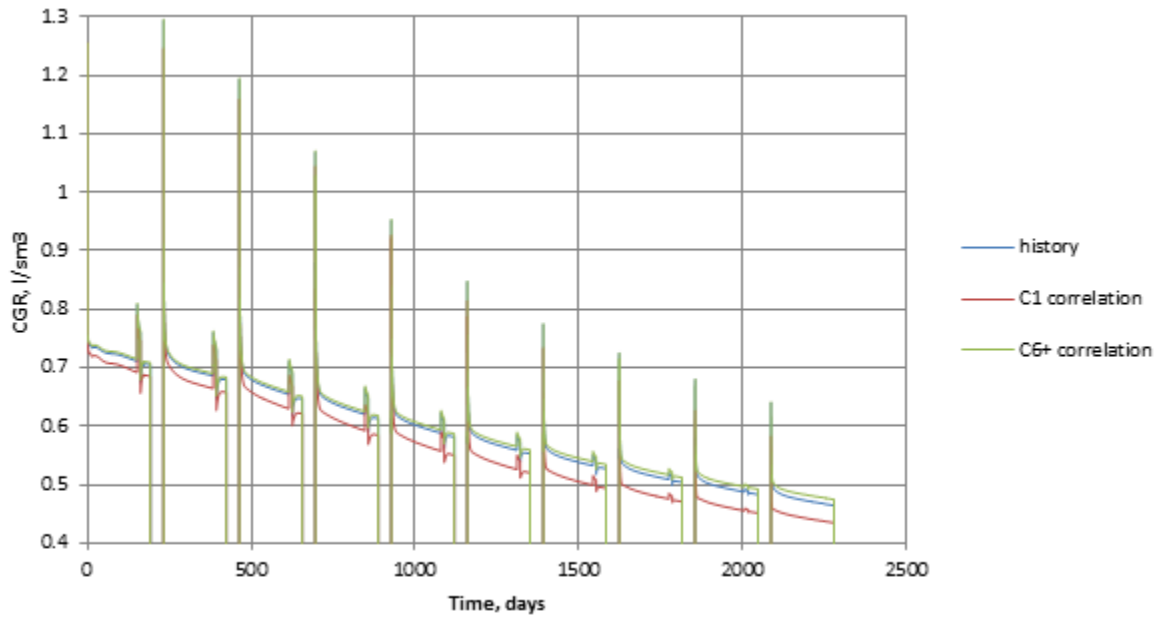


Figure D- 38: Extra rich fluid sensitivity study, relative permeability

Table D- 3: Extra rich fluid sensitivity study, RMS Error

Correlation	RMS Error, %					
	C1			C6+		
Time interval	1	2	3	1	2	3
Parameter						

k, mD	10	0.50	1.9	2.9	0.41	0.81	1.6
	70	0.64	2.1	2.4	0.40	0.90	1.8
Φ	0.15	0.66	2.7	3.2	0.37	0.86	1.7
	0.25	0.67	2.8	4.0	0.31	0.69	1.4
h, m	40	0.66	2.7	3.2	0.37	0.86	1.7
	60	0.67	2.8	4.0	0.31	0.69	1.4
L_f , m	50	0.64	1.9	2.8	0.39	0.83	1.6
	200	0.63	2.0	2.8	0.39	0.83	1.7
k_{fw} , mD·m	500	0.68	1.9	2.8	0.38	0.81	1.6
	1500	0.60	2.0	2.7	0.40	0.84	1.7
P_{res}^0 , bar	300	16	27	39	6.2	10	14
	400	18	57	97	3.0	8.0	12
Depression factor	0.85	0.50	2.1	2.6	0.42	0.89	1.7
	0.95	0.90	1.5	2.8	0.36	0.72	1.4
Relative permeability		2.8	5.0	5.8	0.54	0.95	1.6

Appendix E: Base Case Final Condensate Saturation

Objective: Demonstrate final condensate saturation distribution in the model for each sensitivity study case with initial reservoir pressure below dewpoint.

Rich Fluid

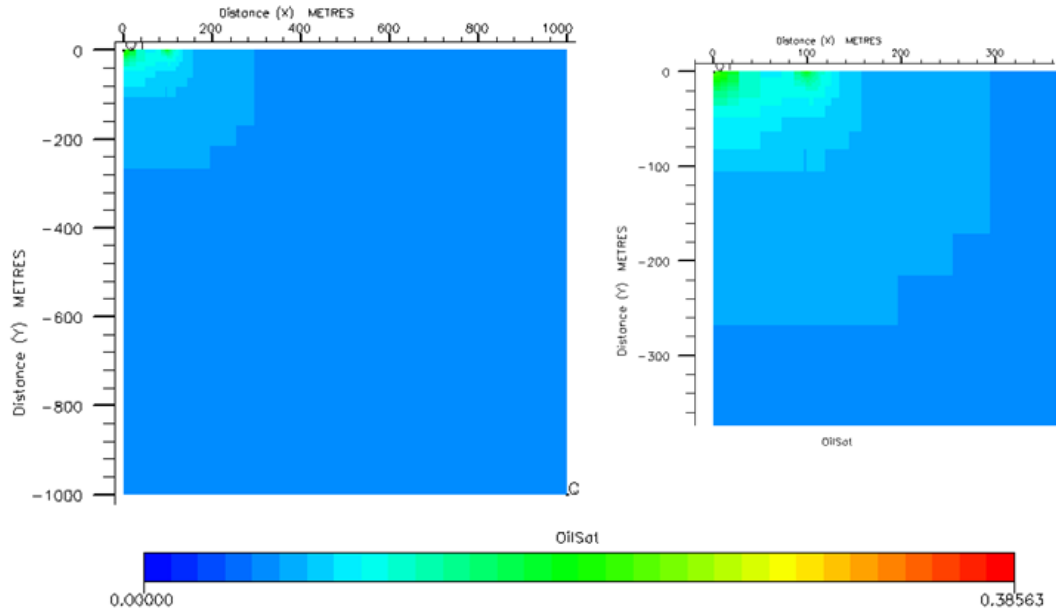


Figure E- 1: Rich fluid final condensate saturation for whole model (left) and detailed view of condensate banking phenomena around the well and hydraulic fracture (right)

Lean Fluid

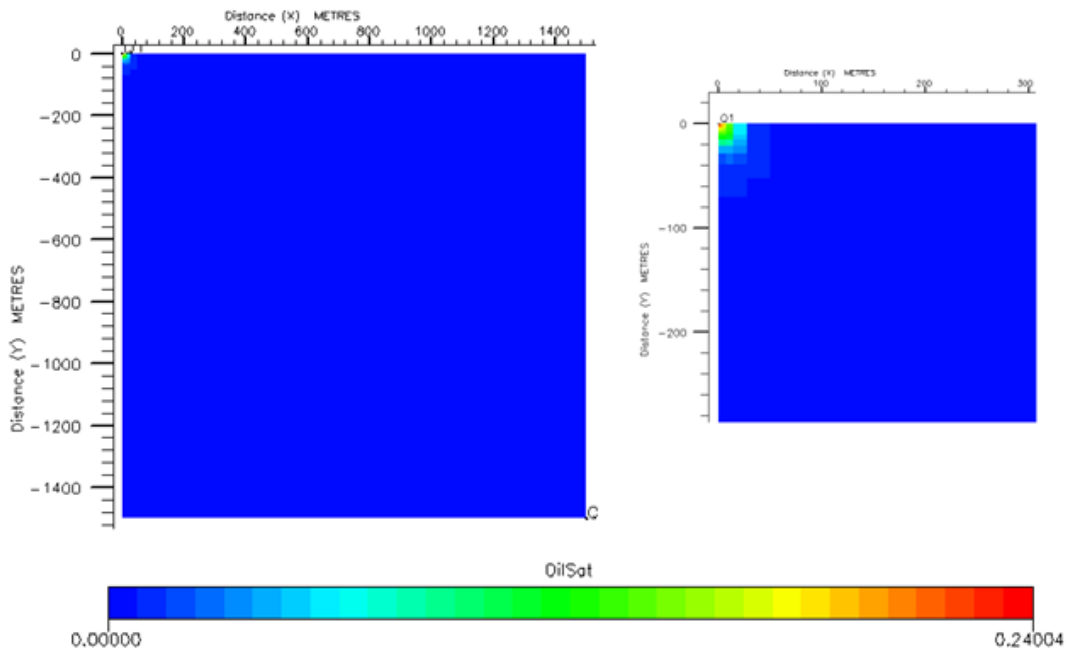


Figure E- 2: Lean fluid final condensate saturation for whole model (left) and detailed view of condensate banking phenomena around the well and hydraulic fracture (right)

Extra Rich Fluid

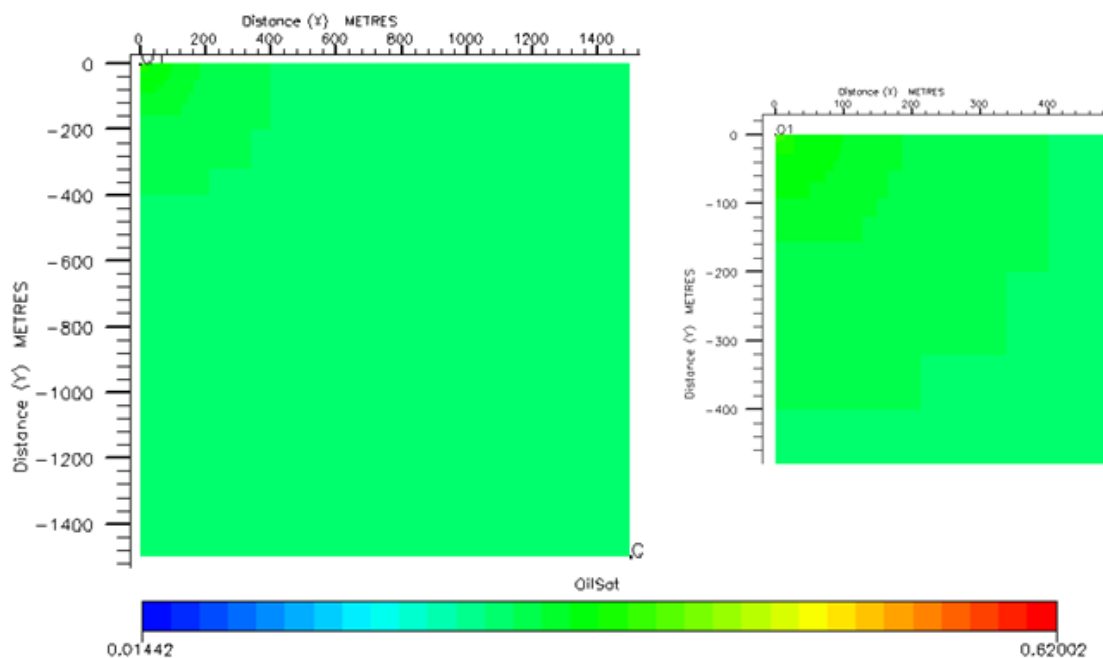
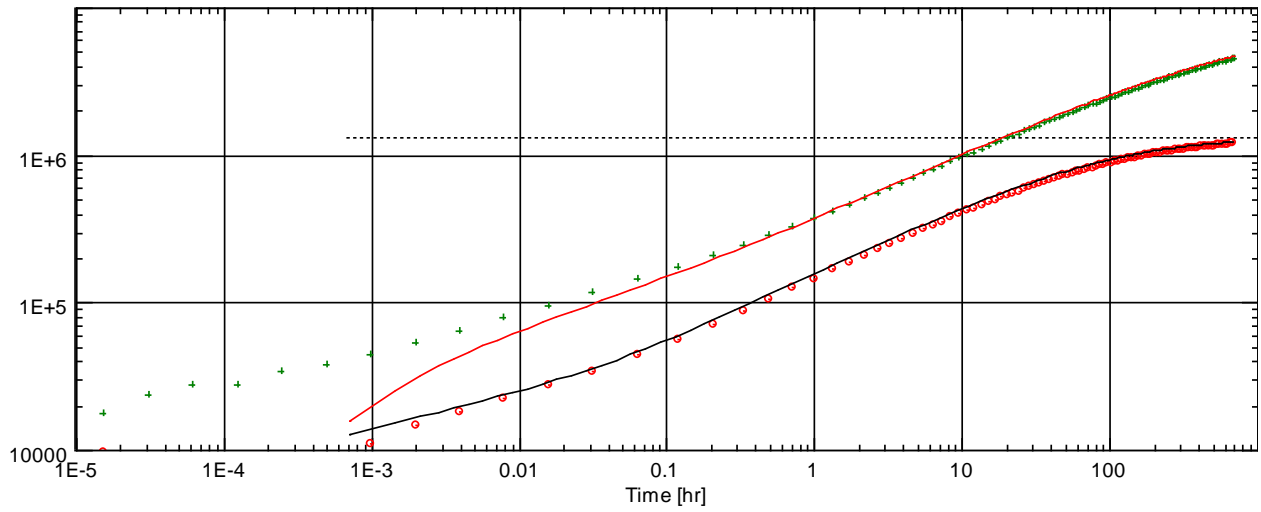


Figure E- 3: Extra rich fluid final condensate saturation for whole model (left) and detailed view of condensate banking phenomena around the well and hydraulic fracture (right)

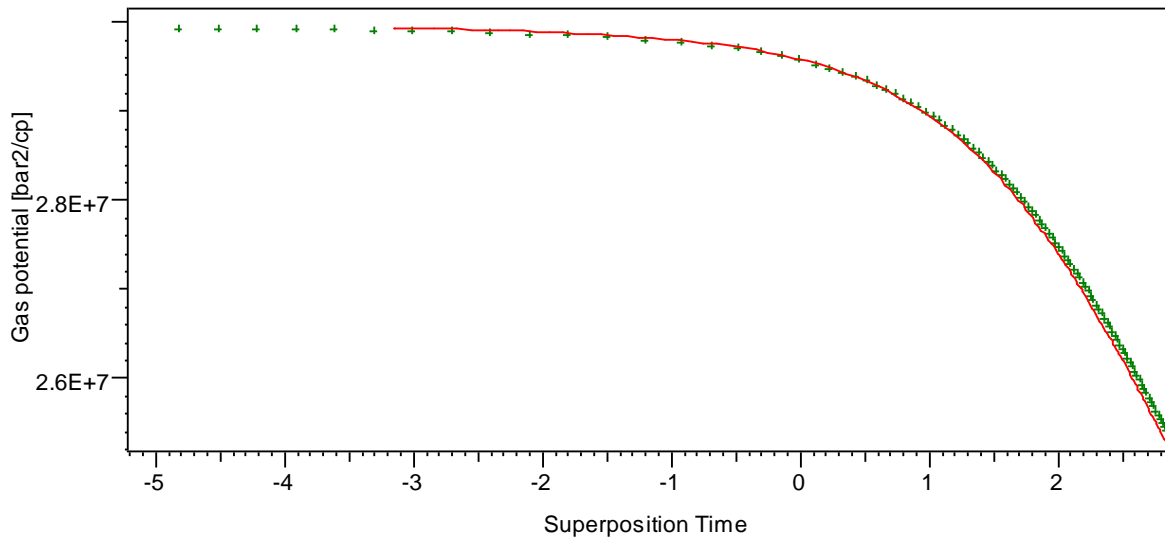
Appendix F: Analytical Solution for Simulation Model Used

Objective: Demonstrate the analytical solution above dew point for the model used. Assumes dry gas.



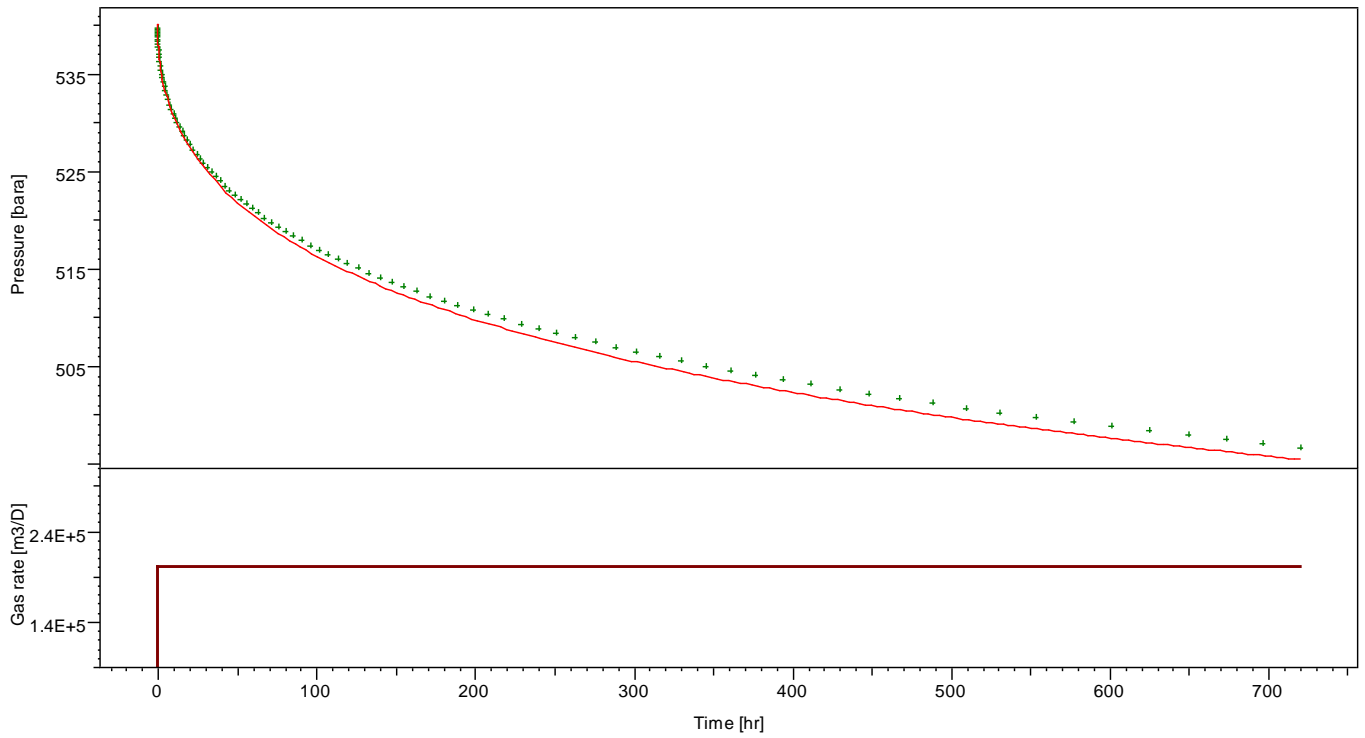
Log-Log plot: $m(p)-m(p@dt=0)$ and derivative [bar2/cp] vs dt [hr]

Figure F- 1: Log-log plot for model analytical solution above dew point



Semi-Log plot: $m(p)$ [bar2/cp] vs Superposition Time

Figure F- 2: Semi-log plot for model analytical solution above dew point



History plot (Pressure [bara], Gas rate [m³/D] vs Time [hr])
Figure F- 3: History plot for pressure and rate for model analytical solution above dew point